HUNGARIAN AGRICULTURAL ENGINEERING

20/2007

MAGYAR · TUDOMÁNYOS · AKADÉMIA
1825

MAGYAR · TUDOMÁNYOS · AKADÉMIA · 1825

Hungarian Agricultural Engineering

N⁰ 20/2007

PERIODICAL OF THE COMMITTEE OF AGRICULTURAL ENGINEERING OF THE HUNGARIAN ACADEMY OF SCIENCES

Published by

Hungarian Institute of Agricultural Engineering
H-2100 Gödöllő, Tessedik S. u. 4.
Director: Dr. László FENYVESI

GÖDÖLLŐ

St. István University, Gödöllő
Faculty of Mechanical Engineering
H-2103 Gödöllő, Páter K. u. 1.
Dean: Dr. János BEKE

Gödöllő, December, 2007

HU ISSN 0864-7410

PREFACE

The Agricultural Engineering Board of the Hungarian Academy of Sciences which supervises the development of this branch organises annually a conference at Gödöllő, which is the central place of the Hungarian agricultural scientific activity.

During the sessions, research scientist, developing engineers, experts of institutions engaged in agricultural engineering development strong in numbers the organizer, the hungarian universities and other higher grades of education, the research institutions: Hungarian Institute of Agricultural Engineering at Gödöllő, Faculty of Mechanical Engineering of the St. István University at Gödöllő and foreign guests give account of their results obtained in the research work and development of agricultural machinery.

This yearly English-Language publication the "Hungarian Agricultural Engineering", started at 1988, contains selected papers presented at the conference of 2007. We do hope that this publication will be found interesting to a big part of agricultural engineers.

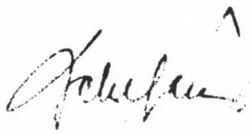

Dr. János Beke
Dean

Faculty of Mechanical Engineering
St. István University

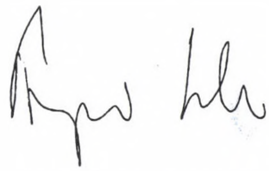

Dr. László Fenyvesi
Director

Hungarian Institute of Agricultural Engineering
Gödöllő

PART I.

ABSTRACT OF SELECTED PAPERS

PHYSICAL PROPERTIES OF CORN STOVER PELLETS

Csaba FÁBIÁN[1] - István J. JÓRI[1] - Péter TÓVÁRI[2]
[1]Budapest University of Technology and Economics (BME) Institute of Machine Design
[2]Hungarian Insitute of Agricultural Engineering, Gödöllő

Corn stover is an abundant by-product of agriculture, which as valueable biomass, could have important influence on renewable energy economics. For safe and wasteless storage and transport, as well as efficient industrial firing it is expedient to compact the material. One of the compacting technologies is producing pellets. About physical properties of corn stover pellets exigous information could be found. Therefore in our laboratory research work at the Hungarian Institute of Agricultural Engineering we investigated some physical properties of corn stover pellets. Testing material was produced using a laboratory pellet mill, without additives, applying different moisture content, particle size of material, and different hole diameter of the pelletizing matrice as variables. Abrasion and geometry tests, as well as material and bulk density tests were prosecuted on pellets. Pellet durability index varied from 87 to 97, pellet length between 5 and 22 mm, bulk density were from 500 to 1000kg/m^3. It was established, that increasing moisture reduces pellet length. Consequence of decreasing particle size and hole diameter of pellet matrice are provide better resistance to abrasion and increasing density of the pellets. The average heating value of corn stover pellets of 10 % moisture content was found as high as 15,5 MJ/kg. Based on these results can be stated, that pellets made of corn stover without additives provide a heating material of good quality.

BIOETHANOL FROM SWEET SORGHUM

Zsuzsanna LÁSZLÓ[1] - Sándor BESZÉDES[1] - Szabolcs KERTÉSZ[1] Cecilia HODÚR[1] - Gábor SZABÓ[1] - Imre KIRICSI[2]
University of Szeged
[1]Faculty of Engineering, Department of Technical and Process Engineering
[2]Faculty of Sciences, Department of Applied and Environmental Chemistry

Two varieties of sweet sorghum (Monori and Cellu) were investigated as raw material for bioethanol production. The juice yields of the two varieties were compared, and the self-life of fresh chopped stam and the juice were investigated during a 12 h storage period. The sugar content decreased rapidly because of the high microbe content of the plant in both cases. During fermentation experiments, the effect of temperature, nutrients and the pH of the juice on the alcohol yield were investigated. Cellulase enzymes were added to the juice before fermentation. In order to experience the remained fibre content that could be converted into alcohol, cellulase enzymes were added to the juice before fermentation. Results showed that the increase of alcohol yield was higher than it was expected from the cellulose content of the juice.

Keywords: bioethanol, sweet sorghum, fermentation

SORGHUM LIKE A BIOGAS INCREASING ADDITIVE

Imre KALMÁR - Eszter KALMÁRNÉ VASS - Emese SZABÓ - Valéria NAGY
Szolnok College Technical and Agricultural Faculty, Mezőtúr

In the Technical and Agricultural Faculty of Szolnok College, within the frame of Ányos Jedlik programme, we are making experiments for producing biogas with methods like giving Chinese sugar to manure.The aim of experiments carried out under factory conditions is to prove that different additives enlarge the produced gas volume and methane the volume of produced methane and the power of fermentation content differently.

QUANTITATIVE AND QUALITIVE ANALYSIS OF THE BIOGAS PRODUCTION FROM THE MUNICIPAL SOLID WASTE

Tamás MOLNÁR[1] - László SALLAI[2] - Dezső FODOR[3]
[1]University Szeged Agriculture Faculty Science of Animal Nutrition and Engineering Institute, Hódmezővasárhely
[2]A.S.A. Ltd.Hódmezővásárhely
[3]NRG-AGENT Ltd Kecskemét

The storage of the refuse takes place in deponia by adequate compression. During the storage gases, mainly methane and carbon dioxide, are developed due to the biological decomposition. We must prevent these gases to get into the atmosphere as they are involved in the global warming of the Earth and so they may cause changes in the environment.
With the regulations getting stricter in the EU where we are going to be members soon it is essential that a refuse dump should have a biogas deflector system in order to protect our environment. A compressor drains gases from the waste material, while another compressor is used for taking the gases to the place where they are used. From utilisation point of view a considerable quantity is developed, which can be diversely utilised.
Keywords: landfillgas, aneorob digestion

ECONOMIC EVALUATION OF SCALING OF AGRICULTURAL BIOGAS PLANTS

Attila BAI - Gábor GRASSELLI - János SZENDREI - Szilvia KORMÁNYOS
University of Debrecen, Centre for Agricultural Sciences and Engineering

In the different size categories, biogas investment can be facilitated economically even under present macro-economic conditions, though using different technological solutions. In small-sized plants, heat energy utilization is to be considered, with 50-60 Ft/m^3 production price (preferably to cover own demands), because of the lesser electric efficacy and extra material costs, and extra investment costs of cogeneration. This can be an alternative to natural gas firing even under present price conditions, especially when the biogas investment is weighed strategically, together with its complex (environmental, employment-assuring) benefits. In middle sized and large plants the own consumption is not realizable because of the greater quantity, therefore, cogeneration production of electricity is advised, under partial or full heat utilization. Under worsening

Hungarian conditions of "green" electricity take-over, the transformation of biogas to another marketable product, bio-methane, is to be considered. This involves no waste-heat generation, the utilization of which is always a critical point of operating cogeneration. Based on waste materials, or, perhaps, also with utilization of the carbon-dioxide from purification, in large plant sizes with 20-30 Ft/m^3 biogas prime cost this can mean a profitable way of green energy production.

EFFECT OF THE VERTICAL WIND PROFILE UPON THE OPERATION OF WIND-POWER PLANT

István PATAY[1] - László TÓTH[2] - Norbert SCHREMPF[2] - Lajos FOGARASI[2]
[1]'Tessedik Sámuel' College, Mezőtúr
[2]Institute of Engineering and Water Management
'Szent István' University, Gödöllő

During operation the blades of wind generators work with different wind speed areas in the course of the rotating. It has results in the different dynamic loading of the blades. The vertical wind profile is determined by the Hellmann coefficient. The dynamic equations are given to analyse the power and torque relations for the blades of wind turbines.

COMBINED SOLAR SWIMMING POOL HEATING AND HOT WATER SUPPLY

Richárd KICSINY - István FARKAS
Szent István University, Gödöllő

This paper presents the results of a monitored solar swimming pool heating system that installed at the campus of Szent István University, Gödöllő, for making preheated water for a swimming pool and preparing domestic hot water for a kindergarten. The recorded data are for the period of 2001-2006. The amounts of solar energy irradiated on collectors' plane, utilized energy directly by the collectors calculated daily. Additionally, directly used up total (supplied by gas and solar sources) and solely solar energy by the consumers have been all calculated daily both in swimming pool operation and in kindergarten operation. On the basis of these data the efficiency of the system has also been determined. The calculations have been carried out by using MATLAB® software.

APPLICATION OF MEDIUM-DEEP SUBSOILERS IN THE AGRICULTURE

(Tests on the Working-Quality by Measuring the Electric Conductivity of Soil)

Péter RÁCZ - Zsolt SZÜLE
Szent istván university, Gödöllő

The present article reports an experiment of the research in the frame of which I search after the relationship between the looseness L of soil characterizing the operating quality of the chisel-type subsoilers of a medium working depth and the change in the electric conductivity in the soil caused by the loosening cultivation. The investigation was carried out with the help of the mobile electric-conductivity measuring device – accounted as a novelty in field-land tests – type *Veris 3100* with disc electrodes, in field-land operating conditions. As the results of the investigation, the characteristic diagrams of the electric-current conductivity are presented in this article, recorded along arbitrary test lengths, for before- as well as after-loosening soil states. In addition, the shapes of the functions related to the individual soil states are also shown.

BRUISE INVESTIGATION OF THE CULINARY PAPRIKA

Károly PETRÓCZKI
Szent István University, Gödöllő

The culinary paprika has an important role in Hungary not only in production, but in the consumption, too. During hand picking and mainly in case of automatic picking and expanding machinery packaging summarily in crop handling the paprika is loaded by many mechanical influences. If the mechanical load remains below a critical level then there is no bruise or the bruise can regenerate. In other case above a critical level an irreversible bruise occurs and so the quality decreases with a considerable degree. The popular V-shaped paprika has a disadvantageous behaviour namely the peak of the paprika is very sensitive to the bruise. As the first step toward analysing it and because of the simple method of approach this article tries to find the limit of the mechanical load which can bruise only the side part of the paprika. The investigation was supported by Hungarian Scientific Research Fund (OTKA T 46917).

A MICRO-CONTROLLER-BASED ALGORYTHM FOR SORTING WHITE PAPRIKA

Zoltán GERGELY - Endre JUDÁK
Szent István University, Gödöllő

There is no device available on the market of sorters (pickers) which is suitable especially for sorting the sweet white paprika, and capable of fulfilling the standard requirements. The most of the sorting machines is suitable for selecting roundish, sub-spherical vegetables and fruits (tomato, potato, apple, apricot, cantaloupe etc.) by applying the weight measurement. The function of the system is to qualify the paprika of which most important parameters are its size and shape – measuring them and processing the measured data have to be solved. The record of shape is realized by CCD photoelectric linear array sensors with the help of which the processing with regular accuracy can be provided. An algorithm running in the micro-controller developed by us provides the assorting process; it determines the size fraction from the length and the shoulder-width, the centre-line length, the perimeter and area data.

DISCHARGE COEFFICIENT DETERMINATION OF SWIRL-TYPE NOZZLES BASED ON HYDROLOGICAL ANALOGY

István SZTACHÓ-PEKÁRY
College of Kecskemét

In a number of early papers presenting a simple mathematical, analytical treatment of swirl atomizers the discharge coefficient, in spite of the weir flow analysis

was determined by the use of the principle of maximum flow. This was by analogy to the principle of maximum flow as applied to swirl atomizers. This paper demonstrates that the principle of maximum flow can indeed be applied, in theory, to the air-core diameter at the outlet region and the discharge coefficient of swirl atomizer.

COMPARISON OF INERTIA TYPE SHAKERS IN A SOUR CHERRY ORCHARD

Zoltán LÁNG
Corvinus University of Budapest

A slider crank type inertia shaker produced in series and an experimental shaker with rotating eccentric masses with similar output parameters were tested in the same sour cherry orchard. Acceleration of the tree and power consumption of the machine was recorded at different PTO speeds. In "Érdi bőtermő" sour cherry variety the performance of the two machines was different. At the same specific power consumption (kW/ms^{-2}) the shaker with rotating eccentric weights produced higher acceleration amplitudes and consequently higher fruit detachment ratio. Test results are analysed and conclusions are drawn to help shaker machine design.

REDUCTION OF FRICTION AND CUTTING LOSSES IN FORAGE HARVESTERS

Péter KAJTÁR - Péter SZENDRŐ - Andreas HAFFERT
Szent István University, Gödöllő

Self-propelled forage harvesters are currently the preferred means for chopping green forage such as grass or maize. A major part of the energy is required for the chopping and transportation of chopped material in the harvester. This energy can be reduced by minimisation of the friction coefficients between the housing and the chopped material or by reduction of the friction processes as the result of design optimisation. The friction process between the chopped material and different surfaces is investigated by means of practical tests and analysed based upon theoretical analyses. First results from theoretical analysis are initially shown. The investigations have the purpose of showing those potentials that allow minimisation of friction processes. Results from cutting tests on a test bed with knives with a slotted geometry (uneven cutting edge) are then presented.

PARTICLE-SIZE DISTRIBUTION OF GRINDS

Theoretical and empirical discussion

Lajos FOGARASI - Péter KORZENSZKY
(OTKA research project No. T 048 446)
Szent István University, Gödöllő

In the comminution, the fineness of grinds (grits) is the most important quality character. However, it can be interpreted and determined only in an indirect way. Using the data base gathered during the several-year research in laboratory conditions, we derived such simple and definitive relationships between the different accepted fineness parameters – empirical and theoretically created nominal particle sizes as well as the specific surface area of the grinds – and we proved their validity in a wide operating and material-property range from the experimental results as well. These are the characteristic curves of the materials to be ground and the comminution procedure as well.

EFFECT OF HAMMER SPEED ON PARTICLE SIZE DISTRIBUTION IN HAMMER MILLS

Péter KORZENSZKY
(An OTKA research project No. T 048 446)
Szent István University, Gödöllő

In the frame of the research project carried out for several years on comminution of different agricultural materials, and comminuters, we improved the earlier conservative measuring system. The new electronic 8-channel, computer-aided testing system and the well instrumented laboratory-size hammer mill equipped with a frequency converter makes possible to carry out multi-parameter measurements and to gain multi-variable plotted and calculated theoretical functions. In the present article I show the effect of the rotor speed of the mill upon the size distribution and the fineness of the produced grits, and some other selected geometric and energetic parameters when grinding maize.

AUTOMATIC STEERING OF POWER MACHINES WITH GPS NAVIGATION AID IN AGRICULTURE

József HAJDÚ[1] - István FÖLDESI[1] - András FEKETE[2] - József DEÁKVÁRI[1] - László KOVÁCS[1] - László MAGÓ[1]
[1] Hungarian Institute of Agricultural Engineering, Gödöllő
[2] Corvinus University of Budapest, Budapest

The objective of the research work performed was to determine the characteristics of steering with GPS navigation aid. The purpose was to determine the accuracy when following the edge of the working width with different tractor and implement combinations.
The best results were obtained when steering with a GPS based automatic steering system both when following a straight leading line and when following the edge of the working width made during the previous test run.
Keywords: Error, Global positioning systems, Navigation, Precision, Tracking

CREATION OF DEVELOPMENT SYSTEM FOCUSING ON PRODUCT-RANGE

Lászó FENYVESI - Szilvia KÉSMÁRKI-GALLY ERDEINÉ
Hungarian Institute of Agricultural Engineering, Gödöllő

The macro-economic location, evaluation, operation of subsidy systems, CAP-reform and necessity of agricultural production are sources of debates all over the world. Besides certain balance explanations they are the traditions and mainly political reasons that are behind the agricultural "regulations" formed in separate regions. The European subsidy system is most probably due to change that results definitely in production support decrease.
The current system is not only deforming the real economic situations deteriorating the healthy development of entrepreneurs but also eliminates the need and importance of development and innovation.
The change in the agrarian-regulatory system is increasing the competition and makes innovation more important in the economic production.

Agricultural production can be successful via its products consequently creation of development system focusing on product-range is the main target. The method of „market-conscious technology development" is suitable for this task.

QUALITY MANAGEMENT SYSTEMS FOR SUSTAINABLE DEVELOPMENT

Klára BÉRES - István HUSTI
Szent István University, Gödöllő

To lead and operate an organization successfully, its necessary to direct and control it in a systematic and transparent manner. Success can result from implementing and maintaining a management system that is designated to continually improve performance while addressing the needs of all interested parties. Managing an organization encompasses quality management amongst other management disciplines. A quality management system is a sustainable system to direct and control an organization with regard to quality.
The quality and its continual improvement is one of the most important area for the organizations of competitive economy. These organizations depend on their customers and therefore should understand current and future customer needs and strive to exceed customer expectations. That is why the sustainability of the customer focused organizations depends on the level of satisfaction of their customers. The producing and servicing companies – apart from their activities – therefore turn higher attention to implementing and sustainable developing of their quality management systems.

LOW COST MECHANISATION SOLUTIONS FOR EFFECTIVE FARMING ON SMALL AND MIDDLE-SIZED ARABLE FARMS

László MAGÓ
Hungarian Institute of Agricultural Engineering, Gödöllő

It is essential to develop a cost effective fleet of machinery for the present day various standard sizes of plants. In the case of the small units it is essential to develop equipment and cost saving mechanical solutions, but there is also demand for the building up of systems of machinery with modern, cutting edge technology and profit improving attributes for the middle-sized farms, which more favourable specific cost level.
The changing and modernising of the Hungarian fleets of machinery, the majority of which is obsolete is unavoidable. Farmers working from different amounts of capital on farms, which provide different levels of mechanical development potential, have to develop mechanisation solutions using the wide range of types and price range of the power and work machinery.
Taking into consideration the current partitioned structure of the farms the goal was established to determine that in the case of the different branches of plant production on small and middle-sized farms which combination of fleet of machinery can be used effectively.

BASIC TASKS OF THE AGRICULTURAL INVESTMENT PROCESS

Miklós DARÓCZI
Szent István University, Gödöllő

The elaboration of the **methodology** and the **computer program** have been performed in order to support the complex decision preparation processes, serve the **efficient utilization of the development resources** and be a well-applicable tool for the management of the enterprises having even average professional skills, minimal computer facilities and knowledge, diverse production structure and plant size.
I set up a model for seeking answer for the **six basic questions** emerging in the phase of **preparation** of complex **decisions** of agricultural investments. It helps to evaluate or rather tender the different investment possibilities and versions. Certain elements of the model **can be altered in a flexible way** considering the current circumstances, and they can be utilized in different sequences or even separately.
I prepared the computer-aided version of the model for MS Excel, which supports the most rapid completion of the **versions, calculations** or even **sensibility analysis** related to the decision preparation. Based on the results of model-calculations, the program is suitable for not only the preparation of agricultural investments but also for the decision preparation of **other tasks of technical development**.

ABRASIVE WEAR TESTING OF ENGINEERING POLYMERS

Gábor KALÁCSKA - László ZSIDAI - Zoltán BORS
Szent István University, Gödöllő

To improve the abrasive wear behaviour of a certain tribo system - modifying the system -, there are more keys e.g. replacing the metal surface with a plastic one. If in a given tribo system the engineering plastic part can be acceptable from other engineering points (e.g. strength, life period and fatigue) than the proper plastic selection may improve the abrasive wear performance of the system. The proper plastic material selection is considered as a keyword, because each tribological system is different. Taking these into account, first, we have carried out some simply laboratory test have already been published. Following that we designed a real machine element test systems applying different plastic/metal gear pairs running in abrasive media. The conclusion of the systems and the comparison of the systems were published in different journals and a PhD thesis work was written.
But to clarify the real plastic material behaviour in case of abrasive particles we had to design a further test system, where the sliding plastic surface always act on a pure abrasive contact surface, which is not covered with transfer layer or third body particles. So, the sliding path to run is always clear. Some mechanical properties of the tested materials were measured at the Hungarian Institute of Agricultural Engineering and tribotesting was carried out at SZIU and UNBM. (OTKA T42511, NI 62729, INNOCSEKK, GVOP 3.3.)
Keywords: engineering polymers, abrasive wear

THE IMPACT PATHWAY METHOD FOR ESTIMATING EXTERNAL COSTS OF ELECTRICITY GENERATION

Sándor MOLNÁR[1] - Nenad DEBRECIN[2] - Tea KOVAČEVIĆ[2] - Márk MOLNÁR[1]
[1]Szent István University, Gödöllő
[2] Zagreb Unviersity, Faculty of Electrical Engineering and Computing

External costs of electricity refer to the costs of damage imposed on society and the environment by an electricity generation chain, but not accounted for in the market price of electricity. Electricity generation impacts include effects of air pollution on health, buildings, crops, forests and global warming; occupational disease and accidents; and reduced amenity from visual intrusion or emissions of noise. Effects of air pollution on human health are the most significant among them. The equivalent monetary value of health damage, i.e. external cost, is calculated here for two types of fossil fired power plants, located in Croatia, with the analysis covering Croatian- and European-wide scope of effects.

PART II.

SELECTED SCIENTIFIC PAPERS

PHYSICAL PROPERTIES OF CORN STOVER PELLETS

Csaba FÁBIÁN[1] - István J. JÓRI[1] - Péter TÓVÁRI[2]
[1]Budapest University of Technology and Economics (BME)
Institute of Machine Design
[2]Hungarian Insitute of Agricultural Engineering, Gödöllő

1. Introduction

Agriculture produces corn stover in waste quantities in fields sometimes regarded as unwanted biomass hindering soilworks, consuming surplus plant nutrients, time and power to eliminate. In spite of its uneasy features corn stover is available for industrial heating by means of mechanical transformation, mainly compaction. One of the most expedient transformation procedure is pelletizing.

Important properties of heating pellets are resistance to abrasion, material and bulk density, geometry, and heating value. In this paper we publish the results of our research on these physical properties of corn stover pellets to be made with different parameters of processing.

2. Materials and methods

Corn stalk with leaves were collected for experimental procedures in the autumn of yr. 2005. After harvest stalks were being collected in sheafs and stored in a linney. This way the experimental material was kept dry and its consistence was saved in good condition and without wastes.

2.1. Preparation

At first corn stover was chopped with a chaff-chopper to 25 mm size, then it was ground using a Fritsch cutter grinder with four different screen sizes: 10, 6, 4, 2 mm. Before pelletizing grinds were humidified to 25, 35 and 45 % moisture content. Prepared material was pelletized by a CPM Laboratory Pellet Mill, which was cleaned before every pelletizing process. Steady-state condition was accounted when pellet matrice temperature reached 50...60°C (depending on the type of pellet matrice). Commonly the pellet matrice temperature reached the steady-state temperature within half an hour after starting the machine. After drying and cooling down , pellets produced were sieved to avoid dust and chippings. Sieves sizes were specified to pellet diameters.

In all cases pellet samples were taken for measuring under MSZ 6962-84 with a sampling ladle. A sample divider was used for preparation of the elementary samples and sample reduction . Mass measurements were made with three diffenerent balances (Precisa 30000D, Precisa 6200D, Kern RH 120-3) according to the mass to be measured [2].

2.2. Pellet durability (abrasion) test

Pellet durability was measured by a Pfost-tester. The tester had two boxes, which were able to abrade 500-500g of pellet samples. The boxes were made of steel, prismatic and chambered. Sizes of the boxes were 300x300x127 mm with a 228x50x5 mm welded baffle on the 300x300 mm side wall. On one side of the box was openable for inserting and getting out samples. The boxes had the possibility to be rotated around an axis on the 300x300 mm wall with 50±3 rpm. Up to the home standards we stopped the tester for measuring samples when 500 rotations were done [1].

2.3. Density and geometry analysis

Dimensions of pellets (diameter and length) were fixed with a slip-gauge by the terms of the pellet testing norm of the Hungarian Institute of Agricultural Engineering, which prescribes the sample mass for the different pellet diameters. Material density was scaled using the analytical balance of a Kern RH 120-3 laboratory drier (0,001 mm precision). Bulk density was measured in pursuance of CEN/TS 15103 with 3 different measure dish .

2.4. Heating value and elementary composition analysis

Heating value has been determined using an IKA calorimeter. Measured value needed to be corrected with the Hydrogen and moisture content of the fuel. Therefore an elementary composition test (CHNSOX) was conducted with a Vario Macro Elementar measurement unit. Both tester have been found in the Accredited Energetic Testing Laboratory of the Hungarian Institute of Agricultural Engineering.

3. Results and discussion

We analysed durability, density and geometry of the pellets as physical properties.

3.1. Pellet durability

The pellet durability (specified in PD index), in fact the resistence to abrasion is one of the most important characteristics of the pelleted material. PD index shows by fixing the percentage of dust and chipping wastes the resistance to abrasion under transport, loading, storage and other handlings.

During durability tests carried out by using the Pfost-tester 500-500 grams of samples were measured. Dust and chippings were sieved after the abrasion process. Screen size of the sieve has been specified according to the pellet diamater by the terms of FVMMISZ 39-71-3-1-01 D95. After testing sieved samples mass were measured and net weight was fixed.

The PD index can be defined in pursuance of ASAE S269.4 DEC96 as follows:

$$PDindex = \frac{Q}{500} \cdot 100 \qquad (3.1)$$

where:

Q – pellet sample mass after abrasion test and sieving [g].

The formula (3.1) gives actually the percentage mass of the abraded pellet sample compared to the mass before abrasion. PD index must be given as the average of two measure results with one decimal precision. As it has been mentioned above Pfost-tester comprises two boxes. As a consequence one testing process gives two measure results. The durability test is valid if the variation between these two results of one test is maximum 5 %.

Diagrams 3.1. and *3.2.* represent PD indexes of different corn stover pellet samples in function of moisture content. Parameter of the curves is the particle size of pelletized grinds.

The pellet samples can be evaluated by the PD indexes as follows:

Value of PD index	> 90	very good
	85 – 90	good
	80 – 85	acceptable
	75 – 80	bad
	< 75	not acceptable.

The received results of durability tests show that with the exeption of one of them the PD index values of the measured corn stover pellet samples were laying above 90. Thus these samples have been classed in the „very good" category. One pellet sample belonged to the good class. We have found the pellets of 6 mm diamater made of 2 mm particle size grinds with 25 % moisture content to show the highest resistancy to abrasion (PD value: 98,9), while the 13 mm diameter pellets, produced of 10 mm grinds, with 45 % humidity, belonged to the lower (still „good") durability class (PD value: 89,2).

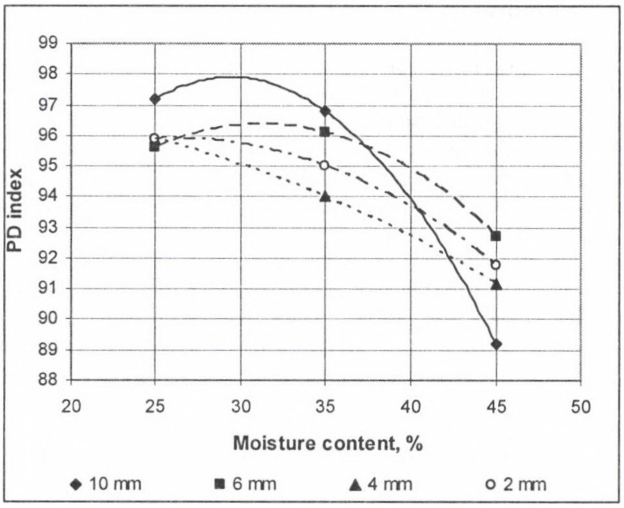

Diagram 3.1 PD indexes of 13 mm diameter pellets as a function of moisture content

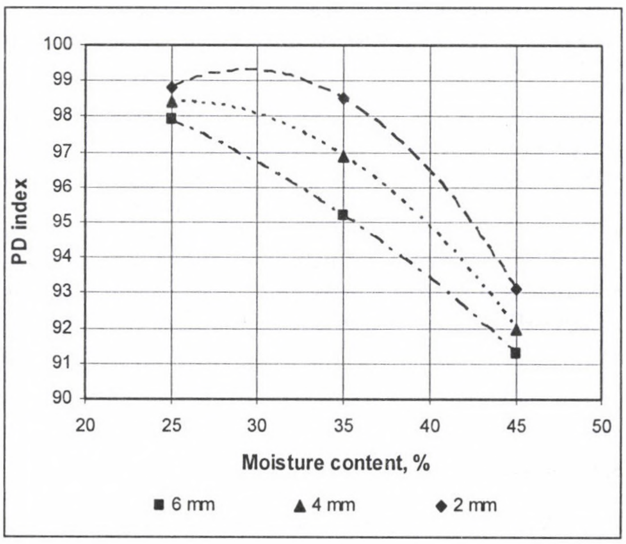

Diagram 3.2 D indexes of 6 mm diameter pellets as a function of moisture content

The pellets made of coarser and more humid grinds have commonly lower quality. In any case, pellets produced of basic material of 45 % moisture content could be found as more abradable than that of made of 25 or 35 % grinds. As it was perceptibe by the 13 mm particles the role of the decreasing grind sizes is not consistent in increasing pellet durability.

3.2. Pellet geometry

As it is strongly determined by used pellet matrice the variation rate of pellet diameter is low. Just elastic follow-up strain can be defined in diameter variation.

Pellet length brings information about the pelleting process and pellet quality. Cohesion of freshly produced pellets coming out directly from the pellet matrice is not always enough to resist the rough mechanical effects. This is why dust and fractions are generated spontaneously in pellet piles. Average percentage of pellet length and diameter (l/d ratio) characterizes a pellet agglomeration, which refers to the fragility too.

Tables *3.1* and *3.2* show results of pellet geometry measurements. As a consequence of increasing moisture content the diameter growths of outspring of the material is clearly observable. The impact on the pellet length of the humidity of the basic material is adverse as it reduces cohesion power. L/d ratio shows the same tendency as diameter growth variation is low compared to length reduction. Observably, particle size of grinds has no effect on the diameter, however in case of length it is not clean-cut. Icreasing particle size causes growth in length of 13mm pellets, but a decrement of length by 6 mm diameter pellets, as the l/d ratios reflect too. It ican be stated , that increasing moisture content causes growth of pellet diameter and reducement of pellet length, while particle size develops only by length, but contrasting in cases of the different pellet diameters.

Table 3.1 Average dimensions and l/d ratios of 13 mm diameter pellets

		Matrice hole diameter: 12,7 mm			
		Grinds particle size, mm			
		10	6	4	2
Moisture content, %		Average pellet diameter, mm			
	25	12,7	12,55	12,76	12,69
	35	12,93	12,84	12,98	12,87
	45	13,06	13,07	13,06	13,89
		Average pellet length, mm			
	25	18,73	17,75	16,87	16,33
	35	16,02	15,76	13,13	13,06
	45	12,74	12,98	11,44	12,01
		l/d ratio			
	25	1,47	1,41	1,32	1,29
	35	1,24	1,23	1,01	1,02
	45	0,98	0,99	0,88	0,92

Table 3.2 Average dimensions and l/d ratios of 6 mm diameter pellets

		Matrice hole diameter: 6 mm		
		Grinds particle size, mm		
		6	4	2
Moisture content, %		Average pellet diameter, mm		
	25	6,17	6,27	6,2
	35	6,33	6,26	6,24
	45	6,3	6,31	6,34
		Average pellet lentgh, mm		
	25	13,1	15,27	22,49
	35	7,95	9,93	13,15
	45	5	6,49	6,49
		l/d ratio		
	25	2,13	2,43	3,63
	35	1,26	1,59	2,11
	45	0,79	1,03	1,02

3.3. Material and bulk density

Material and bulk density show the size of required space of the material by transport and storage. For defining material density volume data was needed, which were assigned out of geometry analysis results. Mass data of the pellets were measured with a balance. Bulk density was measured using three different dishes.

Diagrams 3.3. and *3.4.* show the results of material and bulk density analysis. 6 mm diameter pellets, produced of 2 mm particle size grinds with 25 % moisture content have highest density, while 13 mm diameter, 10 mm particle size, 45 % humidity pellets have lowest volume mass. These results show, that increasing humidity reduces the material and bulk density. The same effect can be observed by decreasing particle size. The 6 mm diameter pellets have higher material density, but not always higher bulk density. By comparing volume mass data it is commonly perceptible, that in case of a high l/d ratio the bulk density reaches only near the half value of material density of the same sample.

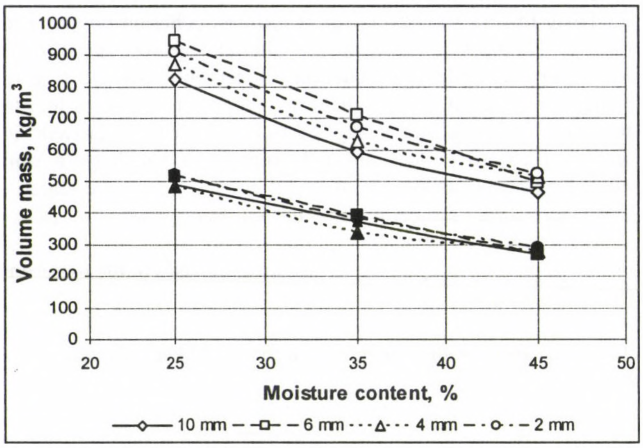

Diagram 3.3 Maretial and bulk density of 13 mm diameter pellets as a function of moisture content

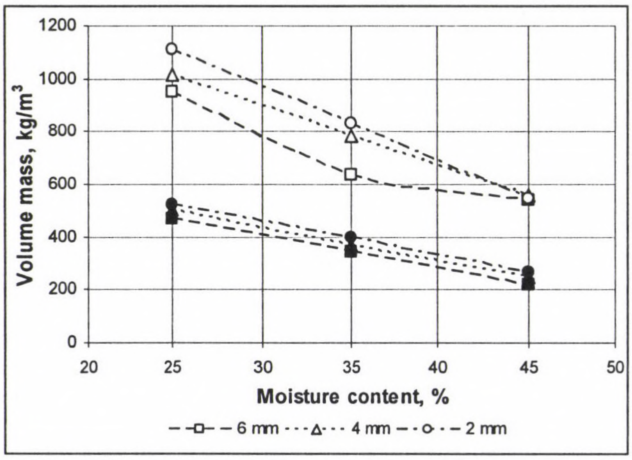

Diagram 3.4 Material and bulk density of 6 mm diameter pellets as a function of moisture content

3.4. Heating value and elementary composition analysis

Heating value and elementary composition test were conducted with automatic measuring units. In the elementary composition test were fixed N, C, S, H, O, Cl, ash and moisture content. Results of elementary composition test and heating value corrected with hydrogen and moisture content are shown by *table 3.3.*

It can be seen from the chart, that the average heating value of the measured corn stover pellet samples are as high as 15,5 MJ/kg, specified to volume: 17,7 MJ/m^3. These results show, that corn stover can be classed by heating value in the same category as firewood.

4. Conclusions

Analysing the results of durability, geometry, material and bulk density and energetic tests conducted with corn stover pellets the following conclusion can be drawn:

- Results of durability tests show, that the measured corn stover pellets have very good or good quality. Moisture content causes lower durability, while the greater particle size has not consistent impact on that.
- It can be seen that the pellet diameter grew if the humidity of grinds is high, because of elastic springing out of the material after coming out of the pellet matrice. Higher moisture content reduces pellet length, because decreasing cohesion and highest fragility of the material. Effect of particle size on geometry develops only by length.
- Increasing moisture content causes lower density. The effect of decreasing particle size results higher volume mass. Material density of 6 mm diameter pellets is higher than that of 13 mm diameter pellets, but tendency of bulk density data is not always the same.
- Larger hole diameter of pelletizing matrice reduces both material and bulk density, and pellet length, but with growing l/d ratio to higher material density is accompanied with lower bulk density.

Based on the results were shown before we have a plan to prepare new project in the following topics:

- Widening of corn stover pelletizing tests to pilot or factory scale, industrial technology, high-power machines.
- Tests of corn stover pellets produced with additives – adhesives, lubricants and burning process improving mateials.
- Investigation the effects to the physical-mechanical and firing characteristics of mixing with other agricultural by-products – rape or sunflower cake grinds.

5. References

[1] FVMMISZ 39-71-3-1-01 D95: Durability tests of feed pellets. Factory standard of the Hungarian Insitute of Agricultural Engineering. 2001.

[2] CEN/TS 15103: Solid biofuels – Methods for determination of bulk density. Technical Specification. 2005 CEN.

Table 3.3 Results of elementary composition and heating value tests of corn stover pellets

	N	C	S	H	O	Cl	H_2O	Ash	Ho	Hu
	%	%	%	%	%	%	%	%	MJ/kg	MJ/kg
Corn stover pellet 1	0,780	45,100	0,140	3,537	37,648	0,126	9,870	2,800	16,498	15,477
Corn stover pellet 2	0,770	45,300	0,130	3,571	37,632	0,137	9,760	2,700	16,450	15,424
Corn stover pellet 3	0,800	45,300	0,140	3,629	37,756	0,136	9,590	2,650	16,621	15,586
Average	**0,783**	**45,233**	**0,137**	**3,579**	**37,678**	**0,133**	**9,740**	**2,717**	**16,523**	**15,496**

BIOETHANOL FROM SWEET SORGHUM

Zsuzsanna LÁSZLÓ[1] - Sándor BESZÉDES[1] - Szabolcs KERTÉSZ[1]
Cecilia HODÚR[1] - Gábor SZABÓ[1] - Imre KIRICSI[2]
University of Szeged
[1]Faculty of Engineering, Department of Technical and Process Engineering
[2]Faculty of Sciences, Department of Applied and Environmental Chemistry

Objective

The vegetable oil and the vegetable alcohol are environmentally friendly motor fuels for replacing crude oil. These materials are usable as motor fuels alone or as fuel additives. The bioethanol can be used as petrol additive up to 20%, the optimal ratio of petrol:ethanol is 85:15. Generally the ethanol is produced from sugar or starch by fermentation with yeasts or bacteria, following by distillation. For ethanol production the raw material should contain sugar, starch or cellulose. The production of bioethanol is a very energy consuming process (e.g. concentration, distillation of alcohol), the energy balance of the conventional bioethanol process is negative. It means that the use of bioethanol as motor fuel could be cost effective only in the case of the permanent and remarkable increase of the price of crude oil, and/or in the case of using other alternative energy sources (e.g. wastes as raw material, biogas etc.) for bioethanol production.

In Europe the main raw material of bioethanol is the beetroot, wheat, maize, in North-America it is the maize and wheat, and while in South-America it is the sugar-cane. Beside these, ethanol can be produced from cellulose-containing materials, e.g. maize stalk, forest-products wastes, grasses or sorghum.

The sweet sorghum belongs to the grass family of *Poaceae*. The most important types of sorghum are *Sorghum vulgare var. technikum*, *Sorghum vulgare var. frumentaceum*, *Sorghum bicolor L. Sorghum vulgare var. Saccharatum*, *Sorghum vulgare var. Sudenense*.

The sorghum is a warm requiring plant, Hungary lies in the northern border of the sorghum culture area. The region of south Great Plain is appropriate for the sorghum culture, the yield is 80-120 t/ha, and even in weak soils (which are unsuitable for maize production) can be achieved 60-70 t/ha green mass [1]. Other authors give 47-52 t/ha annual yield for different types of sweet sorghum.

The juice content of sweet sorghum is in the range of 60-65% [2], and by others it is near 50% [3]. The sugar content of the juice is in 15-20% range. The anaerobic fermentation results in ethanol and carbon dioxide: the theoretical alcohol yield is 51% of the sugar content, i. e. 51 g ethanol can be produced from 100 g sugar. The commonly used yeast for ethanol production is *Saccharomyces cerevisiae*.

The aim of our work was to characterise two sweet sorghum varieties (Monori and Cellu) samples by sugar and dry matter content, and to determine the juice yield and the characteristics and self-life curve of the juice. The optimal conditions of fermentation, the ethanol yield were investigated also.

Methods and Materials

Two varieties of sweet sorghum (*Sorghum bicolor* var. Monori and Cellu) were investigated.

The particle size of sample was 0.5-2 cm. after chopping. The dry material content of the chopped sorghum, juice and bagasse were determined by drying at 105°C. The sugar content was determined by refractometer (BRIX%) and by spectrophotometrically, by means of 3,5 dinitro-salicylic acid method [4], after calibration. The juice extraction from chopped sorghum was carried out with a stainless steel screw-type extruder machine, the power of the engine was 750 W, the rotary speed was 50 1/min or 98 1/min. During self-life experiments 200 g chopped sweet sorghum or 200 ml freshly extracted juice was stored at 15, 20 or 25°C in a thermostat for 12 h. Before the fermentation the yeasts were pre-fermented aerobically, in a 200 ml juice-water mixture (50-50%), with 10 g dried selected yeast (*Saccharomices cerevisiae*), at 38°C during 30 min. This pre-fermented yeast culture was used for anaerobic fermentation at 6.25% concentration. In the case of experiments carried out with non-selected Baker's yeast the concentration of yeast were 0.85, 1.25 or 1.67 m%. The anaerobic fermentations were carried out in a 500 ml continuously mixed fermenter, the temperature was either 20 °C or 30 °C. The duration of anaerobic fermentation changed between 24-72 h. The pH was adjusted to 4.5 with 1 M H_2SO_4 solution. In some cases yeast nutritive was added, containing 1 mol/dm^3 diammonium-hydrogen phosphate (DAP) and 3 mol/dm^3 urea. Investigating the effect of cellulase enzyme for the juice fermentation, 15 µl of cellulase enzyme (Cellulast 1.5L, Novozymes A/S, Denmark, 700 U/g) and 15 µl of β-glucosidase enzyme (Novozym 188, Novozymes A/S, Denmark, 250 U/g) were added to 400 ml juice.

The distillation of fermented juices was carried out in two steps, the alcohol content of the second fraction was determined by a refractometer and a gas chromatograph (Agilent 6890N-5976 GC-MS).

Results and Discussion

In the first series of experiments the characteristics of sweet sorghum varieties were determined.

Table 1. Sugar content and juice yield of different parts of sweet sorhum varieties

	Monori		Cellu	
	Juice yield	Sugar (m%)	Juice yield	Sugar (m%)
Chopped raw material	66.3%	12.0	61.8%	12.8
Leaves	52.3%	10.5	50.7%	10.3
Truss	31.4%	10.6	29.4%	8.5

The results show that the juice yield was higher in the case of Monori sample which can be explained by the less fibrillar structure of this sorghum variety, because the difference of the dry matter content could not cause this difference. The juice yield from leaves or truss was less, than from chopped whole plant, but the difference (concerning the mass ratio of these parts in the chopped material) was not so large, it did not give grounds for the separation of the different parts of plant.

In consideration of the extremely high microbe count of sweet sorghum, during our work the most important aspect was to minimize the loss of sugar, so the change of sugar content of harvested sorghum and juice was followed. The chopped samples were stored aerobically, at 20°C, and the sugar content of freshly pressed juice was measured in every 2 hours. The Fig. 1. shows that the sugar content both in the chopped material and in the juice decreases very rapidly, in absence of any preservation. This loss of sugar content is more than 50%. The measurements were carried out at 15°C and 25°C, in these cases the decrease of sugar content did not differ significantly from the results received at 20°C .

In the next series of experiments the alcohol yield of sorghum by use of different yeasts were investigated: wild yeast (natural flora of squeezed juice), non selected Baker's yeast (*Saccharomices cerevisiae) and* selected *Saccharomices cerevisiae* (T22 and F).

The results showed that the self-fermentation is considerable. Similar ethanol yield (30 %) was observed using either selected yeasts or Baker's yeast, but the amount of microbes was much smaller in the case of selected variant, and the yeast concentration did not affect the alcohol yield. In order to get comparable results, the next series of experiments were implemented with 0.3% selected *Saccharomices cerevisiae*.

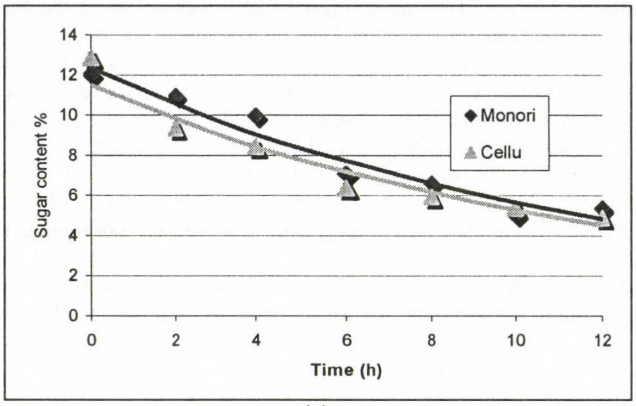

(a)

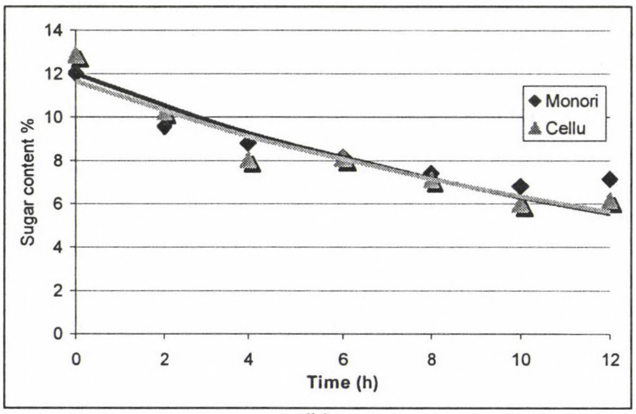

(b)

Figure 1. ***The change of sugar content of chopped sweet sorghum (a) and the juice (b) at 20°C during aerobic storage***

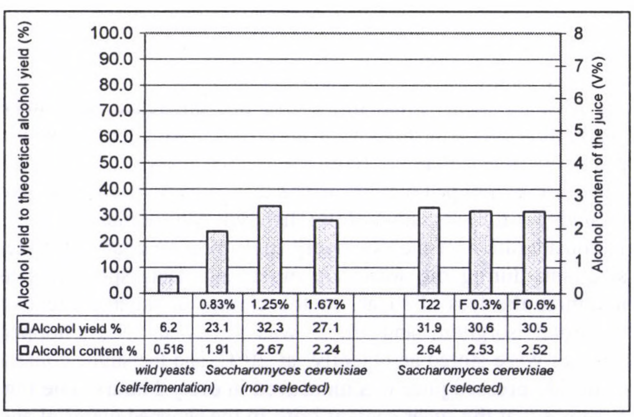

Figure 2. ***Alcohol content and alcohol yield to theoretical yield of fermented Cellu juices, the fermentation temperature was 20°C, with different yeasts applied in different concentration***

After the fermentation the product was twice distilled, and the composition of the alcohol fraction was analysed by a GC-MS. Besides the ethanol, a little amount (less, than 1% of the total alcohol content) of methanol, propanol and acetaldehyde was detected by using of Baker's yeast. In the case of selected yeasts, the ethanol did not contain any impurities.

In the next series of experiments the effect of fermentation temperature and the amount of added nutritive on the alcohol yield were examined (Fig. 3.).

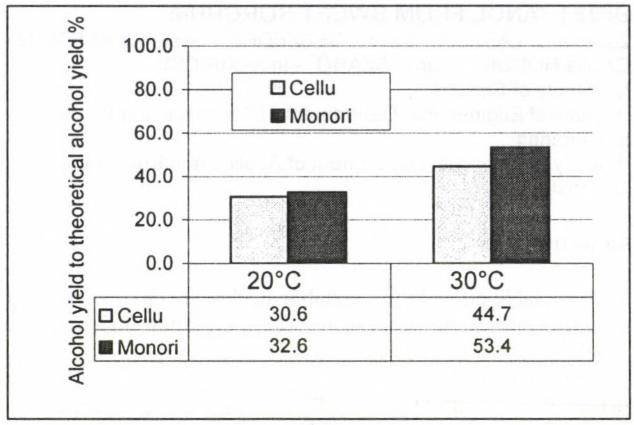

(a)

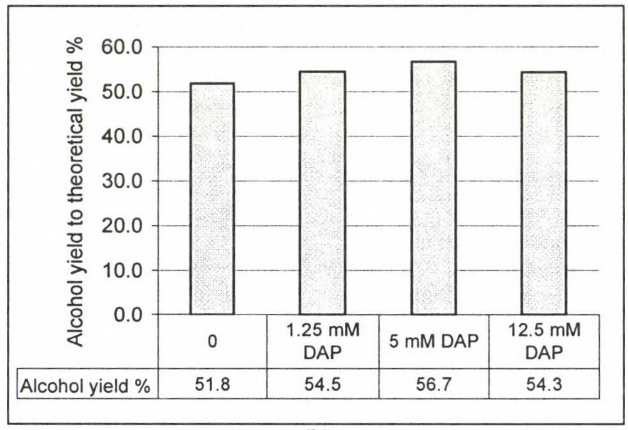

(b)

Figure 3. ***The effect of fermentation temperature (a) and the amount of added nutritive (b) on the alcohol yield/theoretical alcohol yield ratio***

It was found, that the alcohol yield was higher in the case of Monori both at 20°C and 30°C as well. The fermentation at 30°C produced significantly higher alcohol yield (45-50%) during 24 h fermentation time. Examining the effect of nutritive on the alcohol yield, the pH was adjusted to 4.5, and DAP was added to the samples in different concentrations. The results showed, that the DAP caused only a little increase in alcohol yield. The optimal concentration of the DAP was 5 mM.

It was examined, that the alcohol yield could be enhanced by adding cellulase or glucosidase enzymes, regarding that the juice contains a lot of filamentous, floating material. On the basis of lignocellulose content of the juice, the theoretical alcohol yield increase is about 10%. (Fig. 4.)

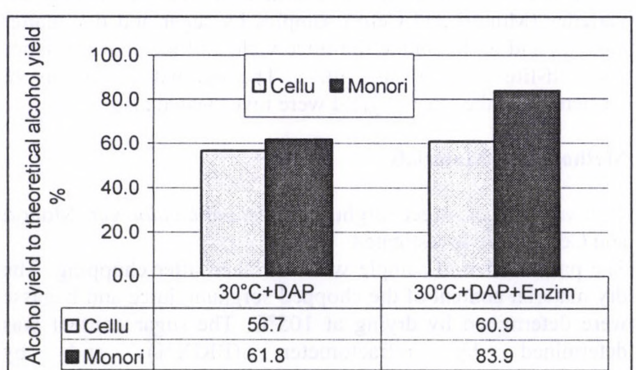

Figure 4. ***The changes of alcohol yield by addition of cellulase and β-glucosidase enzymes during fermentation at 30°C, pH=4.5, 5 mM DAP, 24 h***

Comparing the alcohol yield from sugar only, and from sugar and lignocellulose by addition of enzymes, it was found, that the addition of enzymes considerably enhances the alcohol yield, more than it is expected theoretically on the basis of lignocellulose content, in the case of Monori instead of 60% to about 85%. It can be explained if we consider that the enzymes took part of the glucose production instead of other reaction pathways.

Conclusions

In this work the amount of fermented alcohol from sweet sorghum juice was determined, and the effect of operation parameters on alcohol yield was investigated. The juice was not pre-treated or filtered. It was found, that the maximal (theoretical) alcohol yield could not be achieved, but it can be enhanced by optimization of fermentation parameters, and adding enzymes to the juice.

Acknowledgement

The authors are grateful to the National Research and Technology Institute (NKTH) and the Research and Development Competition and Research Utilization Agency (KPI) (RET-07/2005).

References

[1] Sándor Kocsis: „Megújuló energiaforrások II." Gépészet VII.(2), 2003.

[2] Gnansounonou, E., Dauriat, A., Wyman, C.E.: „Refining sweet sorghum to ethanol and sugar: economic trade-offs in the context of North China" Bioresource Technology 96 pp. 986-1002. 2005.

[3] Mamma, D., Christakopoulos, P., Koullas, D., Kekos, D., Macris, B.J., Koukios, E: „An alternative approach to the bioconversion of sweet sorghum carbohydrates to ethanol" Biomass and Bioenergy 8(2) pp. 99-103, 1995

[4] Élelmiszeranalitika, Ed: Lásztity Radomir, Törley Dezső, Mezőgazdasági Kiadó, Budapest, 1987.

SORGHUM LIKE A BIOGAS INCREASING ADDITIVE

Imre KALMÁR - Eszter KALMÁRNÉ VASS - Emese SZABÓ - Valéria NAGY
Szolnok College Technical and Agricultural Faculty, Mezőtúr

1. Objectiv

The views of multifunction agriculture, which aim at increasing the rate of non-food production apart from the function of food and fodder production, have appeared in the agriculture policy of the EU. The EU has prepared directives towards the gradual increase of the utilization of environment friendly and renewable energy resources, which accordingly determine the guiding values for each member state on the basis of the results to be reached till 2010, taking into account the divergence in the energetic, social, political and technical relations of those. The Technical and Agricultural Faculty of Szolnok College has been dealing with environment protection researches, including waste utilization and biogas production technologies for over a decade. Our earlier experiments have certified that biogas production takes form spontaneously from pig thin manure even without any additive. When we applied continual industrial technology, the intensity of gas development independent of the microbiological treatment increased to a great extent as well. The intensity of gas production or the quantity of the originating methane in harmony with this did increase accordingly.

The objective of the application of additives in our earlier experiments was in the first place the utilization of wastes used as admixture. However, we chose such vegetation additives, i.e. biomass plants for energetic biogas production, which can be economically cultivable as renewable energy resources taking into account the agro-ecopotential of the region, the development conceptions of the agrarian sector and of environment protection as well as the results of the researches so far or can secure the raw material need of biogas and ethanol producing plants on this base throughout the whole year.

Among these utilizable objective plants is the Sorghum too, as a possible biogas yield increasing additive. The biomass yield of Sorghum types cultivable in our country is 80-85 t/ha green mass; their sugar content is about 13-17%; their cultivation technology is relatively of low energy need; they are draught resisting and are well cultivable in more poor productive land.

Our objective is to certify that various co-ferments with the aid of experimental fermentor system representing the industrial circumstances in our laboratory experiment series – depending on the added Sorghum type or organic dry material content – increase the quantity and methane content of the produced biogas in different degrees, too.

2. Methods and materials

We performed our experiments in a specially self-developed laboratory within the frame of Ányos Jedlik programme number NKFP3-00006/2005: *"Complex, connected heat- and electrical energy production technology based on biomass"* (***Figure 1***). We can contribute to the preparatory work reducing the risk of realisation, to the work serving as the base for the establishment of domestic biogas workshops with laboratories including the formed experimental fermentor system.

We can contribute to preparatory work reducing the risk of realisation, to the work serving as the base for the establishment of domestic biogas workshops with laboratories including the formed experimental fermentor system.

During the comparative experiments we modelled the continued biogas producing technology in the fermentors under mezophyl conditions. Continuities were performed daily in conformity with the determined proportion of 50 dm^3 fermentors. 14-21 days of average retaining time were allowed during the quantity to be emptied or continued. ***Table 1*** summarizes the course of the experiments.

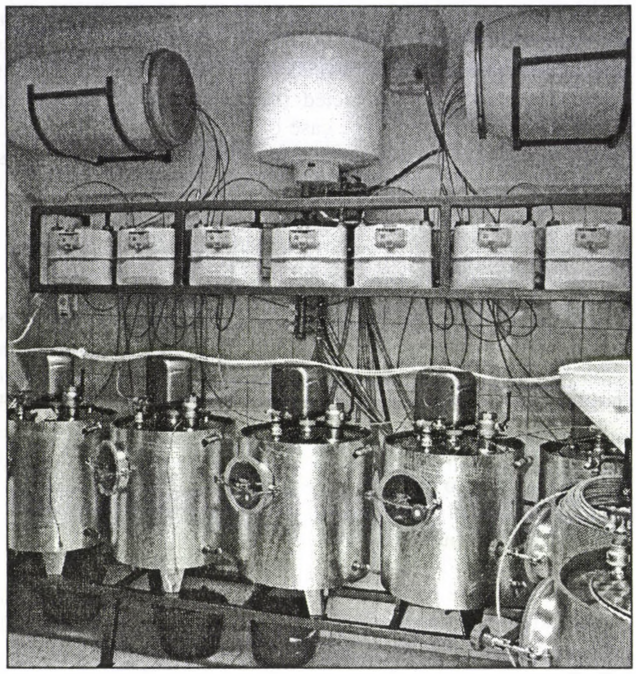

Figure 1 Further improved fermentor line

Table 1 Experimental processes

No	Process period	Time period [day]	Manipulation per fermentors			
			1. control	2. Sorghum (Berény)	3. Sorghum (Sucro-sorgho)	4. Sorghum press residues (Berény)
1	Homogeneity	3-7	Similar conditions, homogeneity of input materials			
2	Stabilization	14-21	Refilling of basic materials, securing similar starting conditions for comparison			
3	Comparison	14-42	Combination of manipulation, continuous operation			
4	Fermentation	14-28	No manipulation, periodical operation			

Adjusted to the industrial conditions, the dry material content of the fresh thin manure was 4% and 3.25% of organic dry material. In order to increase the dry material content we added Sorghum ripped at different times and of different sugar content to reactors 2 and 3. Press residues with low sugar content that remained after the pressed Sorghum were added to reactor 4 for ethanol production, thus increasing the dry material content of the reactor by this. The sugar content of Sorghum ("Berényi") to be added to reactor 2 in the period of the experiment was 10%, the sugar content of the type to be added to reactor 3 ("Sucrosogho") was 8%, while the press residues of "Berényi" type went into reactor 4.

During the experiment we measured the quantity of the input basic materials and additives, the content of the dry substance as well as the intensity of gas production, the quantity and component of the produced biogas by following the traces of changes taking place during decomposition. The results achieved on the course of the instrumental measuring were evaluated in the function of the set parameters.

3. Results

The production of biogas and methane in relation to the input organic dry substance was the following: the production projected on 1 kg of organic dry substance in the control fermentor was the least, while most of the biogas and methane gas was developed specifically by adding high sugar concentrated whole Sorghum biomass in the fermentor. Besides the 55-57% of methane content typical of the control reactor

(*Diagram 1*) 117 dm³ was the specific methane production (*Diagram 2*) projected on 1 kg of dry organic substance.
The gas production of the control reactor having been examined, it can be concluded that in the given period much less biogas was produced, projecting on 1 dm³ of the volume of the fermentor, than the other two biomass based on pig thin manure. In many cases it did not even reach half of the biogas production of the manipulated reactors.
In the function of the added Sorghum types less-greater divergence was experienced during the continued experimental period. The methane production of the reactors is divergent, the reason of which can be looked for in the diverse ripe states and different sugar concentration of the types. They brought forth divergences in the constituents of biogas. Nearly 40% more biogas was produced by the addition of ("Berényi"), a high sugar concentrated Sorghum type in projection to the unit fermentor volume of the reactor than the Sorghum ("Sucrosorgho") with low sugar concentration.

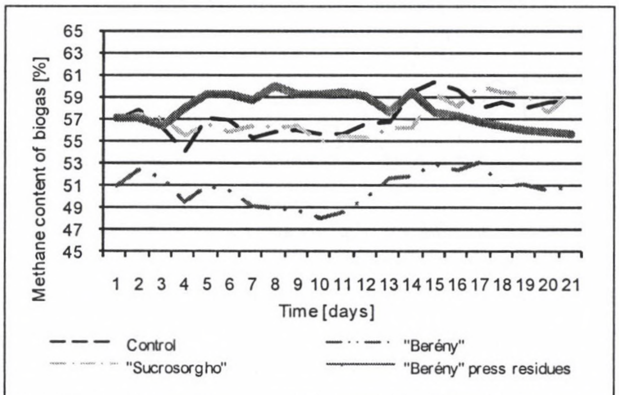

Diagram 1 The formation of the originated methane from the biogas in the comparative experimental periods

Similar Sorghum ("Berényi") were put in fermentors 2 and 4. The ("Berényi") biogas production of the reactor that received the whole harvested plant biomass was nearly 20% higher than that of the reactor possessing such press residues –("Berényi" press residues) – that no longer possessed easily decomposable sugar. There were differences in the constituents of the produced biogas by the two reactors, because ~5% less methane biogas was produced in the fermentor that received the "Berényi" sorghum type than in the remaining reactors (*Diagram 1*).
There is no further great difference in the methane production of the fermentors that receive additives – due to different composition – as is in the biogas yield (*Diagram 2*).

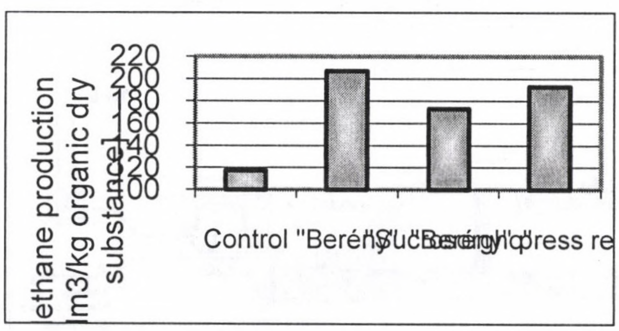

Diagram 2 Specific methane production of fermentors during the comparative experiments

The methane production of the fermentor that receives lower sugar concentration "Sucrosorgho" and the "Berényi press residues" is one and a half times great as that of the control fermentor's (*Table 2*).

Table 2 Gas production of the fermentors during the comparative experiments

	Specification of the examined indices	Control	„Berény"	„Sucro-sorgho"	„Berény" press residues
Specific	biogas production dm³/kg organic dry substance	206	408	303	348
	Methane production dm³/kg organic dry substance	117	207	173	193

4. Conclusions, suggestions

A great quantity can be produced on unit area relatively, from different sorghum types compared to the biomass varieties. Owing to the results of our production experiments on biogas, it can be established that sorghum may be a promising source of energy in the future, with which the fossil energy carriers will be produce-able to a certain extent. Respectable quantity of biogas suitable for renewable energy production develops from totally green plants and even from the press residues. The advantage of the utilization of sorghum as energy plant is that the pressed liquid can be used for the production of ethanol, which can be utilized directly as propellant, or, out of which electrical energy can be gained by the implication of energy modification.
The rate of the utilization of renewable energy may increase in our homeland on the influence of our experimental results, and the de-concentration of energy production will become feasible, which will reduce our dependency on foreign energy suppliers. There may also be an increase in the security of energy supply for the population and the economy. Changes in the agricultural product structure may be realised and safeguarding workplaces in the rural regions that are lagging behind or the establishment of new workplaces, which may significantly contribute to bridging the rural regions falling behind in the present difficult hard times, will become feasible as well.

References

[1] Bai A.: A biogáz előállítása – Jelen és jövő. Szaktudás Kiadó Ház, Budapest 2005.

[2] Lehtomaki, A. – Huttunen, S. – Rintala, J. A.: „Laboratory investigations on co-digestion of energy crops and crop residues with cow manure for methane production: Effect to manure ratio", Resources Conservation and Recycling 2006., p 1-19

[3] Kalmár I. – Kalmárné V. E. – Krizsán J.: A sertéshíg–trágyából kinyerhető biogázmennyiség fokozására irányuló kísérleti eredmények. III. Alföldi Tudományos Tájgaz–dálkodási Napok. Mezőtúr, 2002. p 51-57

[4] Kalmár I. – Kalmárné V. E. – Szabó E.: A sertéshígtrágya, mint megújuló energiaforrás. A megújuló energiák kutatása és hasznosítása az Észak-Alföldi Régióban. A Magyar Szélenergia Társaság Kiadványai No. 2., Debrecen 2003. november 24.

[5] E. V. Kalmár – I. Kalmár – I. Balogh: Experiments with bacterium manipulated thin manure. IAMFE/RUSSIA The 12th International Conference and Exhibition on Mechanization of Field Experiments, Saint-Petersburg 2004, p148-152

[6] Kalmár I. – Nagy I.: Kapcsolt bioetanol és biogáz előállítás „Jedlik Ányos" projekt. Energiagazdálkodás 47. évf. 2006. 1. szám 22-24 p.

[7] Kalmár I. – Nagy V. – Vásárhelyi L.: Laborfejlesztés K+F projektek növelt léptékű biogáz hozamfokozási kísér–leteihez. Előadás, V. Alföldi Tudományos Tájgazdálkodási Napok, Mezőtúr 2006., CD kiadvány

[8] Schulz, H. – Eder, B: Biogázgyártás; CSER Kiadó, Budapest 2005.

QUANTITATIVE AND QUALITIVE ANALYSIS OF THE BIOGAS PRODUCTION FROM THE MUNICIPAL SOLID WASTE

Tamás MOLNÁR[1] - László SALLAI[2] - Dezső FODOR[3]
[1]University Szeged Agriculture Faculty Science of Animal Nutrition and Engineering Institute, Hódmezővásárhely
[2]A.S.A. Ltd.Hódmezővásárhely
[3]NRG-AGENT Ltd Kecskemét

1. Introduction

With the growing number of man and with the development of technology the amount of waste is increasing. We must take care of waste management in order to protect the environment. When storing waste material there are two harmful factors. One is the fluid (percolating water) coming out of the waste and pollute the soil and the other is the methane gases from decomposed organic materials, which cases glasshouse effect and thus global warming. The problem of biogas from the decomposition of communal waste got into the focus of attention since it was proved that on the Earth the natural and antopogen methane and the carbo-dioxide emmission contribute to the so-called glass-house effect. As fossile fuels are finite and environment pollutant the attention turned to the exploration and exploitation of other alternative energy sources like for instance the bio-gas. Through the exploitation, collection and utilisation of the deponia gas obtained this way we can create an environment-frienly position. There would be a demand for the optimal utilisation of biogas on the refuse dump where both thermal and electric energy production might be possible electric energy law offers a favourable possibility, which can enhance the development in this field.

1.2. Anaerob waste management

Anaerobes (facultative and obligate) break down organic matter by fermentation without the presence of oxygen. These microorganisms use organic-bound carbon compounds as oxygen-acceptors and the biogas created in this way might contain up to 40% of CO_2. The degradation of the organic matter and their transformation into methane takes place in several steps. The various stages of the degradation is done by the organisms in the food chain, thus they are in close connection depending on each other

Table 1 The steps of organic matter degradation

	Type of process	Type of bacteria	Raw materials	Product
Stage 1.	hydrolysis	fermented	proteins, carbohydrates, fats	amino-acids, sugars, fatty acids
Stage 2.	acid formation	fermented	amino-acids, sugars, fatty acids	organic acids, alcohols
Stage 3.	acetic acid formation	acetogen	amino-acids, sugars, fatty acids, organic acids, alcohols	acetic acid, hydrogen, carbon dioxide
Stage 4.	methane formation	methanogen	acetic acid, hydrogen, carbon dioxide	methane

1.3. The degradation and transformation of organic matter

During hydrolysis fermenting bacteria decompose polymer compounds, carbohydrates, proteins and fats with exoenzymes. Both obligate and facultative anaerobe organisms take place in the procedure. In the second stage organic acids, alcohol, hydrogen, carbon dioxide, ammonia and hydrogen sulphide are produced from the monomer compounds. Further decomposition processes are carried out by acetogen and metanogen bacteria living in symbiosis. Out of the products of the second stage metanogen bacteria can use only acetic acid, hydrogen and carbon dioxide to produce methane directly. During the fermentation methane is produced from organic matter. The maximum amount of methane gas that can be produced depends on the composition of the organic waste materials (table 2.) In practice the realistic gas yield is approximately 300–600 l fermentation gas/kg organic dry matter with 50-70% of methane content. During fermentation 40-85% of the organic matter is decomposed.

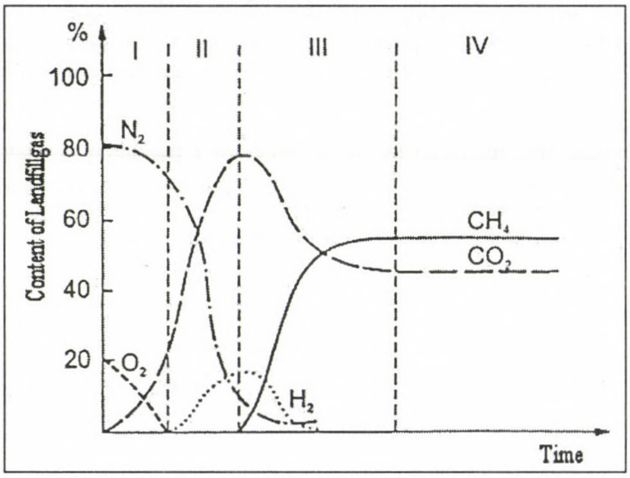

Figure 1 Landfill gas (deponia gas) components in the various stages of fermentation

Table 2 The maximum gas yield from various raw materials

Raw material	Gas yield (l/kg d.m.)	Methane content (volume %)	Heating value (Hu) (kJ/Nm³)
Carbohydrate	900	50	17 800
Protein	700	70	24 900
Fat	1 200	67	23 700

2. Materal and method

2.1. Place of egzamination

The Hódmezővásárhely refuse Ltd.'s communal solid refuse unloading place works in the outskirts of Hódmezővásárhely on the area No. 01957/1. The nearest dwelling house is far away (2500m). The refuse dump of Hódmezővásárhely is situated 20 ha and the top height of deponias are 30m.

2.1.1. The elements of deponia gas extracting system (Figure 2)

Gas well⇒Gas collecting pipes⇒Gas controller unit⇒Compressor unit⇒Torch

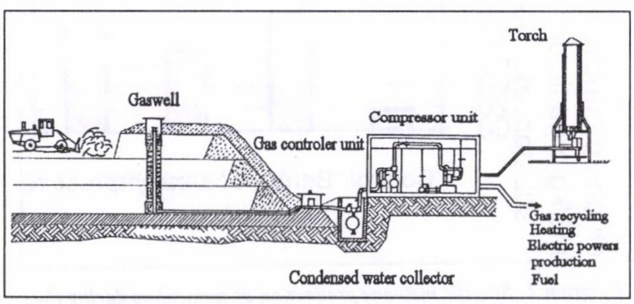

Figure 2 Process figure of gas production[2]

2.2. The way egzamination

To carry out the examinations on the biogas quality and quantity on the refuse dump I have a computer data collection system, container measuring equipment and a gas-motor container .

2.2.1. During the examination I plan to measure the following parameters:

Vacum [mbar]

- Pressure[mbar]
- Methane content of biogas [%]
- Oxigen content of biogas [%]
- External temperature [°C]
- Inletgas temperature [°C]
- Momentary gasproduction [m^3/h]
- Total gasproduction[m^3/h]
- Tempeature of waste gas [°C]
- 1 Compressor [operation time]
- 2. Compressor [operation time]
- Danger register [%]

3- Results

3.1. Communal waste biomass potential in the Hódmezővásárhely micro-region

According tho the analysis based on the MSZ 21976 standard to determine the biologically degradable organic-material-content of the communal waste we can state that 53% of the collected total amount (14.441,965 tons) of solid communal waste that is **7.654,24 tons** can be considered biologically degradable and in this way it is biomass potential.

***Table 3** Energy utilisation of the communal waste*

Settlements	Biomass potencial [t]	Utilisable biogas quantity [m^3/t]	Produced biogas [m^3]	Biogas calorific value [MJ/m^3]	Potential thermal energy [MJ]**
Hmvhely	6488,5	256	1.661.056	21,5	35.712.704
Mindszent	826,36	256	211.456	21,5	4.546.304
Mártély	151,04	256	38.666,24	21,5	831.324,16
Székkutas	188,34	256	48.215,04	21,5	1.036.623,36
Micro-region **	1500	190	285.000	21,5	6.127.500
Összesen	**7.654,24**	**256**	**2.244.424**		**48.255.116**

**biogas quantity of the organic communal waste*
256l/kg=0.256 m^3/kg=256 m^3/t
total of green waste from the territory of the micro-region, approx.* ***1500 t

The above table shows the communal waste produced and generated in Hódmezővásárhely and in the micro-region and the biomass potential and biogas yield produced from it in the year of 2006. According to the table the amount of biogas produced from the wase is 2.244.424m^3. In my calculation I took into account the most favourable biogas yield. From these values we can see that the estimated gas yields in the literature are different from the measured data

3.2. The amount of biogas in the landfill

According to theoretical calculations and depending on the constitution of the waste when the amount of the rubbish is between 40-300 m^3/t an average of 2-3 m^3 /t biogas can be produced annually.

3.2.1. Rettengerger formula

The amount of biogas can also be estimated with formulas, for instance

$V_t = 1.868 \times C_O \times (0,014 \times v + 0,28) \times (1-10^{-kt})$ where

V_t = the specific biogas volume in m^3/t waste, which is produced in *t* time,

C_O = the organic carbon rate of the waste kg/t

v = temperature °C

k = degradation constant (-)

t = time, in years

Usable empirical values are:

C_O = 200 kg/t v = 35 °C k = 0,035

3.2.2. Dr.Weber-Dr.Doedens model

$Qat=1,868*M*TOC*fao*fa*fo*fs*k*e^{-k*t}$

3.2.3. Rettenberger/Tabasaran model

$Gt=1,868*TOC*(0,014T+0,28)*\_ab*\ \_f*\ \_M*(1-10^{-k*t})$

3.2.4. Stachowitz estimation

T(O)C organic carbon content:~200 kg/t

Gm amount of gas:~260 m^3/t

3.3. The amount of biogas produced in the landfill

When calculating the amount of biogas produced in the landfill we can consider a maximum of 3.900.000 m^3 waste. In theory the amount of biogas according to Tabasaran/Rettengerger is

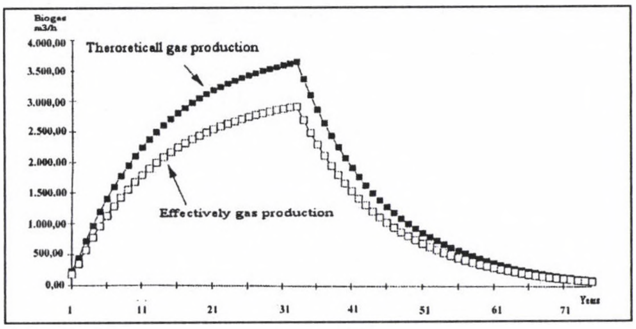

***Figure 3** The amount of biogas produced in the landfill*

When calculating I considered the most favourable biogas yield. From these values we can see that the gas yields estimated on the basis of the literature data are different from the measured gas yields.

***Table 4** The results of one measurement as an example*

The time of the measuring 2005.06.24	Volume [%]	**On the basis of the mesured data the biogas**
methane	60%	88 m^3/hour
carbon-dioxid	26,2%	2112 m^3/day
oxygen	2,4%	770880 m^3/year
nitrogen	11,4%	

**ASA Hodmezovasarhely Scavenger Ltd.*

4. Conclusions

On the refuse dump of Hódmezővásárhely originating biogas can be recycled for heat production and energy production.

4.1. The recycling of the electritical energy

The orinating biogas in the refuse dump of Hódmezővásárhely is burnt up in gas engine. Because of this heat energy and electritic energy originate (Figure 3)

- We have to choose whether we will produce as much power as we can use for our own aim or we will produce as much as we can do and we can install the plus power into the electrical system.
- The islands works have some advantages that we are indepedent of the national electric power system. The operation isn't influenced by neither a rise in prices nor quantity regulations.,
- In case of parallel works we can produce as much power as the biogas can make possible and we can sell the surplus for the energy service.

The surplus eletric power:

- Local electric service called DEMÁSZ Ltd. has to buy the energy power which we can't use inside the works.

References

[1] **A.S.A. Hódmezővásárhely Köztisztasági Kft.**: Maroslelei úti hulladékdeponáló és kezelő létesítmények üzemeltetési utasítása. Hódmezővásárhely, 1995

[2] **A.S.A. Hódmezővásárhely Köztisztasági Kft.**: A hódmezővásárhelyi hulladéklerakó telep környezeti hatástanulmánya. Hódmezővásárhely, 2000

[3] **BARÓTFI, I.: Környezettechnika kézikönyv**. Mezőgazda Kiadó, Budapest: 2000.

[4] **MOLNÁR T., SALLAI L., BARNA V., KISS K.** Energetikai célú biomassza-potenciál vizsgálata a Hódmezővásárhelyi kistérségben. SZTE-MGK Hódmezővásárhely, 2007

Table 5 The data of the cogeneration power plant

The electric power of a block			160 kW
Rated voltage of the generators			400 V
2 blocks to be built in the first step			320 kW
1 block to be built in the second step			160 kW
Produced electric power in full establishment			480 kW [3 blocks]
Produced electric power used up by the branch work			max. 10 kW.
Electric power in the first step			300 kW
Electric power in the second step			450 kW
The data of the cogeneration power plant			Yearly
Gas consumption	m^3/óra	45,5	
Total efficiency	%	85	
Calculated annual length of time	%	95	350 days
Calculated daily length of time	hours	24	8400 hours
Gas consumption	m^3/day	165	57750 m3
Gross electric power	kWh/day	3840	1.344000 kWh
Electric power for sale	kWh/day	3450	1.207500 kWh

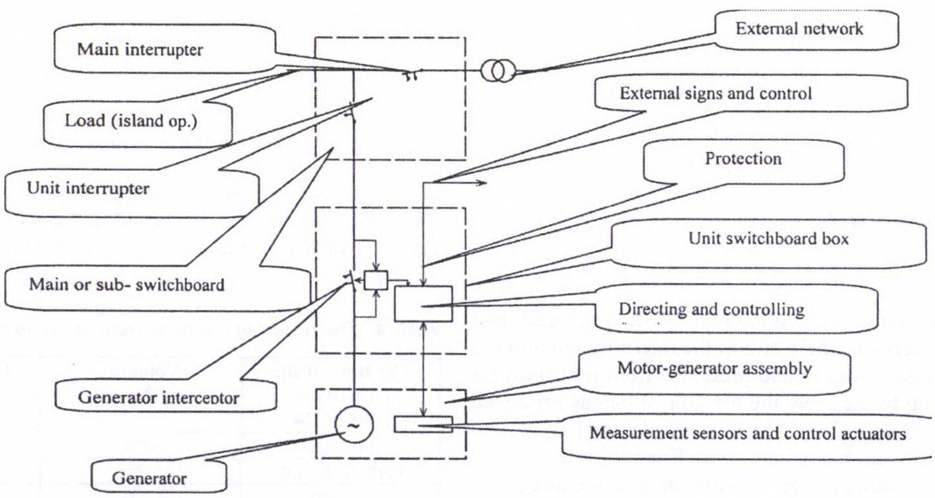

Figure 5 Instalation of cogenerational power station

ECONOMIC EVALUATION OF SCALING OF AGRICULTURAL BIOGAS PLANTS*

Attila BAI - Gábor GRASSELLI - János SZENDREI - Szilvia KORMÁNYOS
University of Debrecen, Centre for Agricultural Sciences and Engineering

Introduction

Biogas production enjoys a special position among renewable energy processes, because of the variety of products achievable (biogas, "bio-natural gas", electricity, carbon dioxide, domestic hot water, fuel, bio-manure). Among these, market of "green" electricity and bio-natural gas is assured by the government – under conditions varying in time and space. In an indirect way, also the regulations on the treatment of municipal organic wastes and manure from animal breeding promote the spreading of biogas plants. In Hungary, the most important preliminary for successful operation of agricultural biogas plants is the economy of the animal breeding division that supplies the input materials. Profitability of biogas production lies namely not only in the produced goods, but also in the maintained profitable operation of the division that would be environment pollutant without biogas production. On animal breeding plants with unprofitable or in the long term insecure operation such an investment is not to be started and granting it is needless.

Plants based on the principles of economy of scale are capable of profitable operation, on the one hand, and to fulfill the (environmental) authorities' regulations, on the other hand. Since further spreading of biogas technology is hindered primarily by the height of investment costs, scaling of a biogas plant and its equipments is a key factor in successful operation. At the same time, scaling of the plant also determines the scope and economic indicators of producible goods. The aim of this article is to answer the question, what principles are to be followed in the scaling of the facilities, what goods are to be produced and what other activities are advisable.

1. General principles on scaling

Continuous operation and full deployment of the capacities can be achieved only with proper scaling of equipments. In the course of this, the first step is to *estimate* the amount of the input materials, then to determine volume of the digesters based on the length of the digestion (20-40 days), temperature of digestion (35-55 °C) and organic matter load (2-6 kg/m^3). In digesters, reduction of retention time is followed by a decrease in gas production, which can be prevented by increased heating of the digesters. Amount and quality of the biogas produced determines the required size of utilization equipments (boilers, gas engines and gas cleaners). Gas storage equipments – including the space above the materials fed in the digester – must have a storage capacity of the biogas volume produced in a few hours. This can be multiplied with compression. However, excess quantity above this level has to be eliminated by a torch.

Available land area determines the size of a plant both in terms of dimensions and economy. According to rules in force, max. 170 kg/ha N-content is applicable in fertilizing, so the amount and N-content of the manure digested requires an agricultural area adequate to this. Beside this, also irrigation capacity limits to a certain extent the (liquid) manure quantity that can be spread out at low costs. In the winter months, the bio-fertilizer must not be spread out, therefore it needs a 3-4 months' storage capacity. Another solution is to concentrate a part of the manure, or to produce solid bio-manure through drying.

To sum up, an ideal biogas plant is capable of direct utilization of produced biogas and bio-manure, or continuous trade of them (after further processing). At equal expected electric capacity, higher gas content of the input materials and/or higher temperature of digestion reduce the required digester capacity, and through this, the investment and operation costs. Risks of problems arising from accidental breakdowns can be reduced through the application of several smaller digesters, whereas efficacy of waste decomposition can be enhanced with the increase of temperature and duration of digestion. Especially beneficial is when a trigeneration working scheme can be applied. In this case, additional heat stream generated besides electricity can be applied for heating in the wintertime and to operate absorption chilling equipment running on hot water for cooling/air-conditioning in the summer.

2. Aspects of output and input utilization

Utilization of biogas for heating (buildings and greenhouses) can be considered only at lower capacities. High capacity demands (e. g. drying) occur only temporarily, therefore heat utilization at middle-sized and large plants need foresight. However, trade of electricity produced with cogeneration is assured and at cogeneration plants it has a deciding share (54-58 %) in the revenue. Waste heat with a value of 33-36% serves at about 30% the heating of the digesters. To utilize the remaining amount is a key issue. Because of unbeneficial changes in electricity take-over regulations, another guaranteed marketable product can became attractive, the transformation to bio-methane. Share of bio-manure is of little importance (cca. 9%), however – in max. 170 kg/N dose – this can be fully utilized for own purposes, or – after processing – for sale.

To entirely deploy capacities or to the optimal scaling large plants may need to engage in processing off-farm inputs for payment. The uncertainty of availability of these inputs can be reduced with long-term contracts. Extra costs of *waste elimination* are considerable, however, in this case also the revenue of waste handling, the heterosis-effect arising from multiple input materials, and the sinking of overhead costs per unit product apply as a great benefit. Minimum size of waste elimination varies due to different input materials and market conditions, however, this is difficult to operate in an economic manner under 25-30 thousand m^3/year. Large size is desired also from technology aspects, since safe digestion favors longer digestion time, and two-phase – mesophil and thermophil – system. Environmental concerns can include strong odors at the beginning of the digestion, and presence of ammonia-nitrogen, soluble sulfides and heavy metals. In conclusion, to exclude off-farm inputs cannot be the aim of a biogas plant, only minimizing risks coupled with it is advisable. Revenue from waste management is hard to estimate, since environmental regulations are strengthening, but the amount of inputs to be handled is decreasing, whereas the number of companies dealing with it is increasing, so a *supply-dominated* market is in formation.

3. Base data for model investigations

In the investigations, six models with different sizes were examined for heat production and cogeneration. Among these, models 1-5th were based on an input mixture of two-third pig and cattle manure and one-third silage, with 16% dry matter content. The 6th model is based on cca. 50% liquid manure, one-third manure with litter, and the rest made up mainly of corn silage, with 15% dry matter. The 1st and 3rd models are based on actual German plants' data, the 2nd, 4th and 5th on average of German plants' data, whereas the 6th model on the data of one of our newest reference plant. The latter model uses two-phase (mesophil + thermophil) digestion, while the smaller plants use one-phase mesophil technology. The small plants (1st , 2nd model) use Diesel engines with fuel injection, the electric efficacy of which is 4-5% lesser than that of the Otto-engines used at the larger plants (3^{rd}-6^{th} models); moreover, their diesel oil demand is also considerable. The key operational and economic base data of the models investigated are described in table 1. The very good values of model 3 are perhaps describing the achievable optimum (proper mixture, proper sizing).

Table 1 Biogas Plant Models for Heat Generation and Cogeneration

Model	*1*	*2*	3	4	*5*	*6*
Input, t/year	*3 182*	*4952*	17 411	23968	*47936*	*90255*
Volume of Digester, gross m^3	*420*	*750*	2 400	3000	*5500*	*8000*
CHP, kW	*55*	*100*	330	500	*1000*	*1672*
Bio-manure Storage, m^3	*410*	*410*	1700	2770	*2770*	*2770*
Temperature of Digestion	mesophil					*M+T**
Investment costs, MFt	*61*	*137*	191	495	*908*	*1400*
Without CHP, MFt	*45*	*93*	112	405	*788*	*1200*
Biogas Produced, thousand m^3/year	*233*	*363*	1 320	1817	*3633*	*6000*
Heat value of it, TJ/year	*5,14*	*7,99*	29,03	39,97	*79,94*	*132*
In Case of Cogeneraion						
Electricity, MWh/year	*410*	*800*	2433	4000	*8000*	*13211*
Heat, MWh/year	*546*	*933*	2780	4667	*9333*	*15412*
Heat, TJ/year	*1,96*	*3,36*	10	16,79	*33,57*	*55,44*

*Legend: * mesophil + thermophil digestion*

4. Results of Model Investigations

In case of heat generation, the weaker economic performance of the smaller plants derive from the improper sizing of the different equipments, the higher specific purchase costs of the smaller equipments and from the higher proportion of personal costs. The prime cost of biogas in medium sized and large plants is 50 Ft/m^3, in smaller capacities 60 Ft/m^3. The biogas with a prime cost of 50 Ft/m^3 (with 60 % methane content) is competitive only compared with a natural gas above 83 Ft/m^3 purchase cost. Difference between gross and net production costs derive from the utilization of byproducts. Full utilization of bio-manure – which has a considerable area and capital demand – reduces the prime costs of biogas with 7 Ft/m^3 (Figure 1.)

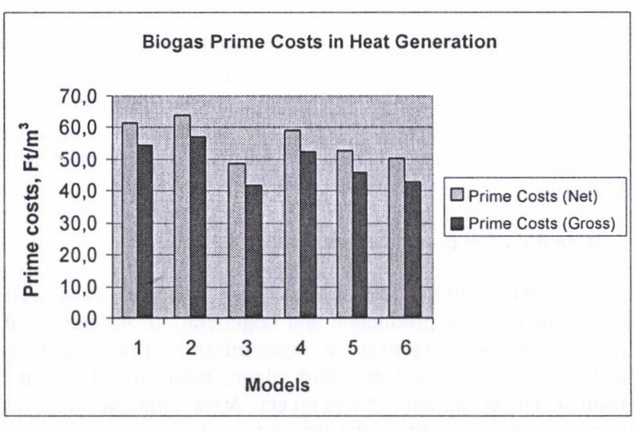

Figure 1 Biogas Prime Costs in Heat Generation

In case of sole heat generation the most profitable way of utilization is to feed into the district heating system, because this guarantees an assured and entire utilization. In small plants, the utilization of the entire amount can not be considered assured, even though the production is more expensive.

Energy can be made more marketable when transformed to electricity, although this involves extra investment. This increases the prime cost of biogas with 4-6 Ft/m^3 in medium and large sized plants, and 15-20 Ft/m^3 in small plants. Because of the higher specific price of electricity, the investment indicators remain almost the same in 4^{th}-6^{th} models, if the smaller amount of waste heat that is remaining after digestion can be fully utilized. The significant worsening of the indicators of the 1^{st}-3^{rd} models is caused by the fact that a CHP can be purchased only in specific sizes, so in small plants it can happen that the engine capacity is considerable greater than the amount of actually produced biogas would require. The investment indicators of smaller plants (1^{st}-2^{nd} models) tend to zero profitability, and their payment period to the actual lifetime of the plants, which is due to the lesser efficacy and extra material demand of the diesel engines, beside the factors already mentioned at heat generation. Only the latter increases the costs of biogas with 10-13 Ft/m^3. As a result of all these, middle and large sized plants produce electricity 5-8 Ft/kWh cheaper than the selling or purchase price, respectively, whereas in small plants 0 – -3 Ft/kWh specific revenue is to be considered, using only own resources to the financing. In proportion, the same is true to heat energy, too: 3^{rd}-6^{th} models: +800-1200 Ft/GJ, 1^{st}-2^{nd} models: 0 – - 300 Ft/GJ.

Another advantageous possibility for great plants is the production of bio-methane. Gas cleaning itself produces losses with 50 Ft/m^3 specific input material costs. Depending on plant size, 25-34 Ft/m^3 is the marginal cost at which bio-methane is cheaper than the natural gas available for great farms. In producing bio-methane, input material (raw biogas) costs have a 60-80% – in smaller plants a smaller – proportion. Input costs can be minimized, if the input materials are available at no cost (e. g., as municipal organic waste without sterilization needs, or as sewage sludge). Cost minimizing effect can be achieved also through utilization of carbon dioxide obtained from purification for fertilizing in greenhouses, parallel to using a part of the biogas for heating the facilities (in the wintertime). This way a 20-30 Ft/m^3 biogas prime cost can be achieved in grater plants, which can involve a profitable purification of biogas. Another important factor is the proper size, since the size of 250 m^3/h capacity, which is considered as a minimum size, produces bio-methane at double costs as a 1000 m^3/h capacity. The full deployment of only the smallest capacity (with actual production data: 5 days/year repair period) involves 2,16 million m^3 biogas, that is, at least a 600 kWe capacity plant (cca. 30 thousand t/year input with 16 % dry matter). Above this level, the costs of purification increase progressively, however, the prime cost of biogas produced at this size of plants is generally beneficial, so it can make economically attractive this way of biogas utilization.

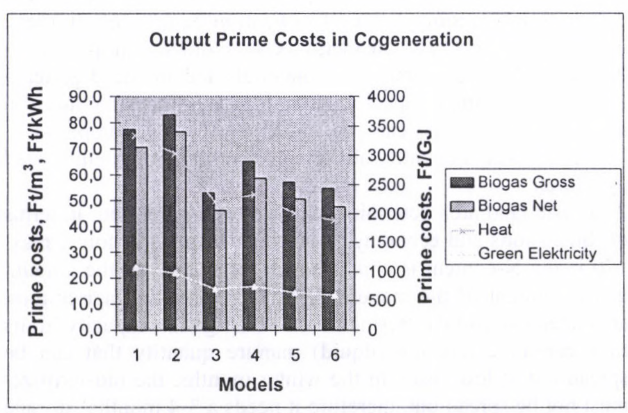

Figure 2 Output Prime Costs in Cogeneration

5. Conclusions

In the different size categories, biogas investment can be facilitated economically even under present macro-economic conditions, though using different technological solutions. In small-sized plants, heat energy utilization is to be considered (preferably to cover own demands), because of the lesser electric efficacy and extra material costs, and extra investment costs of cogeneration. This can be an alternative to natural gas firing even under present price conditions, especially when the biogas investment is weighed strategically, together with its complex (environmental, employment-assuring) benefits. In middle sized and large plants the own consumption is not realizable because of the greater quantity, therefore, cogeneration production of electricity is advised, under partial or full heat utilization. Under worsening Hungarian conditions of "green" electricity take-over, the transformation of biogas to another marketable product, biomethane, is to be considered. This involves no waste-heat generation, the utilization of which is always a critical point of operating cogeneration. Based on waste materials, or, perhaps, also with utilization of the carbon-dioxide from purification, in large plant sizes this can mean a profitable way of green energy production.

EFFECT OF THE VERTICAL WIND PROFILE UPON THE OPERATION OF WIND-POWER PLANT

István PATAY[1] - László TÓTH[2] - Norbert SCHREMPF[2] - Lajos FOGARASI[2]
[1]'Tessedik Sámuel' College, Mezőtúr
[2]'Szent István' University, Faculty of Mechanical Engineering, Gödöllő

Introduction

Wind velocity varies due to the superficial friction of terrain ('wind shear'), depending on the height above the ground surface. The value and the way of the vertical gradient are the function of several factors (relief, ground objects etc.) The effect of the local dependence of wind velocity on height, i.e. the vertical wind profile, upon the operation of wind-power stations is significant. With the changes in wind direction – depending on its speed and character – the wind profile also varies due to the actual relief in wind direction; there may be very significant deviations.

Increasing the tower height (height of rotor shaft) is reasonable, first of all, because of a better utilization of the wind velocities and wind power formed at greater heights. When planning wind-power stations, wind parks and adapting turbines to actual sites, these attendant conditions are generally disregarded especially if the preliminary detailed local wind measurements of energy-yield prognosis at different heights were failed. This measurement and its evaluation are essential because the conditions of the operation of the wind-power stations – the exploitable energy quantity, the specific forces acting upon the devices, including the cost of erection due to the requirements of basement, the expected service and maintenance demand (cost of operating) etc. – basically vary according to the wind profile. These effects can be determined by preliminary, quite a good approximate calculation. This why we have analysed the mechanism of effect and we show one of its segments in the following section.

Material and method of investigation

Wind velocity and wind profiles

The establishments in the international professional publications have been proved by the test measurements in Hungary as well; by the general experience, the wind velocity increases – according to the specific conditions of the regions of the country – in proportion to the height above the ground surface. (*Tóth-Horváth, 2003; Patay, 2003*) With energetic-purpose wind tests, the wind velocity values are measured by cup-anemometers at two or more heights; the wind profiles are computed from these reference points.

Direct information about the prevailing wind directions only for a small part of the cross-section area of the rotor (diameter of the blade wheel) are gained from such measurements. On the base of the measured data, the values of wind velocities for the actual height rang are computed with the help of theoretical relationships. In the wind-energy utilization practice, among several other relationships, the power function with Hellmann's exponent has been propagated (*Lysen, 1982; Johansson, 1994*)

$$\frac{v}{v_{ref}} = \left(\frac{h}{h_{ref}}\right)^{\alpha}$$

where

v is the wind-velocity value to be calculated for the height h,

v_{ref} is the known (measured) wind velocity at the reference height h_{ref} and

α is the exponent of height or Hellmann's exponent.

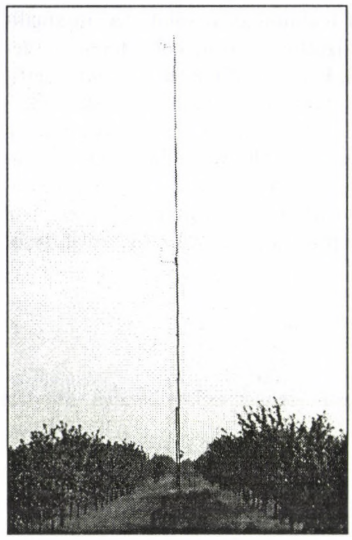

Telescopic tubular column with auxiliary support and anemometers mounted at two heights

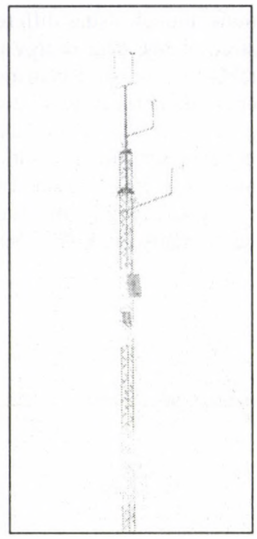

Top end of a lattice measuring column with sensors

Figure 1 Wind measuring columns

Several investigations (*Tóth, 2005; Schrempf, 2007*) and experiences have proved that the above formula can be used well for describing the vertical wind profile; the problem is the determination of the correct actual factor α.

The wind-power chart of Hungary was elaborated in this way; the measurements for the mapping were carried out generally at the heights between 20 and 60 m but the values for 25, 50, 75, 100, 125 and 150-m heights were also calculated with the 'characteristic' factor α of the actual areas. A higher reliability was provided by the data base of the Meteorological Service for several years that was corrected to the 10-m height.

In conclusion, the Hellmann factor can be calculated from the measured data and, with its knowledge, acceptable values are gained. The control measurements were carried out on higher columns and, at some sites, by an acoustic measuring unit (Sodar) which is capable of determining the velocity values up to the height of 250 to 300 m, range by range of 5 to 10 m in the vertical section. The biggest problem with the factor *alpha* determined by the annual wind measurement is that it is an average of the wind profiles in 12 or 16 wind directions. Due to this, the energy yields gained from the winds in different directions and the loads on the parts of equipment are less accurate since the value of the maximum load is determined by the prevailing winds.

Table 1 Annual average Hellmann's exponents by wind directions *(the frequency of wind directions 0, 7 and 8 was 51 %)*

Wind direction	Hellmann, α
0	0.216
1	0.188
2	0.21
3	0.251
4	0.309
5	0.252
6	0.221
7	0.194
8	0.263
9	0.26
10	0.256
11	0.248
Average	**0.24**

Figure 2/a shows the average wind profile while 6 wind profiles from the very different curves recorded in the 12 wind directions gained from the measurement series can be seen in

Figure 2/b. The average *alpha* values gained by the singular wind directions are listed in Table 1; the deviation from each other may be even 50 to 60 %.
According to the measurements of the wind chart of Hungary, covering all land regions of the country, the range of the exponent is between the limits

$$0.15 \leq \alpha \leq 0.45.$$

The lower values have been found in planes while the higher values – in the hill-country regions.

Potential power of the wind

The kinetic energy of the air can be calculated by the following relationship:

$$E_k = \frac{1}{2} \cdot m \cdot v^2$$

If $\rho A v$ is substituted for the flowing mass m, the potential power of the wind is given at an actual point –

$$P = \frac{1}{2} \cdot \rho \cdot A \cdot v^3 \qquad \text{(W)}$$

where
ρ is the density of the air (kg/m^3),
A is the cross-section area of flow (m^2), $A = D^2\pi/4$ (D is the diameter of the blade wheel),
v is the (average) velocity of the air in the cross section flow (m/s).

For unity A, the specific potential power is given in W/m^2.

According to the above functions, the specific power as a function of the height is

$$\left(\frac{v}{v_{ref}}\right)^3 = \left(\frac{h}{h_{ref}}\right)^{3\alpha} = \frac{P_{spec}}{P_{spec\ ref}}$$

where
$P_{spec\ ref}$ is the specific wind power at the reference height. The following formula is derived from the above equation:

$$P_{spec} = P_{spec\ ref}\left(\frac{h}{h_{ref}}\right)^{3\alpha}$$

Power and dynamic conditions of the wind tower

Accordingly, it can be seen that the power is determined basically by the value of the wind velocity since its third power is the factor in the equation. The effect of the diameter of wind wheel is also significant since the area swept by the blades is taken as the cross-section of flow A. The value of v is referred to the centre (axis) of rotation of the blade wheel; it is the same as the value of the formed wind speed according to the wind profile at the height of the nacelle.
The effort to achieve the possible highest power-plant performance explains why the height of tower and the diameter of rotor are to be increased. However, the reasonable tower height and the integral rotor diameter is a critical question. It is worth examining how the course of the vertical wind profile affects the performance of the wind-power plant and the conditions of the energy-production regime.
Let a rotor with three blades to be analysed, of which height of

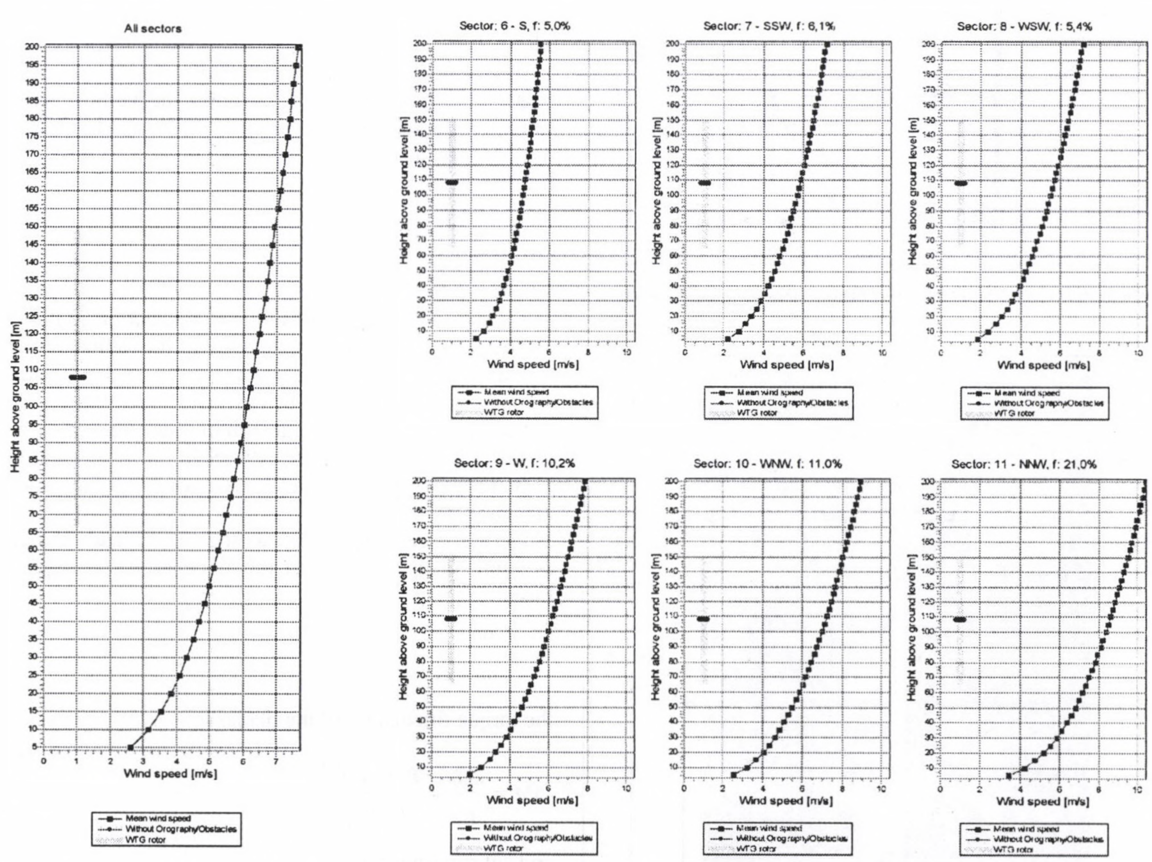

Annual average wind profile

Annual average wind profiles by wind directions (6 from the 12 directions as an example)

***Figure 2** Wind profiles from annual measurement* axis above the ground surface is h_0, and radius – R_0; accordingly, the maximum height swept by the rotor $h_{max} = h_0 + R$ and the minimum height – $h_{min} = h_0 - R$ (Figure 3). The subject of the analysis is to determine the course of the wind power per blade from the upper 'dead centre'; the angular speed of the rotational motion ω is *constant*.

According to the plotted wind profile, it can be seen that the two ends of the blade run in different wind-speed ranges. For the sake of the simplicity, the wind speed prevailing at the locus given with the mean radius (R_{mean}) characterizes the average wind speed acting upon the blade. Accordingly, the specific wind power on the blade in the upper position, the potential maximum, is –

$$P_{spec1\,max} = P_{spec0}\left(\frac{h_o + \frac{R}{2}}{h_o}\right)^{3\alpha} = P_{spec0}\left(1 + \frac{R}{2h_o}\right)^{3\alpha}$$

where P_{spec0} is the specific power at the axis height (W/m^2).

The minimum is the specific power on the blade at the lower point:

$$P_{spec1\,min} = P_{spec0}\left(\frac{h_o - \frac{R}{2}}{h_o}\right)^{3\alpha} = P_{spec0}\left(1 - \frac{R}{2h_o}\right)^{3\alpha}$$

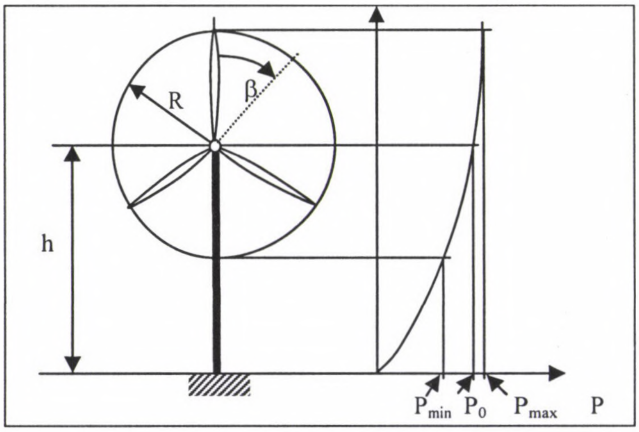

Figure 3 Wind profile and performance conditions of the wind turbine

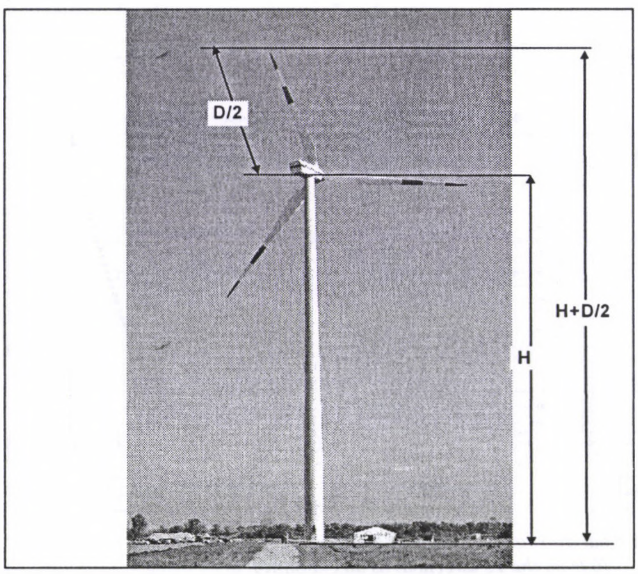

Figure 4 2-MW, 108-m high wind turbine with a rotor of 90-m diameter (Felsőzsolca, Hungary)

The difference between the two specific powers is –

$$\Delta P_{spec1} = P_{spec1\,max} - P_{spec1\,min} = P_{spec0}\left(\frac{R}{h_0}\right)^{3\alpha}$$

where

$\left(\frac{R}{h_0}\right)^{3\alpha}$ is a **dynamic factor** as a resultant from the change in the specific wind performance during a revolution of the blade. Accordingly, after an angular motion of an arbitrary angle β, the actual specific wind power per blade is –

$$P_{spec1} = P_{spec0}\left[1 + \cos\beta\left(\frac{R}{h_0}\right)^{3\alpha}\right]$$

The total wind power is gained in the way that the cross-section area per blade is taken into consideration:

$$P_{spec1t} = P_{spec1}A_1 = P_{spec1}\frac{R^2\pi}{3}$$

Referring to the three-blade rotor, it can be written down that –

$$P_{spect} = P_{spec1t} + P_{spec2t} + P_{spec3t} = P_{spec0}\left[1 + \cos\beta\left(\frac{R}{h_0}\right)^{3\alpha}\right] +$$

$$P_{spec0}\left[1 + \cos(\beta + 120°)\left(\frac{R}{h_0}\right)^{3\alpha}\right] + P_{spec0}\left[1 + \cos(\beta + 240°)\left(\frac{R}{h_0}\right)^{3\alpha}\right]$$

$$P = 3P_0 = 3\cdot\frac{R^2\pi}{3}\cdot\frac{1}{2}\rho\cdot v_0^{\,3} = \frac{1}{2}A\cdot\rho\cdot v_0^{\,3}$$

where v_0 is the wind velocity measured at the axis height; this is, of course, the expected result. However, the essence is that a relationship has been found between the vertical wind profile and the main geometric dimensions of the wind turbine which is worth analysing.

It is the dynamic factor –

$$\eta_d = \left(\frac{R}{h_0}\right)^{3\alpha}$$

and it shows the degree of the load fluctuation of the blades. It can be seen clearly that the increase of the radius, in the case of the same axis height, increases the value of the dynamic factor i.e. load fluctuation of the blades inside a revolution. The effect of the Hellmann exponent determining the vertical wind profile is similar; with a constant ratio R/h_0, at a site featured by a greater α, the dynamic load on the wind turbine exponentially increases.

Since the angular speeds ω of the rotor blades are equal, the dynamic factor determines the fluctuation of torque as well. From

$$M = \frac{P}{\omega}$$

the torque fluctuation of the blades is –

$$\Delta M = \frac{\Delta P_1}{\omega} = \frac{P_o}{\omega}\left(\frac{R}{h_0}\right)^{3\alpha}$$

and substituting P_0 –

$$\Delta M = \frac{1}{6}R^2\pi\rho\frac{v_0^3}{\omega}\left(\frac{R}{h_0}\right)^{3\alpha} = \frac{1}{6}\pi\rho\frac{v_0^3}{\omega}\left(\frac{R^{2+3\alpha}}{h_0^{3\alpha}}\right)$$

All factors influencing the blade dynamics can be substituted in the latter equation and the degree of their effects also can be developed.

Evaluation

At the upper 'dead point' where the wind velocity is greater even by 1 to 2 m/s than its actual value at the lower one, a much stronger bending force is applied and, obviously, it is in connection with the power as well. Due to the different loads, on a 2-MW wind turbine with 108-m nacelle height (axis of rotation) and 90-m blade diameter, the bending deformation at the upper centre may reach even 1.5 to 5 m while it reduces to 0.5 m at the bottom point. This arises during every revolution of blades so each blade is under a significant dynamic load from this bending, according to the frequency of rotation. With blades of mass of 15 metric tonnes, the varying dynamic load acts upon the whole wind turbine – the bearings of its shaft, the tower (mast) and the basement of the construction as well – the difference between the wind loads in the upper and lower positions may be even 400 to 800 kN. As an additional dynamic effect, there is a considerable irregularity (unbalance) in the wind profile (Figure 5) whereas the degree of turbulence is very changeable due to the layer shear, as a function of the height above the ground surface. Practically, the calculated wind profile provides only an idealized analysis. In order to determine the parameters of the basement of the wind turbine, the above phenomena should be surveyed already during the wind measurements; the turbulence is included in the supplying of data.

Conclusions

As it can be seen, the wind profile changes with the wind profile and, due to this, the load as well as the output power.
All these affect the course of the resultant performance of the rotor and the mechanical load upon the blades and the coupling elements. Accordingly, in terms of this, it is not indifferent what the wind profile is like in which condition a wind-generator construction runs or, contrarily, what wind-power plant is to be designed at a site with an actual vertical wind profile.
For the future a reduction of the subsidy on the electric energy produced by wind-power plants is probable therefore, when predicting the expectable energy yield, the potential powers should be known with the possible maximum accuracy. Today the objective of the manufacturers is to increase the height of tower since a better regularity in the wind profile in continental areas can be observed at the heights above 150 to 160 m. With the devices designed for such heights, much higher performances (by 20 to 30 %) and reduced dynamic load from the smoother irregularity can be expected; it may significantly increase the life of equipment, and the fatigue life of the blades and other parts of construction. By the shown analysis, the subject has not been worked out at all; however, we want to focus of the project-managing and erecting professionals' attention better still on this important problem.

References

[1] Johansson, T.B. et al.: 1994. Renewable Energy Sources for fuels and Electricity Island Press, Washington.
[2] Lysen, E.H.: 1982. Introduction to Wind Energy. S.W.d. Amersfoort.
[3] Patay I.: 2003. A szélenergia hasznosítása (*Utilization of Wind Energy – in Hungarian*). Szaktudás Kiadó Ház, Bp.
[4] Schrempf N.: 2007. Energetikai célú szélmérő rendszer kialakítása (*Energetic-Purpose Wind Measurement System*). Doktori (PhD) értekezés (*PhD dissertation*), SZIE Gödöllő.
[5] Tóth G.: 2005. Energia célú szélmérés (*Energetic-Purpose Wind Measurement*). Doktori (PhD) értekezés (*PhD dissertation*), SZIE Gödöllő.
[6] Tóth L.-Horváth G. szerk.: 2003. Alternatív energia. Szélmotorok, szélgenerátorok (*Alternative Energy; Wind motors, wind menerators*). Szaktudás Kiadó Ház, Bp.

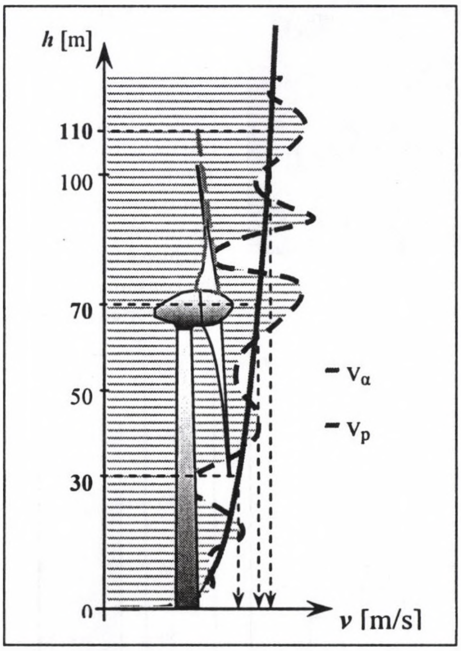

***Figure 5** Ideal (v_α) and real (v_p) (turbulent) wind profile*

COMBINED SOLAR SWIMMING POOL HEATING AND HOT WATER SUPPLY
Richárd KICSINY - István FARKAS
Szent István University, Gödöllő

1. Introduction

Collector based solar energy systems may take the most part in solar energy utilization. Such a system constitutes the basis of our investigation in this paper. The recently discussed evaluation containing quantified results can help for designing and installations of similar combined solar thermal systems in the future.
The evaluation pertains to the solar heat gain of the solar thermal installation that takes part in the heating of the swimming pool in summer time and preheats domestic hot water for the kindergarten in the other period of the year (Farkas et al., 2000).
When designing systems alike the basic aim is to maximize the quantified energy performance and efficiency values of it. Such values have been determined in our investigations by monitorring three kinds of data at suitable parts of the system: irradiance, temperatures of heat carrier fluid and volumetric flow data.

2. System description

The view of the aforementioned solar swimming pool installlation can bee seen in Fig. 1. The system consists of flat plate solar collectors' field (total area is 33.3 m^2, oriented to the south, inclination angle is 45°), two pieces of plate heat exchanger (one of them is for swimming pool operation and the other one is for kindergarten operation), a 700 m^3 outdoor swimming pool, solar storage tank with a volume of 2000 liter in the kindergarten, gas boilers for auxiliary heating both for swimming pool and for kindergarten operations. Inside the solar tank there is no auxiliary heater. The simplified operational scheme of the solar heated swimming pool system can be seen in Fig. 2.

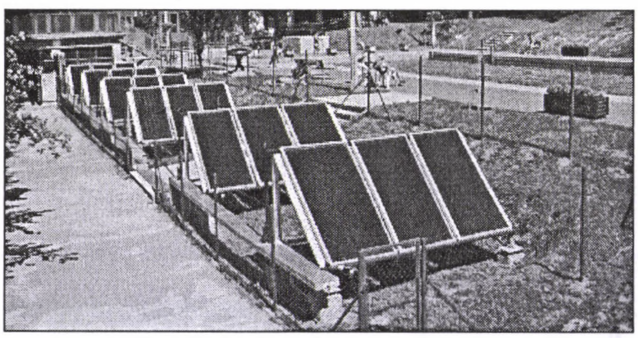

Fig. 1 View of solar collector field near by swimming pool

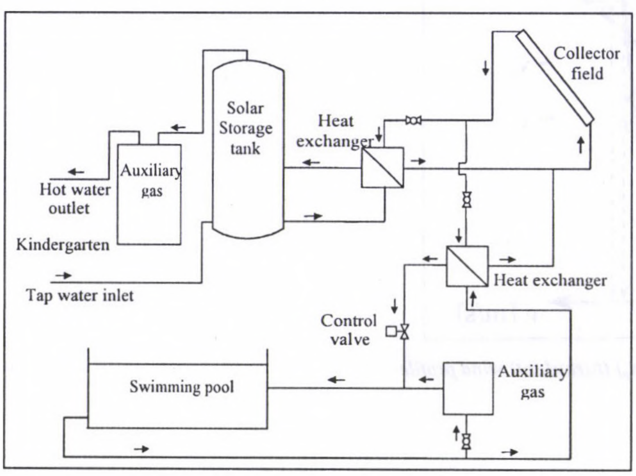

Fig. 2 Simplified scheme of the solar thermal system at the campus of Gödöllő

3. Data used for evaluation

Together with the solar thermal installation a data acquisition and monitoring system is also set up (Buzás et al., 2002). The irradiance and temperature measurements have been achieved at suitable parts of the system. Necessary volumetric flow values was measured or known from pump manufacturer's descriptions A couple of data file was formed every day on the basis of abovementioned measurements and applied by MATLAB® software to calculate relevant daily energy and efficiency values (Farkas et al., 2007).

5. Results and discussions

All henceforward results correspond to the time period of January 1, 2001 – August 1, 2006. The ending date is because of that the data acquisition computer went wrong on August 2, 2006. The most important summarized values for the whole monitored time period can be seen in Table1.

Table 1 Distribution of energy for the period of January 1, 2001 – August 1, 2006

Year	Energy, MWh				
	*Solar radiation	Gathered by collectors	Used for swimming pool heating	Used from solar storage in kindergarten	Total in kindergarten
2001	31,5	18,5	4,9	2,2	11,8
2002	29,4	18,6	5,1	3,5	14,2
2003	22,7	15,3	6,5	3,2	13,2
2004	13,6	7,9	1,7	2,5	11,7
2005	15,6	8,2	1,4	2,3	16,1
2006 (Jan 1-Aug 1)	13,0	5,3	0,4	2,2	10,3
Total:	**125,8**	**73,9**	**20,1**	**16,1**	**77,4**

**during collector loop operation*

We can consider two approaches when calculating system efficiency values and energy distribution of the solar installlation. In the first case we compare the used (directly on consumers' sides) solar energy to solar irradiation gathered during the time when the collector loop pump was on. In the second case we compare the used (directly on consumers' sides) solar energy to solar irradiation gathered during the entire monitored term. Efficiencies calculated by the second approach are certainly lower values comparing to results from the first case.
The total solar energy irradiated on collectors' plane during the entire monitored term and separately during collector loop pump operation are as available solar energy, thermal energy directly produced by the collectors and solar energy directly utilized by the consumers in swimming pool operation adding together with kindergarten operation are all can be seen in Fig. 3.

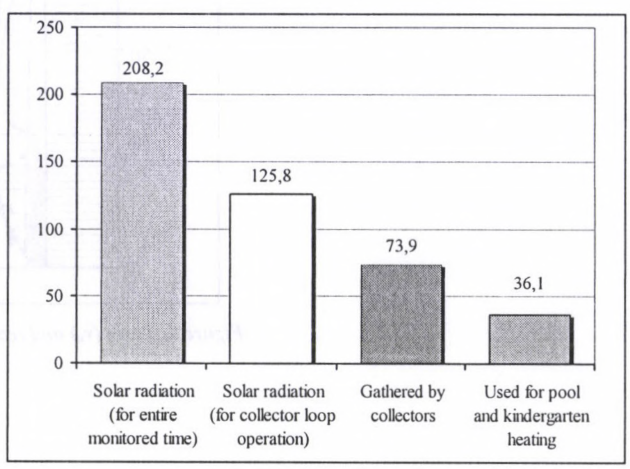

Fig. 3 Available and used solar thermal energies

On the basis of the present discussion, the overall system efficiency in swimming pool operation was 34,8% comparing to solar irradiation during collector loop operation and 25,1% as regarding solar irradiation during the entire monitored term in swimming pool operation. Relevant values in kindergarten operation are 23,5% and 12,5% respectively.
Furthermore the solar heating system covered 26% of the required energy for domestic hot water heating in kindergarten operation (Fig. 4) and 21% of the corresponding energy demand regarding to the entire monitored time period including both swimming pool and kindergarten operation terms (Fig. 5).
According to the long term evaluation the above discussed results are gained and one can conclude that it worth using solar energy in such combined solar thermal systems, with a reason-nable payback period related to the actual installation costs.

References

[1] Farkas,I., Buzás,J., Lágymányosi,A., Kalmár,I., Kaboldy,E. and Nagy,L.: A combined solar hot water system for the use of swimming pool and kindergarten operation, Energy and the Environment, Vol. I. /ed by B. Frankovic/, Croatian Solar Energy Association, Opatija, 2000, pp. 81-88.
[2] Buzás,J., Farkas,I. and Tóth,M.: Performance evaluation of a solar heated swimming pool, The 4th ISES-Europe Solar Congress (EuroSun 2002), Bologna, Italy, June 23-26, 2002, CD-ROM Proceedings, pp. 7.
[3] Farkas,I., Kicsiny,R. and Buzás,J.: Monitoring of a solar swimming pool heating and domestic hot water supply system for the time period 2002-2006, Research Report, Department of Physics and Process Control, SZIU Gödöllő, Hungary, No. 43, December 2007. p. 93. (In Hungarian)

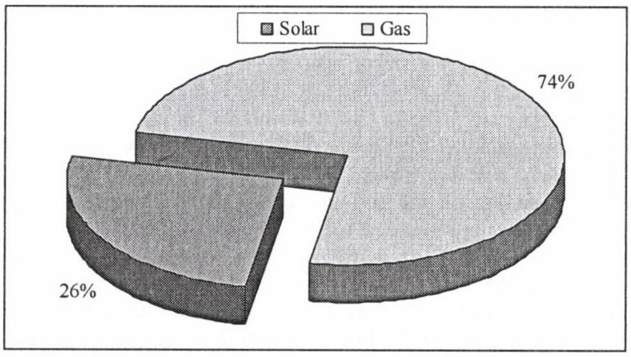

Fig. 4 Distribution of used energy sources in kindergarten during kindergarten operation

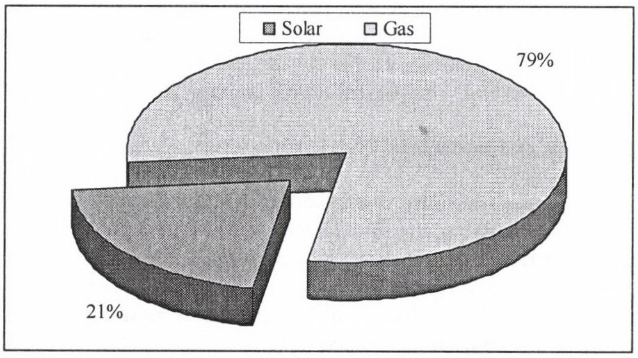

Fig. 5. Distribution of used energy sources in kindergarten during swimming pool and kindergarten operation

APPLICATION OF MEDIUM-DEEP SUBSOILERS IN THE AGRICULTURE

(Tests on the Working-Quality by Measuring the Electric Conductivity of Soil)

Péter RÁCZ - Zsolt SZÜLE
Szent István University, Gödöllő

Scope of the research

The objective of the research is to find a relationship between the degree of the looseness – after the cultivation by subsoilers at medium depth – and the electric conductivity of the soil layer. The reason of the experiments carried out is that several different factors influencing the electric conductivity as well as the looseness degree of the soil exist. Amongst these, the most important characteristic values are e.g. the moisture content of soil [3], the resistance against penetration, the nutrition content of the soil etc. Accordingly, determining the degree of the soil looseness as a function of this electric material characteristic is well founded aim. The present article contains its results.

Methods and materials

The measurement tests were carried out in the last summer under the following conditions: dry, sunny weather, about 30 °C air temperature; plane land, cereal stubble, medium-adherent soil; the moisture content of the soil is 17.5 to 19.5 % in the top layer of 30 to 40 cm, its *Arany's* cohesiveness number is 39, its average penetration resistance is 2.8 MPa; by the physical classification it is a clayey-loam soil.

The loosening was carried out with a chisel-type, straight five-blade subsoiler. For measuring and determining the electric conductivity of the soil, the device type *Veris 3100* made in the US was used. The tests were carried out along the measuring-section lengths 100 m. Before staring the tests the tractor-implement combination as well as the measuring device *Veris* was set on a so-called adjustment field-spot. The *Veris* 3100 type is such a tractor-drawn unit measuring the electric conductivity of the soil which, with the help a GPS working on the principle DGPS, collects the data showing the electric conductivity [1]. This provides the accurate determination of the electric-conductivity data along the measuring-section length.

The measuring cart is a two-wheel closed frame attached to the drawbar unit of an agricultural tractor; 6 measuring electrodes spaced equally are mounted on the frame. These are disks with bearings; the function of the disks is to conduct the measuring electric current into the soil, and to provide the sensing of the voltage drops. In the upper configuration uses the four inner discs (2, 3, 4 and 5). The voltage is measured between the two innermost discs (3 and 4) which are d = m apart. In the under configuration four outer discs (1, 2, 5 and 6) are used and the voltage is measured between discs 2 and 5. When the electrodes (discs) are d metres apart the conductivity is measured to a depth of roughly 1,5d metres.

Knowing the actual amount of the electric current, the value of the electric conductivity can be calculated, in mS/m. The inner two electrodes measure the electric conductivity of the soil in the upper layer of 30 to 40 cm while the two side electrodes – in the lower layer at a depth of 80 cm. Previously the conductivity of the settled (before-tillage) soil was measured along all the five measuring sections and then all measuring section were loosened at a medium depth. Finally, the measurement of electric conductivity (χ) was repeated in the soil along the loosened measuring sections; during these tests the measuring equipment *Veris* was towed along about the same track as that along which the conductivity was determined in the settled soil (*Fig.1*).

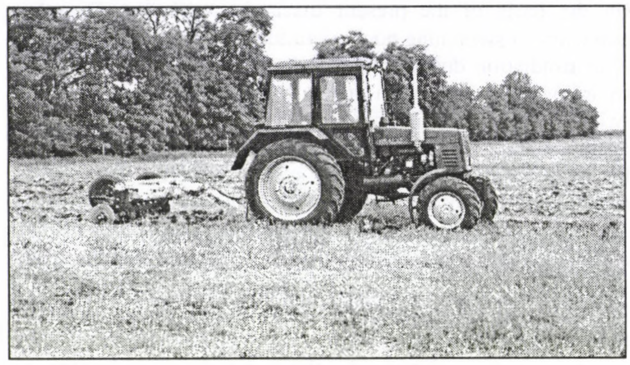

Figure 1 The measuring device Veris 3100 in a field-test on a loosened land

Results

At the so-called evaluating main points (the places along the sections at 20 m lengths), the data were averaged in the course of the data processing so five main points were gained in each measuring section. The evaluating main points are necessary because the soil is a living substance changing in its each part and, depending on the soil properties, there are considerable deviations in the measured values. For answering the problem, this method was used in the research. After processing and evaluating the data for all the five measuring sections, the variation of electric conductivity as a function of the length of the measuring sections – in the top (30 to 40 cm) and the deep (80 cm) layers as well – before and after the medium-deep loosening.

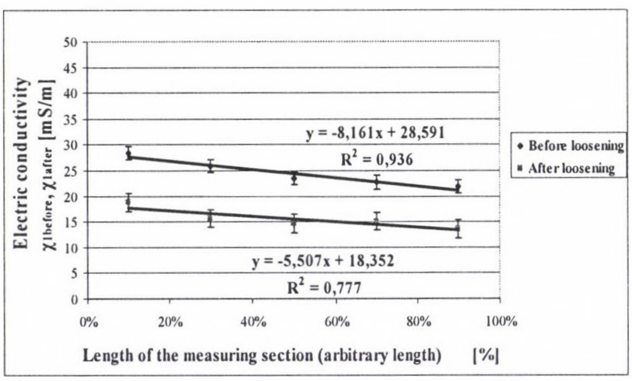

Figure 2 Course of the electric conductivity as a function of the length of the measuring section before and after loosening, in shallow layers (30 to 40 cm)

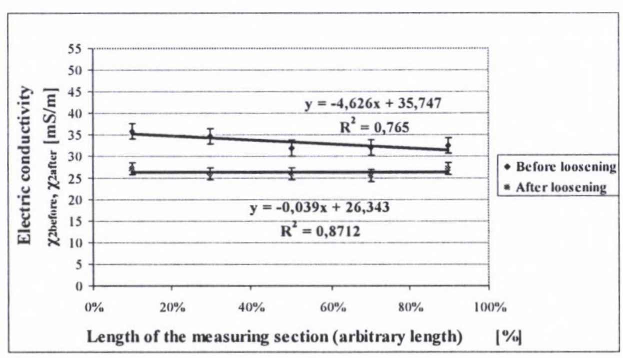

Figure 3 Course of the electric conductivity as a function of the length of the measuring section before and after loosening, in deep layers (80 cm)

When defining the measuring-section length, I considered its total length as a unit.

The indicated slope values as well as the constants clearly decreased at both depths under the impact of the medium-deep soil loosening. (*Fig. 2*) Comparing the gained curves for the different measuring sections, it was established that the course of the relationship may be approximated with a linear function independently of the length of the measuring section, in the top and the deep layers as well. Its physical explanation is that the loosening process is accompanied by two important phenomena which can be interpreted after digging test cross-sections in the cultivated soil layer. One of them is the canal zones cut by the loosening blades in the soil and the other is the distribution and the sizes of the granules, crumbs and clods. The size of the canal zones and the size-distribution of the crumbs and clods formed by the loosening blades depend on the soil conditions at the point where the subsoiler is actually operated. It can be observed that the after-loosening electric-conductivity values are higher in the first part of the curves; its cause is the fact that the loosing blades of the implement reach their set working depth after covering a distance of 5 to 6 m from starting the operation. Accordingly, also the degree of the loosening is worse than that in the other parts of the measuring section. As to the changes at the measuring points in the other parts of the measuring section, its cause is the changing soil properties at each point; the differences in the working quality of the subsoiler arise from this so the electric conductivities – accordingly the measured points – are varying in the same way. These differences can exactly be traced with the help of the measurement of the electric conductivity of the soil; accordingly, the method will be capable of testing the cultivation quality.

The investigation also shows that the effect of the medium-deep soil-loosening in a depth of 30 to 40 cm can be observed in the lower 80 cm layer as well; however, the loosening implement did not work in this depth (*Fig. 3*). Obviously, the degree of the decrease in the electric conductivity is higher in the top layer, in which the functional tillage was carried out, than that in the lower deeper soil layer.

During the evaluation it was also proved that the distribution of the electric-conductivity values is of the Gaussian type. After calculating the deviation values of the measured date, I proved by Bartlett's probe [2] that the empirical deviation values belong to the same theoretic deviations' model.

Then the consistency-analysis of the function was carried out; it has proved that the course of the electric conductivity can be approximated by the following straight line of the general form for the soil states before as well as after the loosening and the top shallow as well as the deep layers:

$$f(\chi) = mx + b \qquad (1)$$

The two parameters (*m* and *b*) of the straight line were calculated for all the four functions, starting from the following regression relationship:

$$\phi(m,b) = \sum_{i=1}^{n} \left[m \cdot x_i + b - \chi_i\right]^2 \qquad (2)$$

This formula has the minimum if its derivatives with respect to *m* and *b* are zero, respectively:

$$\frac{\partial \phi}{\partial m} = 0 = 2\sum_{i=1}^{n} \left[m \cdot x_i + b - \chi_i\right] x_i \qquad (3)$$

$$\frac{\partial \phi}{\partial b} = 0 = 2\sum_{i=1}^{n} \left[m \cdot x_i + b - \chi_i\right] \qquad (4)$$

The equations can be transformed on, by applying the term-by-term multiplication and adding up.

$$m = \frac{\sum_{i=1}^{n} x_i \chi_i - \frac{1}{n}\left(\sum_{i=1}^{n} x_i\right)\left(\sum_{i=1}^{n} \chi_i\right)}{\sum_{i=1}^{n} x_i^2 - \frac{1}{n}\left(\sum_{i=1}^{n} x_i\right)} \qquad (5)$$

$$b = \frac{-m\sum x_i + \sum \chi_i}{n} \qquad (6)$$

Table 1 Values of m and b of the functions with different soil states

Soil state	*m*	*b*
Before loosening, shallow	-7,998	28,509
After loosening, shallow	-5,432	18,341
Before loosening, deep	-4,512	35,387
After loosening, deep	-0,031	26,193

Accordingly, with the full knowledge of the values of the independent variable x_i and the belonging measured values χ_i of the characteristic parameter χ, the most probable straight line can be calculated with the help of the relationships (5) and (6). The above formula of calculation well approaches the computed values accordingly the correctness of the values is proved.

In the functions describing the phenomena, the slope of the curves is the characteristic number indicating the compaction (bulk density) of the soil.

$$\frac{d\chi}{dx} = m \qquad (7)$$

$$d\chi = m \cdot dx \qquad (8)$$

$$\int_0^{40} d\chi = m\int_0^{1} dx \qquad (9)$$

The variable x in the equation means the length of the measuring section. Here, the limits of integration were defined as 0 and 1 while the limits of integration of χ are 0 and 40 mS/m.

After solving the differential equation (7) the general shape of the straight lines related to the single soil states is gained:

$$\chi = mx + b \qquad (10)$$

The formula (10) describes the phenomenon between the indicated error limits accordingly it is suitable for determining it.

Conclusions

On the basis of the results and the experiences of the measuring tests, it can be stated as follows:

- The soil electric-conductivity measuring device with disk electrodes type Veris 3100 is suitable for the measurement of changes produced by the medium-deep loosening.
- According to the tests, the application field of the measuring device Veris 3100 can be extended to the quality tests of other implements working on the loosening principle.
- It was established that the general solution (10) of the ordinary linear differential equation (7) determines the course of the electric conductivity as a function of the length in the shallow (30 to 40cm) or the deep (90 cm) layers, before and after an arbitrarily chosen loosening operation.
- From the results, it can be established that the electric conductivity of the soil decreases under the impact of the medium-deep loosening which is manifested in the significant decrease in the slope and the constant values of the straight-line equations for the singular cases. It can be explained with the great amount of air induced into the soil by this soil cultivating method and the electric conductivity of the air is much worse than that of the soil.

The above results will be very useful in creating exact mathematical relationships between the electric conductivity and the degree of loosening.

References

[1] RÁDICS, J. – JÓRI, J. I. – SZABÓ, I. – DEÁKVÁRI, J. – KOVÁCS, L.: Intelligens munkagépek tervezési – üzemeltetési feltételei. (Designing and operating conditions of intelligent implements) *XXX.* MTA-AMB K+F Tanácskozás. Gödöllő, 2006. p.13

[2] SOÓS, P. – CSORBA, L.: Műszaki számítások. (Technical calculations) Agrártudományi Egyetem. Mezőgazdasági Gépészmérnöki Kar. Gödöllő, 1989. p. 229

[3] VÁRALLYAY, GY.: A talaj vízgazdálkodásának szabályozása, mint a környezetkímélő növénytermesztés egyik kulcskérdése. Növénytermesztés és környezetvédelem. (Regulation of the water balance of the soil – on of the key-question of the environment saving plant production – Plant production and environment protection) MTA Agrártudományi Osztály. Budapest, 1999. p 162

[4] B. Boydell, A. McBratney, B. Whelan & Budiman: Preliminary results with the VERIS soil electrical conductivity instrument. Australian Centre of Precision Agriculture, University of Sydney, 2007. www.usyd.edu.au/veris

BRUISE INVESTIGATION OF THE CULINARY PAPRIKA

Károly PETRÓCZKI
Szent István University, Gödöllő

1. Objective

The culinary paprika has an important role in Hungarian market. The paprika producers try to find their proper positions not only in domestic market, but in European Union, too. The producers are forced by the sharp competition to do everything for the best adaptation to the requirements of the market. Excellent quality must be produced, assorted and packed economically at a given shipping schedule in according to the demand not only of the customer, but the EU regulation itself, too. These requirements are met less and less with tight and occasional man-power, the utilization of machine work in case of sorting and packaging gets urgent. During the machine manipulation the bruise proof operation can be realized, if the mechanical load is in the range of bruise proof values. There are several articles about the technical side of the growing e.g. Dimény et al. (2004); Fekete et al. (2005). Láng (1982, 1983) wrote in his articles about energy flow and the bruises during the operation of the paprika harvester. Fenyvesi (2004) summarized his bruise investigations of agricultural materials in his recently published book.

2. Methods and materials

Machine manipulation has a lot of mechanical influences on the culinary paprika. Reducing the mechanical load to the paprika the probability of the bruise can go down, but together with it the price of the machine and the duration of the manipulation time increases very much. There is no manipulation without mechanical load applied to the surface of the paprika. That's why we try to estimate the critical value of the compressive load. The existence of the bruise can be observed correctly only a few days later with the local appearance of the colour change. So the investigation needs a lot of time. Usually the surface of the biological material is compressed in a testing machine (e.g. Zwick, Instron or Loyd), the load value is recorded and the bruise point can be determined. The mechanical testing machines can press a measuring stud or a special forming pressing surface into the material with low adjustable deforming rate. During the deformation the force can be measured with load cell, and so the deformation – force diagram is recorded. The investigation can carry out with quick and repetitive load with DyMaTest dynamical and programmable testing machine (Petróczki, 2005, 2006) shown at the Fig. 1. In DyMaTest in according to the principle of the instrument the shape of the compressive load can be set and not the deformation rate like the conventional mechanical testing machine. So the deformation is the function of the load here.

After the study of the references above and the preliminary considerations we can say, that at a low compressive load the behaviour of the surface is elastic and not categorically linear. Together with the increase of the compressive force the pressure of the liquid inside the cell increases as well, the load of the cell wall increases, deformation occurs and the force-deformation function is continuous. In case of the bruise a kind of irreversible effect e.g. cell wall tear takes place, which modifies suddenly the slope of the function. So we analyse the step of derivative of the deformation-time function. The force which causes this step is named critical or end force. It means, that below this force there is no bruise yet.

The measurements was carried out at the middle part and at the biggest diameter of the paprika so, that the measuring stud load plane was parallel with the surface of the paprika. The paprika was supported by the sand-bed on a large surface. The diameter of the measuring stud was ø 5 mm. The load function was programmed so, that the compressive force increased linearly up to the maximal value during 1,2 second, next decreased for the same time up to the zero load. Our test lasted for three load-cycles, but only the first rising slope was used for the calculations. The preload was 0,1 N. Two kinds of measurement was carried out with 5 N and 10 N maximal forces.

During investigations we have found no step of deformation in case of 5 N maximal value as can be seen on a "typical" diagram of the Fig. 2.

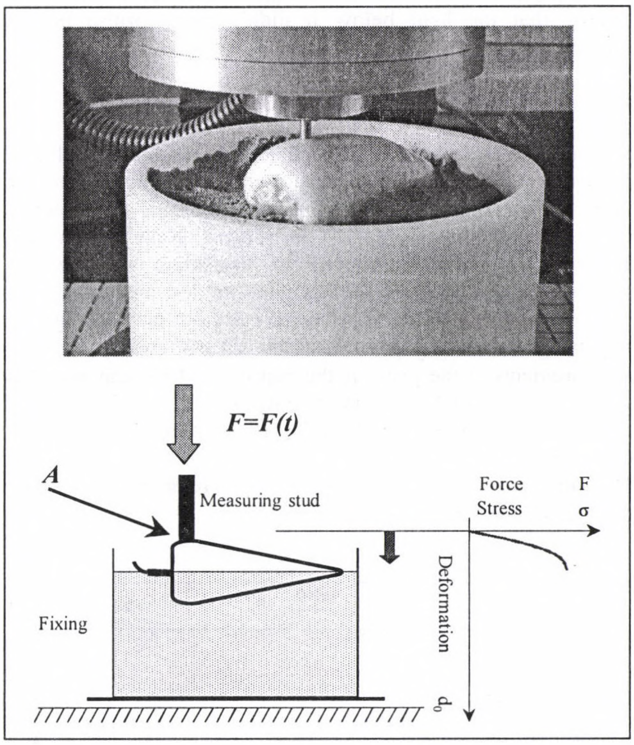

Fig. 1 The loading of the paprika surface with measuring stud in DyMaTest instrument

The compressive force increased up to 10 N in Fig. 3. The deformation (d_0) increased monotonic up to 8,5 N (until 1,02 s) and next a discontinuity appeared on the curve. The whole process can be observed more clearly on the derivative of the deformation, where can be seen, that there is an irregularity already at 0,96 s, but we can say explicitly, that the bruise starts at 8,5 N. This diagram as an example was presented, because the bruise was visible to the naked eye, too. Fig. 4. shows an imperceptible to the eye, but a probable bruise time diagram.

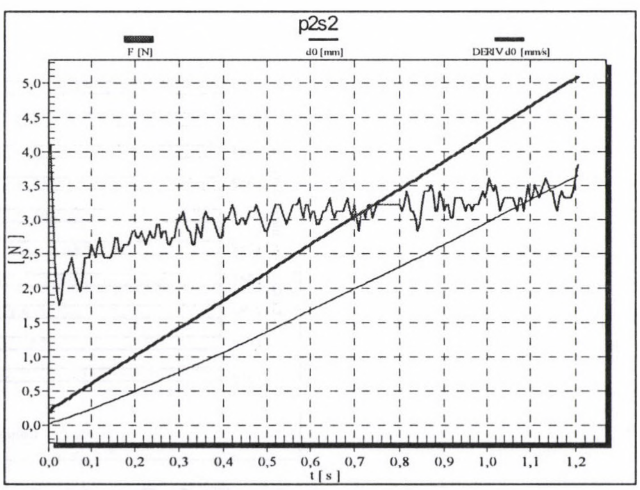

Fig. 2 The increasing compressive force (F) from 0 N up to 5 N, the deformation of the surface (d_0) and its derivative with respect to time (DERIV d_0)

3. Results

We haven't recognized neither visible nor invisible, but probable bruise during our investigations at 5 N maximal load. The number of repetition at max. 10 N load was 16, the number of the visible and the probable bruises was 10 from it. In remaining 6 cases there was no bruise during tests at all. The Fig. 5. illustrates bruise caused force limits and we can state, that the critical value of the compressive force is 6,4 N. It means, that the load below it didn't cause bruise in our investigations.

4. Conclusions

Not only the critical force of the visible bruise, but the value of the force which causes a probable bruise can be determined from the measurements with linearly increasing compressive force generated by DyMaTest instrument. Next time a new investigation is recommended to determine whether the probable bruise comes true or not. The simplest method is to do that, as we have mentioned before, to carry out the investigation of getting brown of the pressed surface after a few days. We did measurements at the peak of the paprika and we can say, that similar effect can be observed, but we can't go into details because of the limited length of the article and more complexity of the problem.

The investigation was supported by Hungarian Scientific Research Fund (OTKA T 46917).

References

[1] Dimény I., Fenyvesi L., Hajdú J.: Piactudatos zöldségtermelés MGI Könyvek, 3. 2004.

[2] Fekete A., Fenyvesi L., Horváth E., Sitkei Gy.: A gyümölcs- és zöldségtermesztés műszaki vonatkozásai. MGI Könyvek No. 4. 2005

[3] Fenyvesi L.: Mezőgazdasági termények sérülésvizsgálata. Akadémiai Kiadó, 2004.

[4] Láng Z.: Terményvizsgálatok az étkezési paprika gépi betakarításához. Kertgazdaság, 1982. XIV. évf. 5. szám.p.45-52.

[5] Láng Z.: Paradicsom és paprika betakarító gépek termésleválasztó szerkezeteinek összehasonlítása. MTA-MÉM AMB Kutatási Tanácskozás, Gödöllő, 1983. febr.1-2. Előadás és poszter.

[6] Petróczki K.: DyMaTest – új műszer a mezőgazdasági reológiai kutatásokhoz. MTA-AMB XXIX. Kutatási és Fejlesztési Tanácskozás (29th Conference on R&D in Agricultural Engineering). Gödöllő, 2005. jan. 18-19. III. szekció – Méréstechnikai eljárások az élelmiszer–gazdaságban. Előadás és poszter.

[7] Petróczki K.: DyMaTest alkalmazása a mezőgazdasági anyagok reológiai kutatásaiban. MTA-AMB XXIX. Kutatási és Fejlesztési Tanácskozás (30th Conference on R&D Agricultural Engineering). Gödöllő, 2006. jan. 24. III. szekció – Méréstechnikai eljárások az élelmiszer–gazdaságban. Poszter.

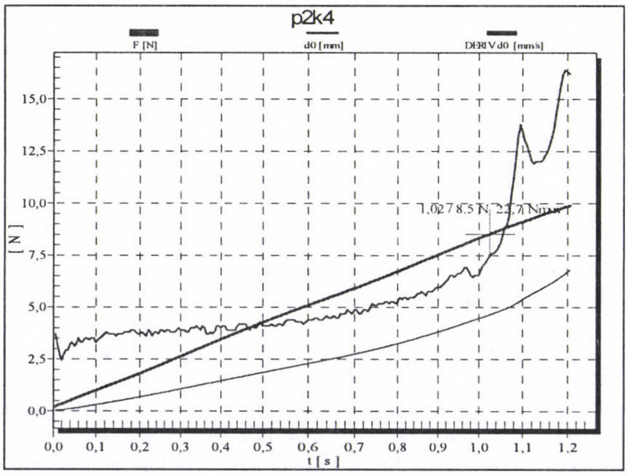

Fig. 3 Diagram of a „visible" bruise. The bruise started at cca. 8,5 N

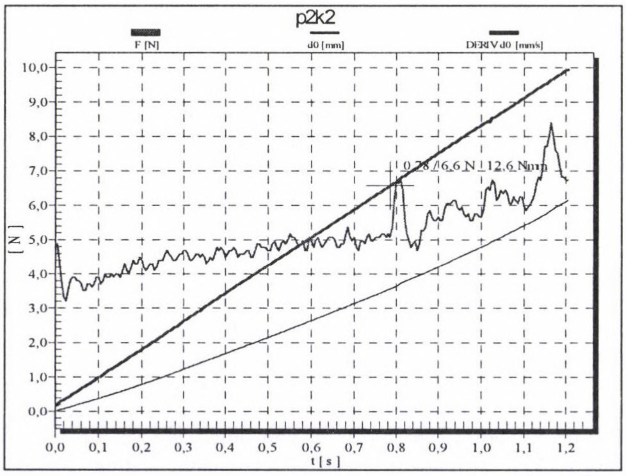

Fig. 4 Diagram of a „non visible", but probable bruise. The bruise occurred at 6,6 N

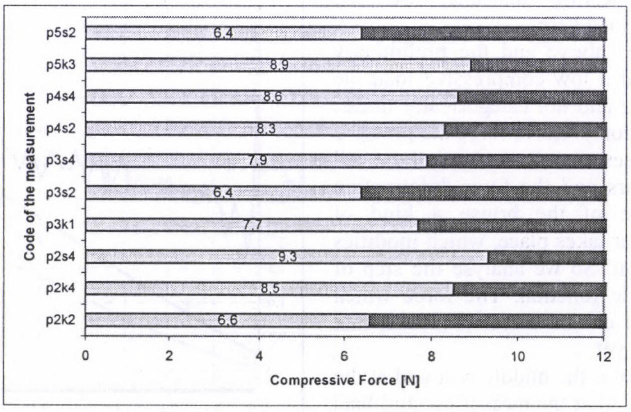

Fig. 5 Compressive force at the starting of the bruise

A MICRO-CONTROLLER-BASED ALGORYTHM FOR SORTING WHITE PAPRIKA

Zoltán GERGELY - Endre JUDÁK
Szent István University, Gödöllő

Introduction

Now the sweet paprika is still picked manually in the small as well as the large-scale plants (farms or works) so paprika generally with peculiar sizes to the producers is put on the market. This does not fulfil the very severe requirements of today. Since at present there is no accurate device available on the market of sorters for sorting the sweet pointed, white paprika accordingly we set the development of a picking system based on the picture processing as a target.

The rapid propagation of the image processing is closely related to the explosive increase in the data processing rate and the store capacity of computers. But it is still a key problem today as well (especially with the real-time applications) to elaborate successfully algorithms **with an acceptable running time**.

The image processing starts with shooting and recording pictures. There are several usable options for this – conventional or infrared cameras, X-ray images and ultrasonic detectors as well. The image is usually an intensity picture or map which certain luminance values assigns to the individual points of the objects; the recorded picture may be analogous or digital.

The wide assortment of new optical techniques looks promising in the rapid determination or, at least, estimation of the quality parameters of the crops. A super-rapid pattern recognition system differing from the earlier practice is shown in the following paragraphs; it facilitates the picking processes of the sweet white paprika with acceptable accuracy.

Method

For achieving a suitable picking performance, the complete recognition of 3 or 4 peppers has to be provided in a second (that is 10,800 to 14,400 bell peppers per hour at a travel speed of 1 m/s). It requires an extremely high-speed picture processing system and, in addition to this, the amount of data to be processed is also multiplied according to the multi-directional mapping.

It turned out during the investigations that the above demands can be satisfied only by the CCD sensor with a low pixel number – by the line CCD sensors (with the type used by us), the pixel data can be read out in 102 µs at the maximal read-out rate. An additional advantage is that the record of contour directly can take place; accordingly, the search of contour through software can be avoided and the recognition algorithm will be speeded up (*Figure 1*).

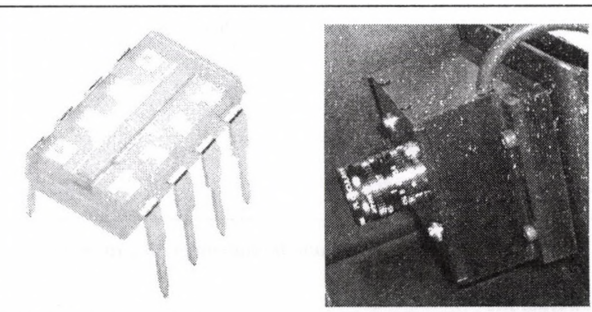

Figure 1 The used line CCD (left) and the boxed design (right)

An embedded system (with microcontroller basis) was elaborated for the sorting algorithm. The pixel data of the CCD are received by a high-rate Microchip DSP. This unit includes the pattern recognition algorithm as well. The high speed of the DSP provides the real-time running of the algorithm. The whole control system as well as the operating software programmes has been developed by us alone. During the experiments the application of PCs was rejected since they did not run reliably in the severe industrial conditions (in spite of their industrial design).

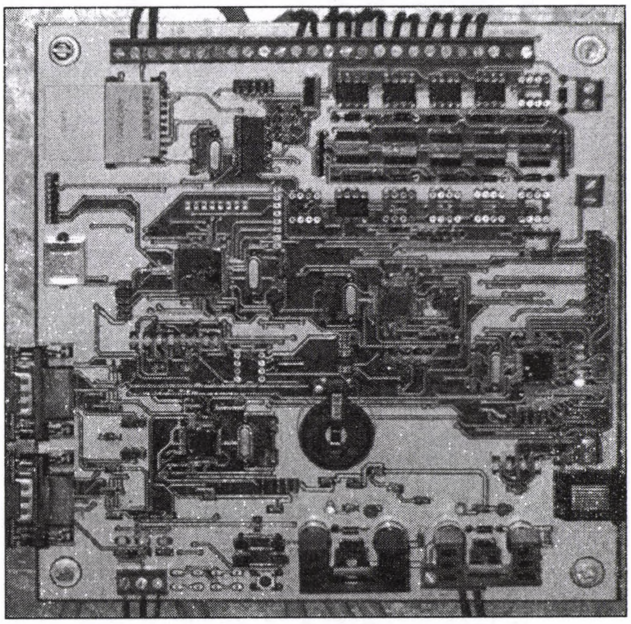

Figure 2 The central processing unit

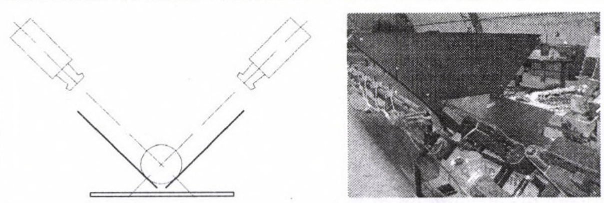

Figure 3 Projection from two directions

To avoid the time-consuming rolling and moving of the crops, the projection has to be provided from several directions. It has been found in the course of our investigation that using more than two cameras does not improve significantly the accuracy, but greatly decreases the rate of processing.

Results

The working of the algorithm in a very simplified form is as follows: As it was mentioned above, only the contour of the pepper is recorded during the measurement. The elimination (image rejection) of the stalk is a serious problem; it is solved by the perception of the decrease or increase in diameter. For determining the degree of malformation, the centre-line is constructed and its length is accurately computed with small triangles. The values gained in this way are compared to the length of the line drawn between the first and the last centre points of the paprika body. The quotient of the two length values is the curvature degree. By this method, the curvature invisible in profile also can be filtered out.

During the beginning phase of the research, many pattern-recognition algorithms had been tested but their running times were not acceptable. With the most algorithms, the re-simplification and the transformation of the pictures caused **significant time losses**. The time distribution of the processes in a general shape recognition algorithm running in the PC can be seen in *Figure 5*. (The running time of the tested algorithm was usually 10 to 30 s, disregarding the data transfer.)

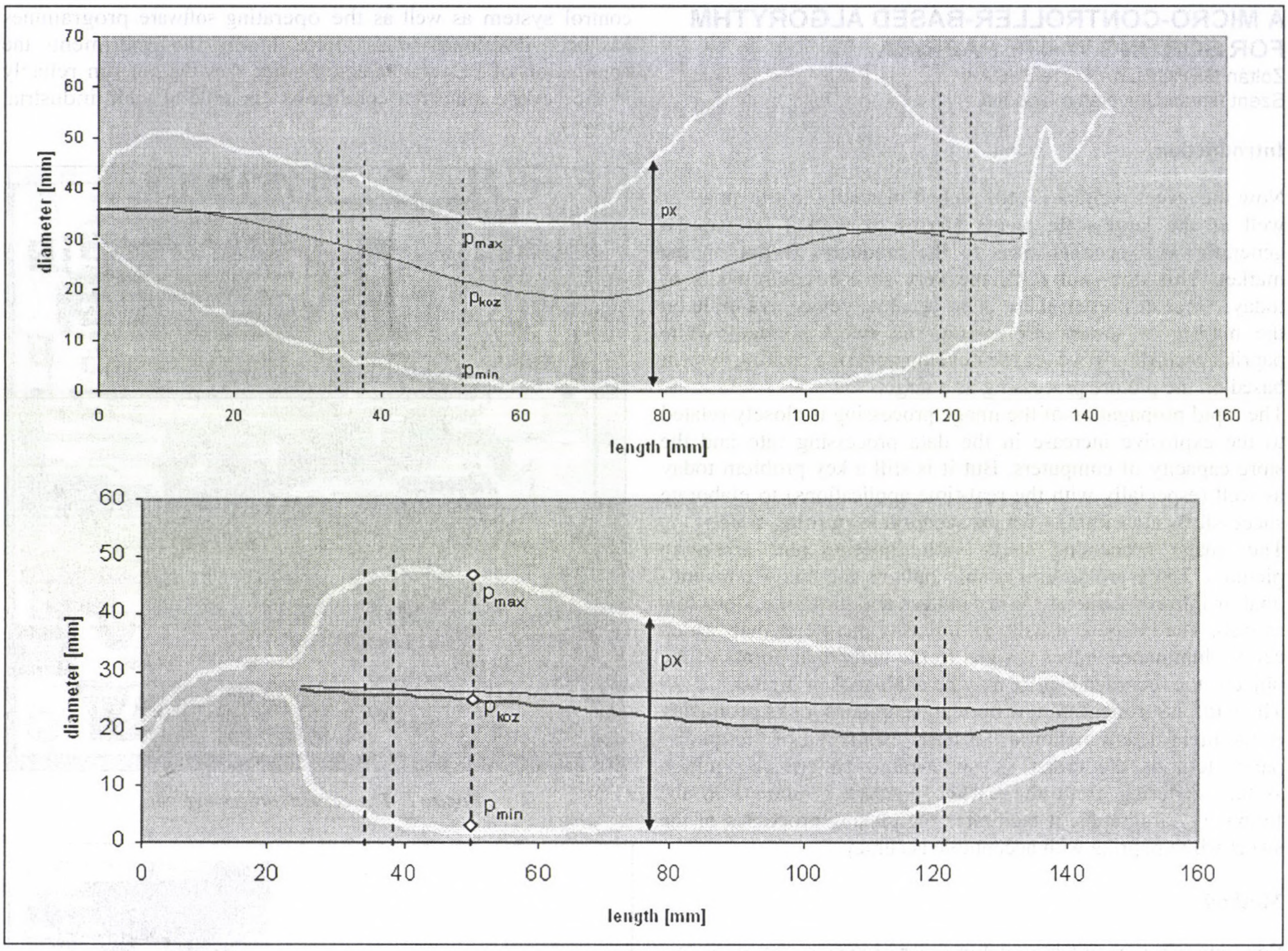

Figure 4 The contour recording process of a malformed and an un-deformed bell pepper

During the elaboration of the algorithm, particular attention was paid to the accuracy and the running rate suiting the requirements. In our self-developed system, the first processing of the data begins already in the camera during the reading-in accordingly the DSP receives the preliminary processed, suitably formatted and packed data flow (*Figure 6*).
With this method, the amount of unnecessary transferred data could have been significantly decreased; accordingly, we managed to reduce the transfer time to its fraction, and minimize the time of transformation jobs as well.

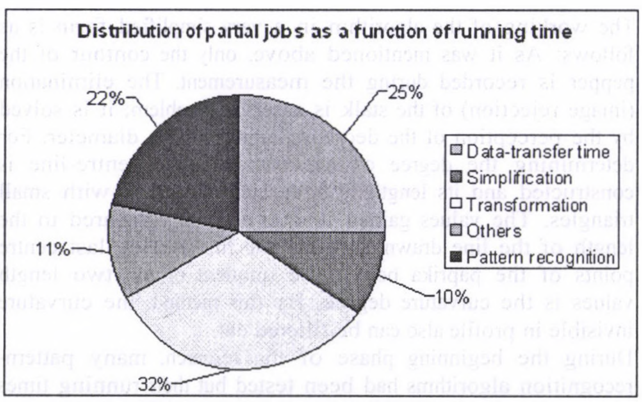

Figure 5 Distribution of the processes during the running time of an algorithm running by PC

In the present state of the system, the following data measured and computed from the records of the two cameras are accessible in about 1500 µs after the input of the last datum:

- length (interpreted without the stalk)
- shoulder-diameter
- perimeter
- length of centre-line
- area of cross-section
- degree of curvature

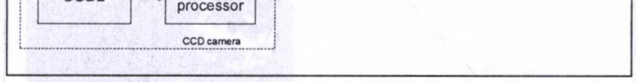

Figure 6 Path of data from the camera to the processor

Conclusions

When searching for the method of sorting, we have found that using the line CCD sensor is the most suitable process for recording contour.
The development of the measuring system was completed; the microcontroller-based pattern recognition seems viable for the further applications as well. The correct determination of the parameters required by the standard is provided by the

algorithm. Even in its present state, the algorithm is capable of recognizing easily the malformed peppers.
The designed measuring system and the algorithm very well performed its part during the long-term tests. The prototype system is working continuously at present as well; the evaluation of the data is also continuous.

Credits

The experimental system was constructed by the 'Furafol Hungary' Ltd in the frame of the R+D project INNODA No. 039/2005.
We owe Viktor Madár and 'Furafol Hungary' Ltd thanks for their help and collaboration in our measurement and the required testing program.

References

[1] Gergely Z., Madár V., Judák E.: Paprikaosztályozó rendszer kialakítása (Development of Paprika Classifying System) -MTA Agrárműszaki Bizottsága, Kutatási és Fejlesztési Tanácskozás XXXI. Gödöllő, 2007

[2] Gergely Z., Madár V., Judák E.: Paprikaosztályozó berendezés a növényházi termesztésben (Paprika Classifying System in Vegetable Growing) - MTA Agrárműszaki Bizottsága, Kutatási és Fejlesztési Tanácskozás XXX. Gödöllő, 2006

[3] Fűrész Gábor: CCD alapismeretek (CCD basics). Budapest: MCSE egyesület, 2003

[4] Sing-Tze Bow: Pattern Recognition and Image Preprocessing. Marcel Dekker Inc, New York, 2002

DISCHARGE COEFFICIENT DETERMINATION OF SWIRL-TYPE NOZZLES BASED ON HYDROLOGICAL ANALOGY

István SZTACHÓ-PEKÁRY
College of Kecskemét

1. Introduction

The discharge of swirl type nozzles depends from the constructional parameters and the working pressure. Spray nozzles are designed to produce certain spray characteristics, most notable of which is the relationship between fluid flow rate and inlet pressure. In attempting to gain some commonality between various manufacturers, styles and capacities, it became readily accepted by the plant protection to use the nozzle discharge coefficient [Koo, 1990]. The flow rate of nozzles is depending of constructional and operational parameters and the working pressure.
The atomization and the flow rate of nozzles can be characterized by the c_D discharge coefficient which includes the constructional and operational parameters. The discharge coefficient can be defined by the quotient of theoretical and real flow rates [Gerencsér, 1981]:

$$C_D = \frac{Q}{\frac{d_0^2 \cdot \pi}{4}\sqrt{\frac{2p}{\rho}}} = \frac{Q}{\pi \cdot r_0^2 \cdot v_x} \qquad (1)$$

where:
Q – the real flow rate [$m^3\ s^{-1}$]
d_0 – the outlet orifice diameter [m]
p – the operating pressure [Pa]
ρ – the density of the liquid [$kg\ m^{-3}$]
r_o – the outlet orifice radius [m]
v_x – the axial component of the discharged fluid velocity [$m\ s^{-1}$]

Numerous researcher attended to determine the discharge coefficient of swirl nozzles [Vörös, 1935], [Giffen – Muraszew, 1953], [Sitkei, 1960], [László, 1975]. The aim of their efforts were to determine the air-core diameter in the outlet region and the half spray angle $\alpha/2$.
In our assumption the air-core diameter will adjust itself so that the volumetric flow rate will be a maximum. Following the usual method of determining a maximum or a minimum, the equation is rearranged so that the discharge coefficient is a function of the air-core. This is then differentiated and set equal to zero. One then obtains one equation in one unknown, the air-core diameter in the outlet orifice.
This paper sets out to show the formulation of the principle of maximum flow for a swirl atomizer by analogy to the standard textbook derivation for the principle of maximum flow for a weir.
Weirs are essentially small, submerged walls placed across a river in order to step the river down a hillside and therefore control its flow velocity and hence prevent undue erosion. The water rises from a deeper level, on the upstream side of the weir and then flows over the top of the weir, to then cascade down over the downstream side. The volume flow over the crest of the weir is of course the same as it is in the deeper upstream region of the river. However, the flow is faster due to the reduced cross-sectional area of the water. The remarkable phenomenon is that the surface level of the water is actually lower, over the top of the weir, than it is in the main body of water in the upstream region. These heights, and the flow velocity, adjust so that the flow rate is a maximum.
In a swirl atomizer the swirl chamber is analogous to the deeper region upstream of the weir and the outlet corresponds to the weir itself. It is also found that the liquid surface level changes between the upstream region and the outlet. In other words the air-core diameter, and the axial velocity, adjusts so that the flow rate is a maximum.
In weir flow the surface topology and dynamics are governed by the volumetric flow rate and the force of gravity. In swirl atomizer flow the surface form and dynamics are governed by the volumetric flow rate and the analogous centrifugal force.

2. The geometrical characteristics and flow conditions of swirl nozzles

The cross-section of the swirl nozzle shows their geometrical parameters and the inner structure (*Fig 1*), where:
D – diameter of the swirl chamber [m]
d_{in} – diameter of the inlet tube [m]
d_{air} – diameter of the air-core in the orifice outlet plane [m]
α – spray angle [rad]
β – slope angle of the inlet tube [rad]
l – length of the swirl chamber [m]

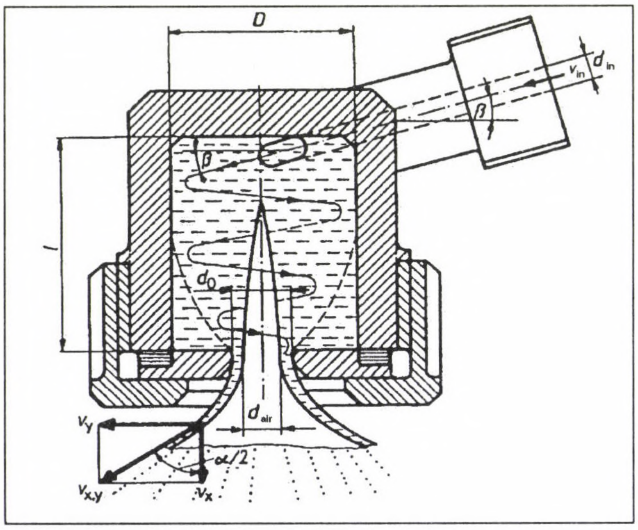

Fig. 1 Cross-section of a swirl nozzle

The axial velocity-component v_x of the discharged fluid:

$$v_x = \frac{Q}{\pi(r_o^2 - r_{air}^2)} \qquad (2)$$

where:
r_{air} – radius of the air-core in the orifice outlet plane [m]

and the inlet velocity a v_{in}:

$$v_{in} = \frac{Q}{\pi \cdot r_{in}^2} \qquad (3)$$

where:
r_{in} – radius of the inlet tube [m]

In first hand the velocity of the individually droplet in the fluid-film is:

$$|\bar{v}| = v_{xyz} = \sqrt{\frac{2p}{\rho}} \qquad (4)$$

and in other hand:

$$|\bar{v}| = v_{xyz} = \sqrt{v_x^2 + v_y^2 + v_z^2} \qquad (5)$$

where:
v_z – tangential component of the velocity [$m\ s^{-1}$]

The *Free Vortex Constant* C_Γ:

$$\mathrm{C}_\Gamma = v_z \cdot r_{air} = v_{in} \cdot \cos\beta \cdot \frac{D}{2} \tag{6}$$

The five equations above [(2)–(6)] contain six unknowns, therefore it is needed a sixth equation too. The sixth equation is given by the outlet conditions. These conditions are similar like the flow conditions above a weir.

3. The hydrological conditions the flow above weirs

The *Bernoulli-equation* for the conditions of flow above weirs – based on *Fig 2* – ca be written in the next form:

$$h(x) + H(x) + \frac{u^2}{2g} = h_0 + \frac{u_0^2}{2g} \tag{7}$$

and the volumetric flow rate:

$$Q = u \cdot h \cdot B \tag{8}$$

where:
h_0 – the depth of the liquid in front of the weir [m]
x – the *x-axis* on the figure
h(x) – the depth of the liquid, from the free surface down to the weir at the location x [m]
H(x) – the height of the weir at the location x [m]
u(x) – velocity for the liquid flowing over the weir at the location x [m s^{-1}]
g – gravitational acceleration 9,81 m s^{-2}
u_0 – velocity for the liquid in the main channel [m s^{-1}]
B – the breadth of the channel [m]

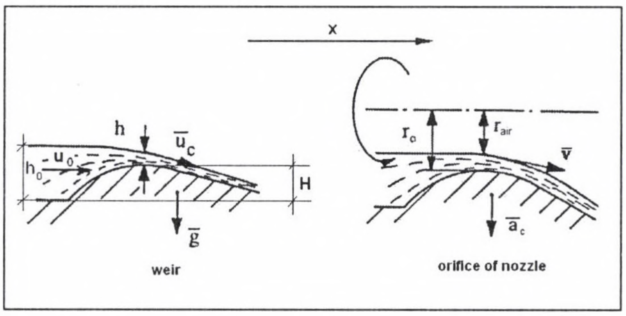

Fig. 2 The analogy of flow over a weir applied to the outlet of a swirl nozzle

The differentiation of equations (7) and (8) with respect to x given by:

$$\frac{\mathrm{d}h}{\mathrm{d}x} + \frac{\mathrm{d}H}{\mathrm{d}x} + \frac{u}{g}\frac{\mathrm{d}u}{\mathrm{d}x} = 0 \tag{9}$$

and

$$\frac{\mathrm{d}Q}{\mathrm{d}x} = B \cdot u \frac{\mathrm{d}h}{\mathrm{d}x} + B \cdot h \frac{\mathrm{d}u}{\mathrm{d}x} = 0 \tag{10}$$

which is equal to zero as Q will not vary with x, the direction of streaming. Both equation (9) and (10) may be rearranged to make d*h*/d*x* subject. The resultant expressions are equated with one another to provide

$$\left(\frac{u}{g} - \frac{h}{u}\right)\frac{\mathrm{d}u}{\mathrm{d}x} + \frac{\mathrm{d}H}{\mathrm{d}x} = 0 \tag{11}$$

At the crest of the weir, $\mathrm{d}H/\mathrm{d}x = 0$. The streaming velocity u(x) will continue to increase with axial direction as it passes over the weir so that $\mathrm{d}u/\mathrm{d}x \neq 0$, at the axial position of the crest of the weir. If both of these, reasonable, assumptions are applied to eqn. (11) then it only remains that, at the crest,

$$u = u_C = \sqrt{g \cdot h} \tag{12}$$

where the subscript c represents the crest, or critical position. This establishes an expression for the velocity of the flow over the crest of the weir and this will be used presently.

4. Hydraulically relations of nozzles based on analogy of weir

Like *Fig 2* shows for the nozzle can be used the centrifugal acceleration $a_c = v_z^2/r$ instead of gravitational acceleration g, and the $r_0 - r_{air}$ liquid-film thickness instead of depth of liquid *h*.

$$v_x = \sqrt{a_c \cdot (r_0 - r_{air})} + v_{in} \cdot \sin\beta \tag{13}$$

In this case the value of the centrifugal acceleration should be calculated for the liquid-thickness $r_0 - r_{air}$, allow for the equation (6) the relationship $\mathrm{C}_\Gamma = v_y \cdot r$:

$$\bar{a}_c = \left(\frac{v_z^2}{r}\right)\Bigg|_{r_{air}}^{r_0} = \frac{1}{r_0 - r_{air}} \int_{r_{air}}^{r_0} \frac{\mathrm{C}_\Gamma^2}{r^3}\,\mathrm{d}r \tag{14}$$

The solution of equation (14)

$$\bar{a}_c = \frac{\mathrm{C}_\Gamma^2}{2(r_0 - r_{air})} \frac{r_0^2 - r_{air}^2}{r_0^2 \cdot r_{air}^2} \tag{15}$$

Substitute equation (13) for equation (15):

$$v_x \cong v_{in} \cdot \sin\beta + \sqrt{\frac{\mathrm{C}_\Gamma^2}{2r_{air}^4}\left(r_0^2 - r_{air}^2\right)} \tag{16}$$

5. Discharge coefficient of the nozzle

The discharge coefficient of swirl nozzle using equations (1), (6) and (16):

$$\mathrm{C_D} = \frac{\pi \cdot r_{in}^2 \cdot v_{in}}{\pi \cdot r_0^2 \cdot v_{in} \cdot \sin\beta + \pi \cdot r_0^2 \cdot \frac{\mathrm{C}_\Gamma}{r_{air}^2} \cdot \sqrt{\frac{r_0^2 - r_{air}^2}{2}} \cdot \cos\beta} \tag{17}$$

and after the necessary replacing:

$$\mathrm{C}_D = \frac{r_{in}^2}{r_0^2 \cdot \sin\beta + r_0^2 \cdot \frac{D}{2 \cdot r_{air}^2} \cdot \sqrt{\frac{r_0^2 - r_{air}^2}{2}} \cdot \cos\beta} \tag{18}$$

6. Conclusions and summary

The resulting air-core radius only applies to non-viscous fluids. An increasing viscosity will lead to a loss in circulation and the centrifugal potential will decrease (among other effects like an increasing boundary layer) and the air-core will become smaller. As a result the flow rate will increase, as opposed to the case of fan nozzles or solid jet nozzles.

The air-core diameter (and on account of that the discharge coefficient) is independent of the pressure; is depends only on nozzle geometry. Since the air-core is constant in diameter the flow rate will be proportional to the square-root of the pressure.

References

[1] AKESSON, N. B. (1952): Recent investigations of spraying accessories. *Proc. 4th. Ann. Cal. Weed Conf.* 58-64 p.

[2] FRENCH, O. C. (1942): Spraying equipment for pest control, cal. *Ag. Exp. St. Bul.* 666.

[3] HINZE, J. O. (1955): Fundamentals of hydrodynamic mechanism of splitting in dispersion processes. *Am Inst. Of Chem. Engrs.*

[4] HOUGHTON, H. G. (1950): Spray nozzles, Chem. Engrs. Handbook, ed. J. Perry, *McGraw-Hill*: 1170-1175 p.

LANE, W. R. (1951): Shatter of drops in streams of air. *Indust. And Engg. Chem.*, 43. sz. 1312-1317 p.

[5] LITTAYE, G. (1943): Sur l'atomization d'un jet liquide. *Compt. Rend.*, Oct. 215, 340-342 p.

[6] SIDAHMED, M. M. (1997): Transport model for near nozzle fan sprays. *Transaction of the ASAE.* 40.k. 3. sz. 547-554 p.

[7] SITKEI GY, (1960): A keverékképzés és égés lefolyása diesel-motorokban. *Akadémia Kiadó*, Budapest, 67-91 p.

[8] SZTACHÓ-PEKÁRY I. (2003): The Energy Balance Method of Characterizing Sprays from Hydraulic Nozzles. *Hungarian Agricultural Engineering* (Gödöllő), 16.k. 38-40 p.

[9] SZTACHÓ-PEKÁRY I. (2005): A hidraulikus cseppképzés erőtani elmélete. Előadás és poszter. *MTA Agrár-Műszaki Bizottság XXIX. Kutatási és Fejlesztési Tanácskozás* (Gödöllő), január 18-19. Kiadvány, in print

[10] YOUNIS, S. M. 1969: Development of modified knapsack sprayer for effective control of cotton pests, M.S. Thesis in Ag. Engg., U. Alex., Egypt.

COMPARISON OF INERTIA TYPE SHAKERS IN A SOUR CHERRY ORCHARD

Zoltán LÁNG
Corvinus University of Budapest

Introduction

The most widespread method for stone-fruit harvest is the catch and shake technology, by witch a shaker unit, including rotating or alternating unbalanced masses, is clamped to the trunk or main branch of the tree. Vibration is due to the inertia force of these unbalanced masses. Figure 1. shows the working shames of the two inertia type shakers: the one with rotating eccentric masses (to the left) and the slider crank type machine.

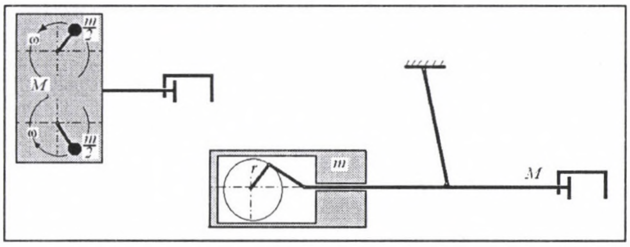

Figurel The two type of inertia shakers: the one with rotating eccentric masses ((left side) and the slider crank type one

According practice the efficiency of the shaker harvest is mostly influenced by the frequency of shaking and the amplitude of the fruit bearing branches. Replacing the fruit tree during shaking by a one degree of freedom damped vibrating system, its amplitude at the catching can be calculated using the following equation:

$$X = \frac{mr\omega^2}{\sqrt{\left(\frac{1}{c} - M_t\omega^2\right)^2 + (k\omega)^2}} \qquad (1)$$

where:
m is the unbalanced mass
M_t is the total vibrating mass, reduced to the catching cross section
r is the eccentricity of the total unbalanced masses
ω a is the frequency of shaking
c is the spring constant of the tree reduced to the catching cross section
k is the damping coefficient of the tree reduced to the catching cross section

It means that, the amplitude of the catching cross section is the function of the frequency, of the masses and of the physical properties of the tree itself.
The momentary displacement of the trunk in this case is:

$$x = X\sin(\omega t - \varphi) \qquad (2)$$

It's momentary acceleration:

$$\ddot{x} = -X\omega^2\sin(\omega t - \varphi) \qquad (3)$$

The maximal amplitude, following from Eqn. 3:

$$a_{\max} = X\omega^2 \qquad (4)$$

Another important characteristic of the shaker harvest is the power demand of the machine. Presuming again that the tree at the catching cross section shows linear viscous-elastic properties, the equation of the driving power of the machines is:

$$P = \frac{1}{2}X^2k\omega^2 \qquad (5)$$

Eqn. (5) shows, that the power demand is determined by the amplitude, damping coefficient and frequency. The values X and k are the functions of shaking height on the trunk.
The simple structural model proposed by Láng, 2006 is suitable for the calculation of trunk amplitude and acceleration due to shaking at any trunk height. For a defined shaking height Eqns. (1), (4) and (5) can be used. The parameters of the tree involved in the equations are shown in Fig. 2. The total mass M_t in Eqn. (1) is the sum of masses taking part in the shaking:

$$M_t = M_f + M + m \qquad (6)$$

where:
M_f is the mass of machine frame
M is the reduced limb mass to the catching cross section

The spring constant c is composed of two parts. The first one characterizes the elastic turning of the main roots with a certain soil mass around a horizontal axis. The second part is due to the elastic bending of the trunk. At the shaking height y their sum is:

$$c(y) = c'(y) + c''(y) \qquad (7)$$

where

$$c''(y) = \frac{64 \cdot y^3}{3 \cdot d^4 \cdot \pi \cdot E} \qquad (8)$$

d is the trunk diameter at y height
E is the viscous damping coefficient of the trunk

As Eqn. (8) shows, the trunk diameter d and modulus of elasticity E are also influence the amplitude and acceleration of the shaken trunk.

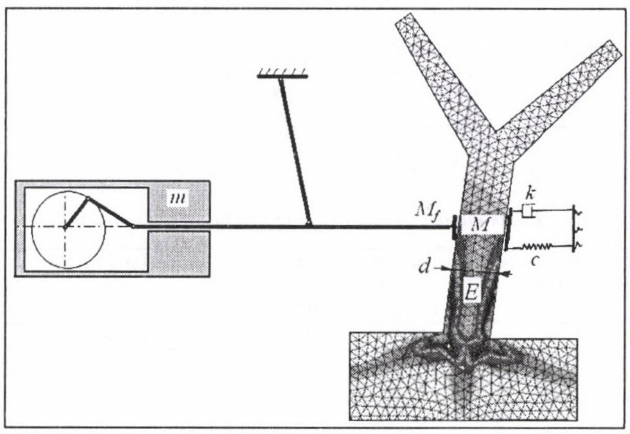

Figure 2 Parameters of the shaker- fruit tree model

In this paper the tests of two type inertia shakers (Fig.1) in sour cherry orchard are described. Measured acceleration and amplitude values on the tree trunk as well as the mechanical power demand of shaking are compared with theoretical values and conclusions are drawn of the model's ability. Also the shaker machine parameters are analysed to clear their effect on the shaker output.

Materials and method

The boom shakers involved in tests are shown in Figure 3 and 4. Both were driven hydro-statically. The first was a series produced one with slider crank type shaker head. The second was an experimental machine with rotating eccentric masses design to have similar output to the first one. The main parameters of both shakers are summarized in Table 1.

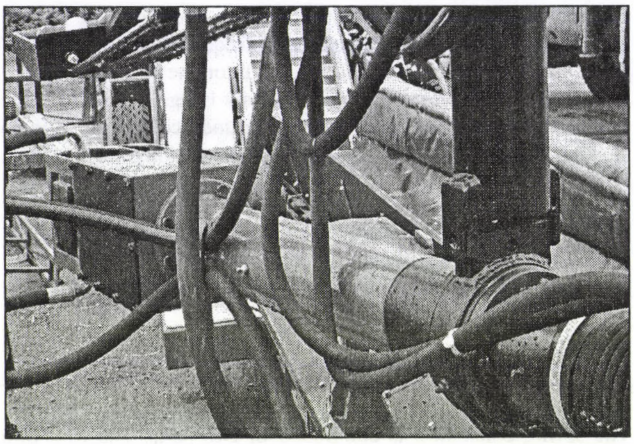

Figure 3 Slider crank type shaker unit

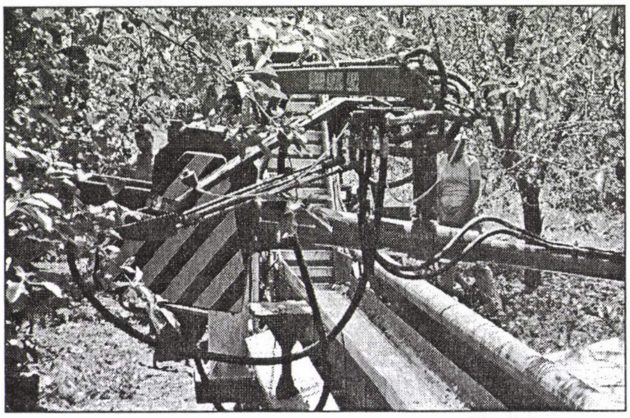

Figure 4 Machine with rotating masses

Table 1 Main data of the two inertia shakers

Shaker type	m, kg	M_f, kg	r, cm
Slider crank	111	75,2	3,5
Rotating eccentric masses	43,5	180,5	9,4

Table 2 Trunk diameters and catching heights of the tested trees.

No. of the tree in test	Trunk diameter, cm at the height of		Catching height cm
	0 cm	100 cm	
1.	12,7	12,7	100 and 78
2.	16,0	13,7	88 and 57
3.	14,6	12,1	91 and 64

The shakers were tested in 9 years old „Érdi bőtermő" vase form sour cherry variety. The same three trees were shaken by the two machines. Trunk diameters and shaking heights are shown in Table 2.
An accelerometer was fixed on the shaker boom. Trunk accelerations and mechanical power demand were measured during shaking the tree trunks at different height and different amplitudes.
Mechanical power demand was calculated by measuring torque and speed of the tractor PTO. All measured data as functions of time were recorded be a data logger.
To be able to compare test results the same trees were shaken by the two machines.

Results and discussion

Calculated and measured amplitudes and peak acceleration in function of shaking frequency are shown in Figure 5 for the tree No. 1. For the calculation Eqns. 1 and 3 were used. Tree parameters were taken from earlier field tests (Láng, 2006).

Figure 6 shows the calculated and measured power demands for the two shaker types in function of shaking frequency. The large differences between theoretical (calculated) and measured values are due to the low efficiency of the hydro-static drive. There is also a difference between the calculated power functions of the two shakers.
At the same power input the rotating type shaker runs on higher frequency (see the ■ dots) which leads – besides almost unchanged amplitude – to higher acceleration (Figure 6).

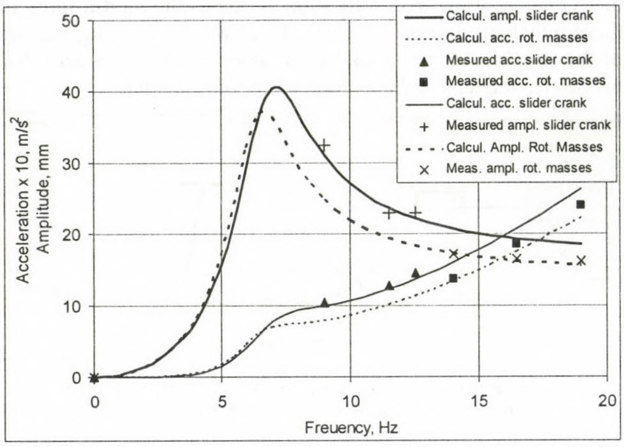

Figure 5 Measured and calculated acceleration and amplitude values for the tree No. 1

The higher acceleration at the shaker with rotating eccentric masses leaded to higher fruit detachment level: after shaking the trees with the slider crank type shaker, during the second shaking by the shaker with rotating eccentric masses about 95% of the fruit remained on the tree was detached.
The explanation for then different trends in power demand may be explained as follows. During shaking the different parts of the limb vibrate in different phases: those are in time delay to the shaker unit. This delay leads to interaction between those. The machine frame mass of the slider crank type shaker is much smaller than the one of the rotating type shaker (see Table 1); that's why its vibration is much more influenced by the limb vibration. As a result of it the acceleration-time function differs largely from the sinusoidal shape (Figure 7). From the other hand the shape of acceleration-time function of the shaker with rotating eccentric masses is closer to the sinusoidal.
Another reason can be the difference in eccentricity of unbalanced masses. As the catching surface between shaker and trunk can be regarded as viscous-elastic, at smaller eccentricity less effective amplitude remains for the displacement of the trunk.

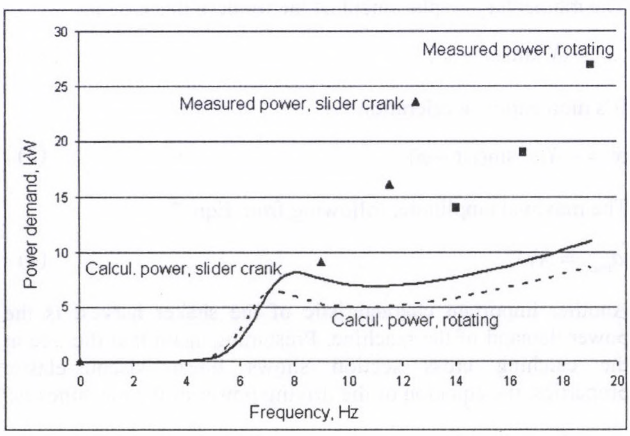

Figure 6 Measured and calculated power demands for the two type of shakers

Discussion

The acceleration and displacement amplitudes resulting from the two machine types coincide well with measured data. This proves the ability of the model used for the calculations.

In 9 years old „Érdi bőtermő” vase form sour cherry orchard higher machine-frame mass and eccentricity of unbalanced masses resulted in higher fruit detachment ratio. Further experiments should however be carried out to prove this phenomenon in different plantations. It can be presumed that orchard with different vibrating limb masses can be best harvested applying different machine frame masses.

References

Láng Z. (2006):Dynamic Modelling Structure of a Fruit Tree for Inertial Shaker System Design. Biosystems Engineering, 93(1), 35-44.

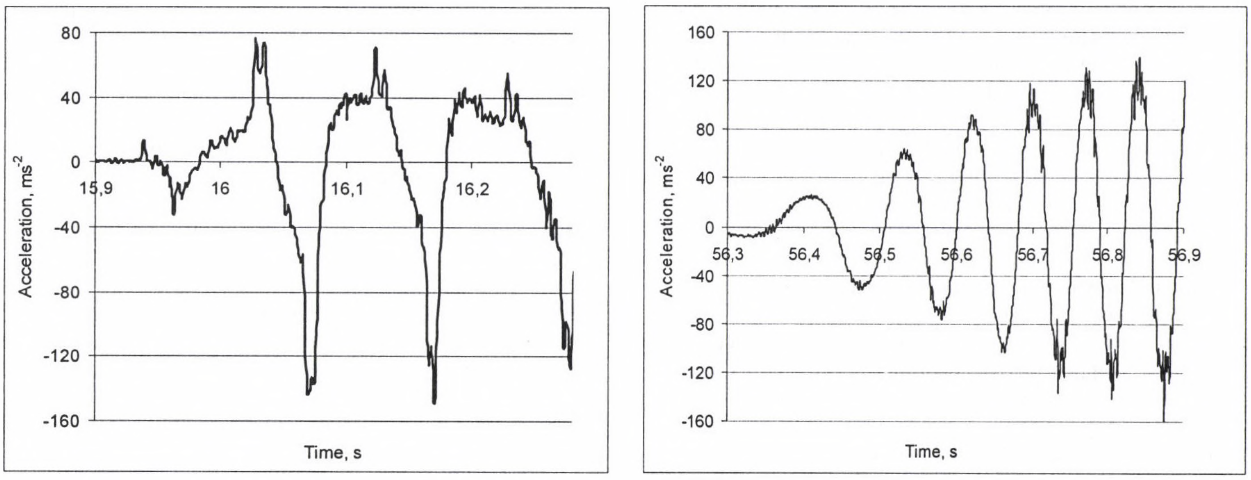

***Figure 7** Acceleration versus time functions for the slider crank (to the left) and rotating eccentric mass type shakers*

REDUCTION OF FRICTION AND CUTTING LOSSES IN FORAGE HARVESTERS

Péter KAJTÁR - Péter SZENDRŐ - Andreas HAFFERT
Szent István University, Gödöllő

Objective

Powerful self-propelled forage harvesters are currently used for chopping green forage for preservation in a silo with maximum harvester throughputs in excess of 300t/h fresh weight. These types of high throughputs can only be achieved by high motor outputs of up to 735kW. A large part of the total energy is required by the actual chopping process due to the fact that the green forage is cut in the chopper drum and then chopped in the steel rollers by pressure and shear stresses. A further significant amount of energy is required for transportation of material in the harvester, a process in which considerable friction losses arise as the result of the sliding processes between the chopped material and the harvester housing. In addition to the sliding friction, there is sliding between the particles (internal friction) in the chopped material. It is only possible to determine the internal friction with extreme difficultly and it is not considered further in this paper.
Tests are used firstly to investigate the friction coefficient between the chopped material and different materials at sliding velocities up to 40m/s. Theoretical investigations are then applied to investigate the effects of different parameters upon friction readings. This shows the potentials for minimisation of friction losses.
During the chopping process the compression rollers firstly feed the chopped material over the chopper drum shear bar. Here the material is cut by the knives positioned at the circumference. Centrifugal force and suitable baffle plates (drum disc and baffle plate) then transport the cut material to the steel rollers. The chopped material is further chopped in the steel rollers by pressure and shear stresses. The discharge accelerator then accelerates the chopped material to a higher velocity with paddles, and the material is then transported through the upper discharge chute onto an adjacent moving transportation unit. Deflection of material causes considerable friction losses in the discharge accelerator with subsequent material centring in the lower discharge chute as well as in the upper discharge chute (Fig. 1).

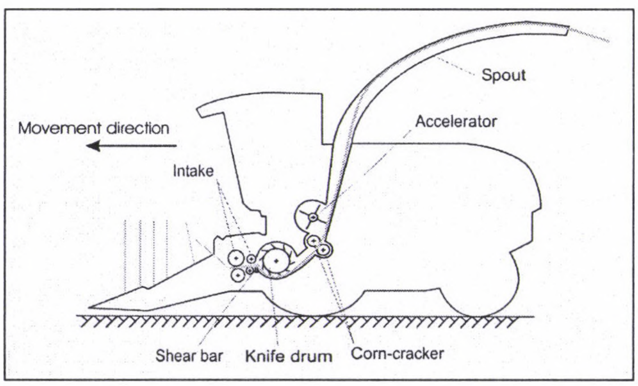

Fig. 1 Forage harvester construction and functional principle [2]

Material and methods

The friction force between two bodies is dependant upon the normal force and the coefficient of friction. In agricultural materials, coefficients of friction are dependant upon other parameters in addition to the type of material. An important parameter is the dampness of the chopped material. It deviates strongly depending upon weather conditions and the degree of ripeness. The friction velocity and level of normal pressure have an effect upon the coefficient of friction. A further problem in determination of the friction coefficient arises from the high inhomogeneity of the chopped material. Studies on the friction characteristics of agricultural materials to date are based upon sliding velocities from 5m/s to 10 m/s [1]. Velocities up to 40m/s are now investigated in order to achieve parameters similar to those in forage harvesters.
Practical investigations on the friction process are performed by using a test bed. The chopped material (e.g. grass or maize) is in a material holding device and pressed against moving plates. The normal force and friction force are measured during the test. The friction coefficient is then calculated from these two measurements.
Theoretical analysis and optimisation of the chopping process with regard to the friction processes are also part of the investigations. This involves analysis of the friction processes and a description of these processes in the form of modelling. The theoretical analyses also allow the possibility of using model calculations to determine the effects of parameter influence in the form of tendencies. Precise modelling of processes cannot be achieved due to the complexity in the form of material parameters. Fig. 2 is a chart of energy against the coefficient of friction derived from theoretical calculations for the whole chopping process. The energy loss increases overproportionally against the friction coefficients. When these losses are applied to the overall energy requirement for chopping grass, the percentage at high coefficients of friction is up to 15% [3].

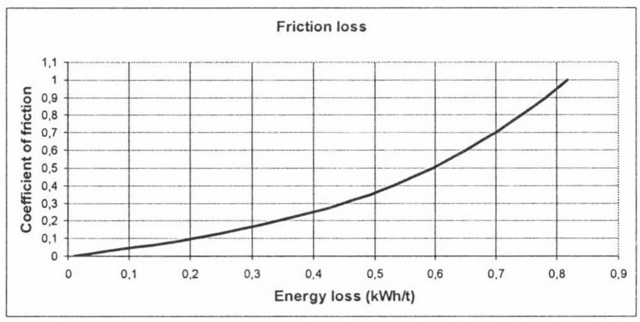

Fig. 2 Friction loss at different coefficients of friction

Fig. 3 shows the components with the respective friction losses of total friction loss in a forage harvester after the cutting process in the chopper drum. It can be seen that the losses in the chopper drum, lower discharge chute and upper discharge chute are about equal and total approximately 90% of the friction losses. The low material deflection in the baffle plate and discharge accelerator produce relatively low losses of approximately 10%.

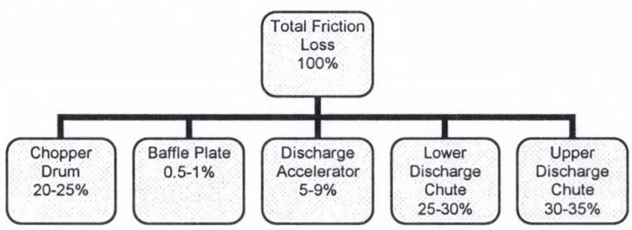

Fig. 3 Friction losses from theoretical calculations for each component in a self-propelled forage harvester

Friction losses at the knife inner edge are also produced during the cutting process in the chopper drum due to deflection of material during the cutting process. The knife geometry is derived from optimisation with regard to the cutting, transportation and delivery functions, i.e. it is the best possible compromise. Different knife geometries are then offered to some extent for use in grass and maize. The knife geometry differs primarily through the angle at the blade and the thickness of the knife. In order to achieve a pull-through cut, the knife is selected as V-shaped in most cases. This produces a reduction in the wedge angle on the knife and even torque readings at the chopper drum.

The cross-section of a maize stalk shows a very inhomogeneous structure. The soft core is surrounded by a hard and strongly fibrous layer. During cutting with conventional straight cutting edges, the stalks are initially squeezed together due to their hard outer layer until the cutting force exceeds the penetration resistance. This means that part of the energy used in the cutting process is required for compression. An investigation is also performed of whether a special knife geometry can bring about a reduction of the proportion needed for compression.

The knife geometries investigated are shown in Fig. 4. A point-shaped loading of the knife point owing to the knife shape is firstly produced when the knife strikes the stalk. This loading is achieved by the V-shaped or round slotted surface on the knife inner edge (Fig. 4).

A modified impact testing machine was used as the test bed. Each knife was attached to the pendulum and maize stalk in a bracket with shear bar in the lower section of the striking machine (Fig. 5).

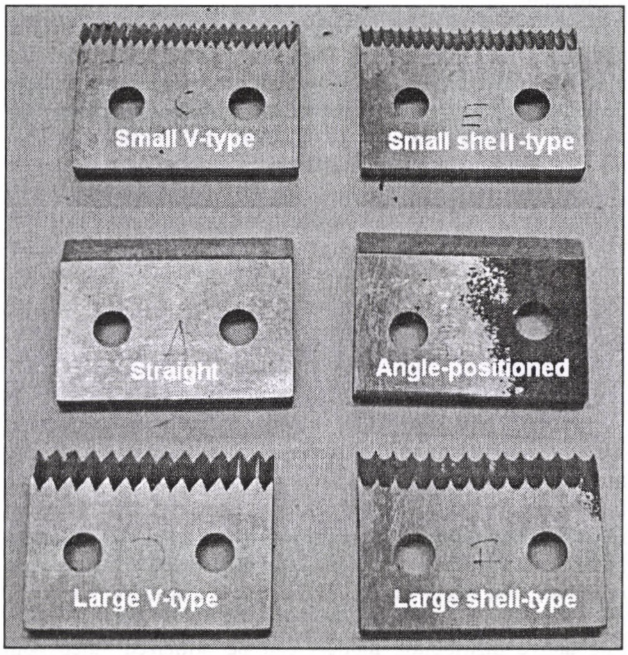

Fig. 4 Test knives

In order to guarantee comparability in the tests, the cutting tests were performed between two stalk nodes. The tests were performed with cutting lengths of between 10mm and 15mm and a cutting velocity of approximately 3.8m/s. The dampness of the stalks was 68%.

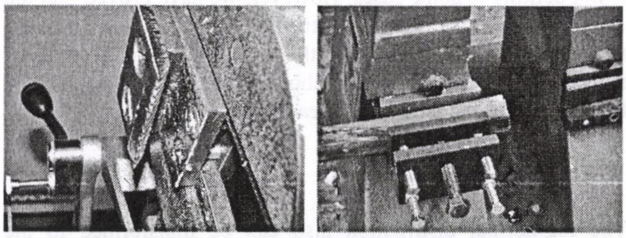

***Fig. 5** a; knife attachment, b; stalk bracket*

Results and discussion

The specific cutting energy was calculated from the measured cutting energy and the cross-section of the stalk,

$$w = \frac{W}{A}\left[\frac{J}{cm^2}\right],$$

where:
W – cutting energy,
A – cross-section of the stalk.

The cross-section was determined by using a special software program. The program used the limit of the cross-section to calculate each limit and from that the cross-sectional area.

The specific cutting energies for all knives are shown in Fig. 6. It can be seen that slotted knives have less energy consumption than conventional knives. Serrated slotted knives have a significantly lower energy consumption of 15% to 20%. A considerable reduction of cutting energy was established for shell-type knives with a small radius.

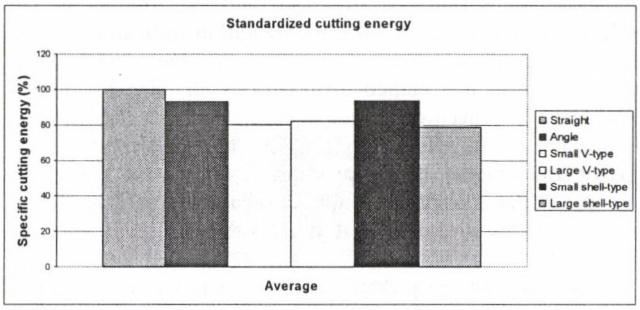

Fig. 6 The specific cutting energy for different knife geometries

Conclusions

Friction and cutting losses occurring in the chopping process cause a considerable increase in energy consumption. A reduction of friction energy losses can be achieved by optimisation of the material flow geometry. The decreasing normal forces achieved by material deflection cause a reduction of friction losses. A further possibility is provided from a reduction of the friction coefficient through the use of special materials in the material flow for which extensive research and testing is needed.

Some of the investigated knife geometries in the test bed show a significant cutting energy reduction of up to 20%. The cutting velocity here of approximately 4m/s is very low. The effect of a rotating knife and high cutting velocities of up to 40m/s can only be established by installation in the forage harvester chopper drum.

References

[1] F. Wieneke: *Reibungswerte von Pflanzen und Faserstoffen.* Munchen: Landtechnische Forschung 1956

[2] Szendrő, P. – Jóri, J. I. – Szüle, Zs.: *Mezőgazdasági géptan,* Bp. Mezőgazdasági Szaktudás Kiadó, 2003.

[3] Werner Röhrs: Untersuchungen zum Schneid- und Förder-vorgang in Trommelfeldhäckslern. Dusseldorf: VDI-Verlag 1988

PARTICLE-SIZE DISTRIBUTION OF GRINDS

Theoretical and empirical discussion
(OTKA research project No. T 048 446)
Lajos FOGARASI – Péter KORZENSZKY
Szent István University, Gödöllő

Objective

One of the most difficult problems is to determine and interpret exactly the quality of the grinds or other comminution products. During its history, for more than 100 years, the scientific analysis of the mills, the comminution processes and properties of the ground or milled materials has used the particle size as the fineness parameter. However, it is well known that an actual grits mass consists of particles with very different sizes – the size distribution range of the particles in a sample is relatively wide – so it is not easy to select the suitable **characteristic particle size** as a single-parameter fineness indicator. With the development of the particle-size measurement and the laboratory analysis as well as the modelling techniques of the size distribution records, quite good distribution model functions were managed to create and, in addition to the selected nominal particle size, the **deviation indicator** became the second characteristic parameter. By the mathematical processing of the gained distributions or size-distribution functions, the **specific surface area of the grits** mass can be calculated and its value may be used – as a **single value** – for **giving the fineness of the product.** It is needless to say that this parameter is not the real surface area of the particles due to the calculation method but it is a useful comparing fineness character.
The objective of the present article is to prove that the **grits samples are well analysable, and can be suitably mapped**, and – with the full knowledge of the used comminuter and the behaviour of the material to be ground or milled – all the conventional size **parameters can be transformed to each other** with an acceptable accuracy; the specific surface area can be computed from the **fineness characteristic function of one variable**.

Methods and materials

In the present research, a small/middle-capacity hammer mill with several different mill screens was used for grinding cereal grains (wheat, barley, maize etc.). The improved test system operated in a wide speed range is capable of producing grits with variable fineness; the kinetic, energetic and other mechanical data are automatically measured and transmitted to the computer control, measurement and data processing system, and recorded. The particle-size measurement is carried out by the laboratory sieve-analysis device. In its standardized form, the particle-size determination by sieving fits in well with the cereal grits of hammer mills.
The results of sieve analyses were plotted in size-distribution diagrams then regression curves were fitted onto the measured point sets. It is not reasonable to directly record the density function of the size distribution – that is the sieve fractions plotted against the sieve sizes in a histogram – because this method may enlarge the subjective and instrumental errors of the measurement, and distort the resultant curve. Instead of this, the particle-size analytical practice determines usually the sieve-oversize curves $R(x)$ – the ratio of the particles retained by the sieve-cloth of size x (*Figure 1*) – and then their characteristic parameters; the method is better compatible with the laboratory sieving process than determining directly the sieve-undersize curves $D(x)$ – the mass-specific size-distribution curves, otherwise the cumulative size-distribution of the grits sample – which is the complementary function of $R(x)$ i.e. $D(x) = 1 - R(x)$.

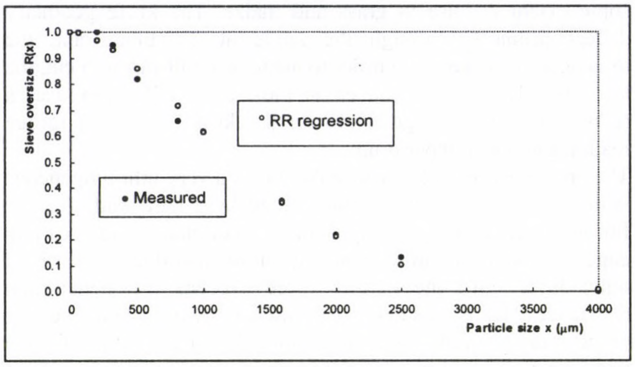

***Figure 1** The x-R diagram of the sieving analysis of a maize-grits sample*
1995; storage-dry maize ground by the laboratory hammer mill with the hammer speed 80.9 m/s, drilled φ5 mill-screen and the mass-flow rate 1.23 t/h

In *Figure 1*, the particle sizes are represented by the sieve sizes of the test screen set. In comparison with the points from the regression function (*see also Figure 2*), the measurement errors – the weaknesses of the sieve analysis – can be observed well in the diagram; however, the incidental deviations do not seem significant.
The regression analysis of the sieve curve requires a special conformal function. After a long complicated theoretical and mathematical research two distribution model functions have been accepted and standardized for the analytical practice – first the *RR* (or *RR(S)B* i.e. the Rosin-Rammler) and after the *log-normal* distribution formula. The former model was applied in the old German (DIN) standard and the latter is the base of the Hungarian and US (ASAE) standards valid at present.

The RR distribution: $R = e^{-\left(\frac{x}{x_0}\right)^n}$ and the log-normal formula:

$$D = 1 - R = \Phi\left[\ln\left(\frac{x}{x_{50}}\right)^m\right]$$

where x – particle (sieve) size; R – ratio of sieve oversize; x_0 – nominal particle size $x_0 = x(R = 1/e \cong 0.368)$; D – ratio of sieve undersize (over-tail); Φ – the Gaussian error (integral) function; x_{50} – nominal particle size $x_{50} = x(D = 0.5 \text{ or } 50\ \%)$ i.e. the median of the distribution; n and m – they can be considered as deviation characters of the particle-size distribution models, respectively.
The above distribution models can be criticized since both models are based on certain arbitrary assumptions however they approach quite well the empirical size distributions of the actual mill outputs. Their advantage is that 'only' two parameters characterize the distribution function. The main problem – especially with the *RR* model – is their uncertain validity in the super-fine range or at the actual limit particle sizes. The calculation of specific surface area of grinds with the *RR* model is not definite in some cases. However, we have proved that the characteristic parameters of the different models can be mutually transformed to each other. The regression analysis of the sieve data is simpler by the above *RR* formula since it can be transformed to the following linear equation:

$$\ln\ln\frac{1}{R} = n(\ln x - \ln x_0)$$

The log-normal distribution also can be transformed to the linear shape but its computer handling is much more difficult. The fitting of a sieve oversize curve can be seen in *Figure 2*; the closeness of the regression curve is very good; N. B. it is a non-linear regression reduced to the linear process. Anyway, it is more precise than the graphical-visual method on the special *RR* diagram net.

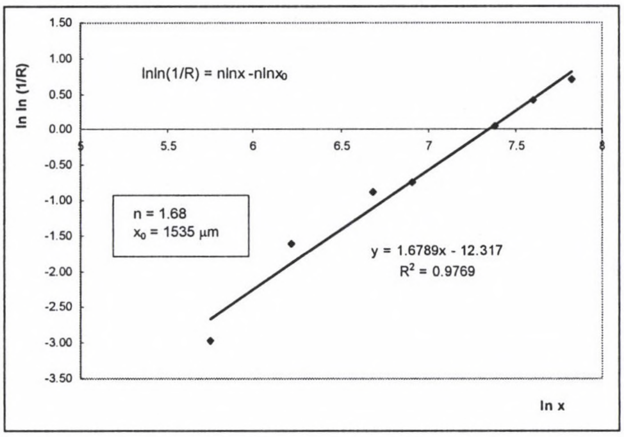

***Figure 2** Curve fitting onto data gained from the sieving analysis of maize grits*
1995; storage-dry maize ground by the laboratory hammer mill with the hammer speed 80.9 m/s, drilled ϕ5 mill-screen and the mass-flow rate 1.23 t/h

Experimental data gained during several years were processed and compared. We managed to synthesize such simple relationships which can be considered as universal characteristic curves of the actual hammer mill and the ground cereal grains (their grits).

Results and discussions

There are simple definite (linear) relationships between the different nominal particle sizes of the size distributions of very different samples produced by the laboratory mill independently of hammer speeds, screen types and sizes. The experimental check proves empirically this ascertainment at quite good correlation co-efficients (*Figure 3 and 4*). The relationship is valid also for other mills operating by the same comminution principle and similar matters. The empirical regression curve of the average particle size vs. nominal particle size x_{80} is better a power function but it only slightly deviate from the straight line (*Figure 4*); however, taking the equation of the regression line into consideration, the linear approximation is valid only in the actual domain.

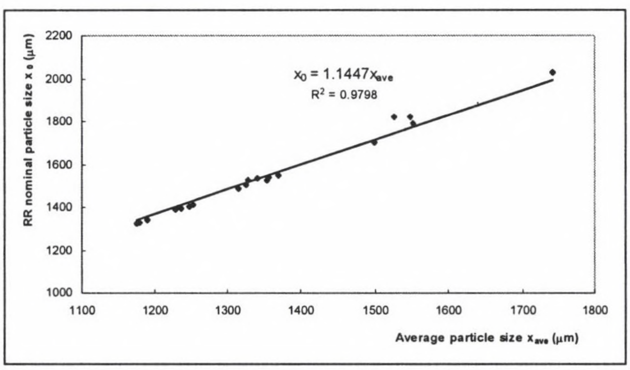

***Figure 3** Linear relationship between the average particle size and the RR nominal particle size of grits, with a close correlation across a broad operating spectrum*
1995, 2005, 2006; storage-dry maize ground by the laboratory hammer mill with different hammer speeds, mill-screen sizes and mass-flow rates

According to the empirical and theoretical analysis, the relationship between any nominal particle size and the calculated specific surface area of grits is a definite function of one variable – a general hyperbolic curve. It does not obviously stand to reason but we proved that the product of the two variables is constant in the whole particle-size range (*Figure 5*). The actual narrow deviation strip is due to different subjective and instrumental or methodical errors, and the unhomogenity of the material. It has to be marked that the random deviations of the independent and dependent variables are cumulated in the product. This hyperbolic function is the **fineness characteristic curve** of the actual material to be ground. With the tested comminution principle, it can be considered as a general constitutive law.

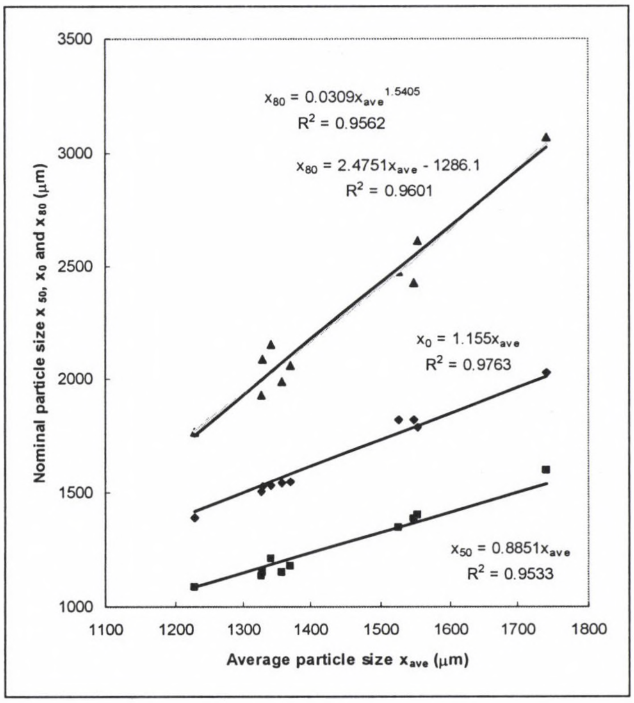

***Figure 4** Relationship between the average particle size x_{ave} and the nominal particle size x_{50}, x_0 and x_{80} of maize grits*
1995; storage-dry maize ground by the laboratory hammer mill with two hammer speeds, drilled ϕ5 mill-screen and different mass-flow rates

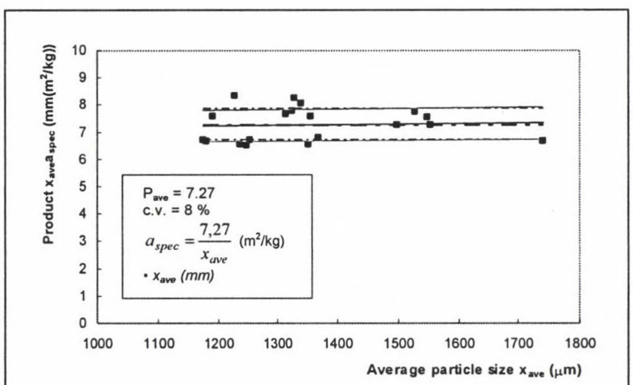

***Figure 5** Empirical demonstration of the general hyperbolic function of specific surface area vs. average particle size of grits*
1995, 2005, 2006; storage-dry maize ground by the laboratory hammer mill with different hammer speeds, mill-screen sizes and mass-flow rates

Conclusions

The mutual convertibility of the different nominal particle-size values into each other by a simple (linear) and definitive relationship is proved. It is very important when interpreting or comparing the results defined and calculated from different – even old – sieve analyses. The relationship between the specific surface area and an arbitrarily chosen nominal particle size (x_{ave}, x_0, x_{50}, x_{80} etc.) of the grits is a general hyperbola; the variation coefficient (relative deviation from the average – 7 to 8 %) of the product of the dependent (a_{spec}) and the independent (x_{nom}) variable is acceptable. It can be explained in the way that the deviation characters of the particle-size distributions (modelled by the *RR* as well as the *log-normal* formula etc.) are also probability variables and their expected values characterize the actual mill (the comminution principle) and the ground material.

References

[1] Mikecz I. – Fogarasi L. – Akdeniz, R. C.: Influence of screen construction on fineness of grits made by hammer mills. Hungarian Agricultural Engineering 1990 No. 2 p. 44-46 HU ISSN 0864 – 7410

[2]Fogarasi L.: Kalapácsos darálók energetikai és főbb műszaki jellemzői új rostakonstrukciókkal (Energetic and other main technical properties of hammer mills with new screen constructions). (Doctoral dissertation) University of Agricultural Sciences – Faculty of Agricultural Engineering Gödöllő 1996

[3] Fogarasi L. – Douba M. – Sembery P.: Relationships between Fineness Parameters of Grits Ground by Hammer Mill. Hungarian Agricultural Research (Journal of the Ministry of Agriculture) Hungary 1997 No. 1, p. 8 – 9 HU ISSN 1216 – 4526

Péter KORZENSZKY
(An OTKA research project No. T 048 446)
Szent István University, Gödöllő

EFFECT OF HAMMER SPEED ON PARTICLE SIZE DISTRIBUTION IN HAMMER MILLS

Objective

The main objective of the research is the detailed effect analysis of the constructional, dynamic and process properties determining the **energetic conditions** and the **efficiency** (which is extremely bad with the mills) of the comminution. The state of motion of the charge is a complex of the motions and collisions of the single particles that are determined by the superposed elementary interactions. So, in the analysis, a critical dynamic parameter, besides the charge mass and the particle-size distribution by mass, is the **peripheral velocity of the rotor** which at once is an input property as well. The measurement system is capable of varying infinitely and continuously the hammer speed.

Methods and materials

The laboratory-size measurement assembly is composed of a hammer mill (type Zenit Junior with three-stage V-belt transmission) driven by a bipolar asynchronous motor (type Leroy Somer LS132ST of 5.5 kW) through the frequency converter OMRON 3G3MV (Figure 1).
With the help of the frequency converter, the rated synchronous rotary speed of motor 3000 rpm (50 Hz) is infinitely adjustable (theoretically) between 0 and 400 Hz.
Because of the design of the motor and some other reasonable parameters, it was temporarily expedient to limit the output frequency of the converter to 60 Hz that is slightly higher than the rated rotary speed; the actual test range was between 0 and 3600 motor rpm.
During the tests the rotary speed of the motor (and the mill) and the position of the hopper slide (feed opening ratio) was selected or adjusted, with each actual material to be ground and screen type and size.
In the course of the experiments, the rotary speeds of the driving and the driven shafts, the power supplied by the frequency converter were measured. With the help of the strain gauges (adhesive measuring tapes) glued on the shaft of the mill, the torque (M_2) was measured from which the net mechanical power input was calculated. At the same time, the rotary speeds (n_1 and n_2) and the temperature of output grits (t_{grits}) were measured and recorded as well. To determine the mass-flow rate of the test material (here corn), the variation in mass of the input and output was recorded with the help of electro-tensiometric dynamometers. The performance of the mill is defined as the **mass flow rates** of the feed (Q_{in} as input) and/or the outflow (Q_{out} as output) material (in kg/s or t/h). The rates are equal to each other in the stationary running.The gained data were recorded by the measuring and data-acquisition device SPIDER 8 (Figure 2).
The particle size distribution by mass was determined by the sieve analysis and, after processing the gained data, the size distribution and the distribution density (frequency) functions of the grits samples was recorded and plotted (Figure 3). Here the RR(S)B distribution model was used for fitting the sieve oversize curves. Different nominal (or denominated) particle sizes (x_{80}, x_{50} , x_{30} etc.) were calculated from the regression functions.
With increasing the rotor (or hammer) speed, the particle size distribution curves are definitely shifted to the left, into the finer range. However, the shift is apparently not in direct ratio to the change of the peripheral speed and the used conventional mill screen of 3.5 mm does not react considerably to the change in speed (Figure 4). In the grinding practice, a frequently used parameter is the reference particle size calculated with different nominal oversize fractions. Figure 5 shows an example plotted from our measurements. The same can be realized: the slope of the curves is relatively slight however the trend of the relationship is quite a clear.

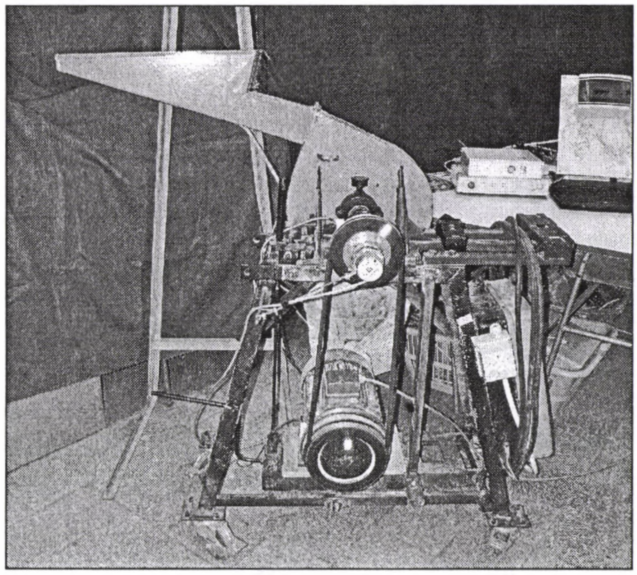

Figure 1 The laboratory measurement system (hammer mill type Zenit Junior)

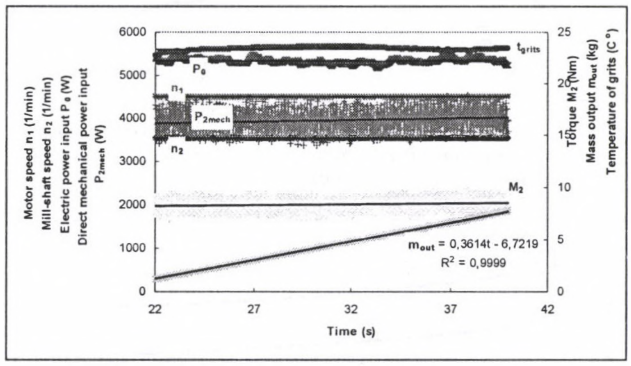

Figure 2 Recorded curves in the stationary range (maize, moisture content: 10.5 %, screen size: 3.5 mm, converter frequency: 60 Hz, feed opening: 100%)

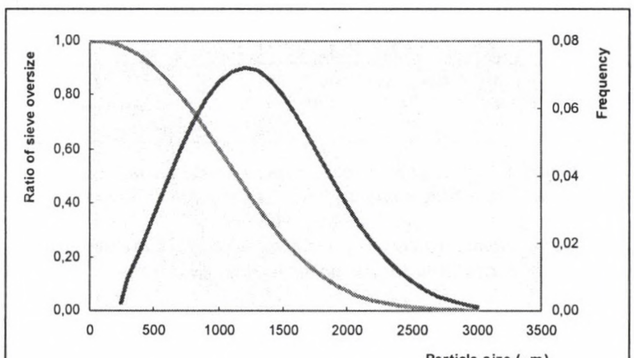

Figure 3 Plotted size distribution curves (maize, moisture content: 10.5 %, screen size: 3.5 mm, converter frequency: 60 Hz, feed opening: 100%)

The specific surface area of the sample – a_{spec} in m^2/kg –can be calculated with the knowledge of the actual particle size distribution function. The surface-area increasing intensity or fineness production – $dA/dt = Q\,\Delta a_{spec}$ (m^2/s) – is the second important characteristic performance parameter of the mill when grinding an actual material.

Results and discussions

The effect of the increase in hammer speed is definitely more considerable upon the produced new surface area of grits in a time unit surface increasing intensity. The diagram of the net power input plotted against fineness production (Figure 6) shows that the relationship is linear with a good correlation (r = 0.968). The angular coefficient (slope) of the straight line is the energy level ν (actually = 2485.3 J/m^2); the energy consumption in the mill per a unity new particle-surface area is considered as the grindability characteristic of the material related comminution principle of the mill.

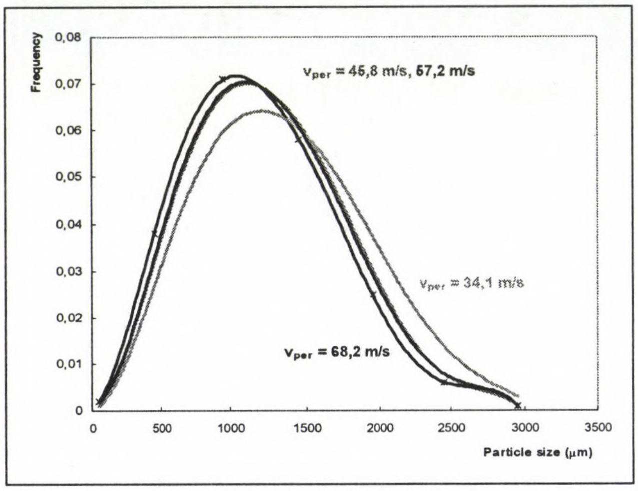

Figure 4 Effect of the hammer speed on the particle size frequency
(maize, moisture content: 10.5 %, screen size: 3.5 mm, feed opening: 100%)

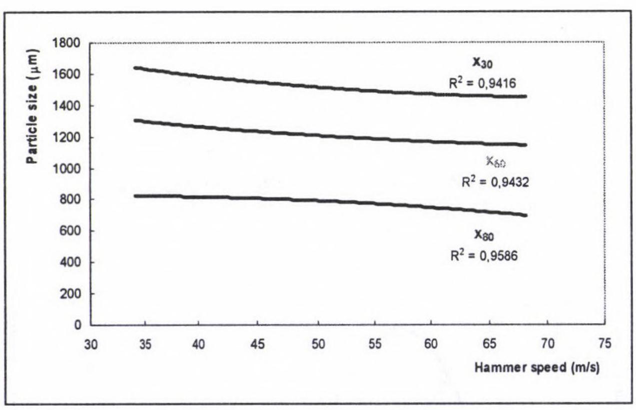

Figure 5 Effect of the hammer speed on the particle size
(maize, moisture content: 10.5 %, screen size: 3.5 mm, feed opening: 100%)
x_{30}, x_{50}, x_{80} – limit particle sizes; the mass ratio of the oversize grits ($\geq x_{lim}$) is 30, 50 and 80 %, respectively

Conclusions

The relationship between the surface increasing intensity (i.e. the fineness production of the hammer mill) and the mechanical power input is **definitely linear** with quite a close correlation, and proves again the earlier gained theoretical main characteristic functions of the hammer mills. It can be considered as the **constitutive operating law** of the actual hammer mill. The angular coefficient of the function ν is the grinding energy level; it is essentially the grindability (i.e. **characteristic) of the material** to be ground. The relatively wide range, in which the fineness production changes, is primarily due to the effect of the mass-flow rate variation; the hammer speed better affects the mass flow rate Q than the grits fineness.

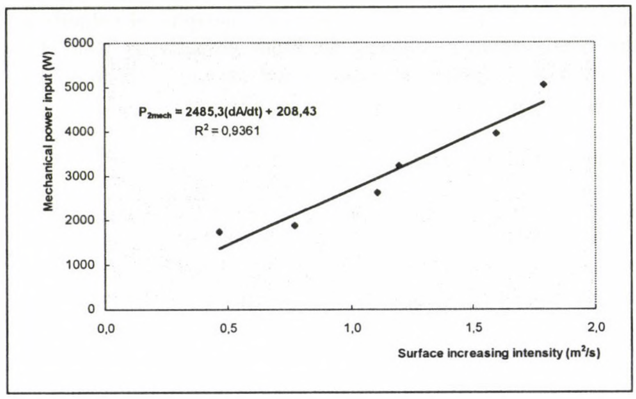

Figure 6 Relationship between the surface increasing intensity and the mechanical power measured on the input shaft of the mill
(maize, moisture content: 10.5 %, screen size: 3.5 mm)

References

[1] Korzenszky P. – Dr. Judák E. (2005): Measurement Assembly for Energetic Analysis of Comminuters. Hungarian Agricultural Engineering, 18/2005 (72-74. p HU ISSN 0864-7410)
[2] Petróczki K. – Aldabbar M.H.M. (2006): Terménydaráló nyomatékának mérése nyúlásmérő bélyeges nyomatékérzékelővel, MTA AMB Kutatási és Fejlesztési Tanácskozás, Nr.30. 131-135 p.
[3] Fogarasi L. – Douba M. – Sembery P. (1996): Grinding Cereal Grains by Hammer Mill. Hungarian Agricultural Engineering 1996 No. 3 (31 – 35. p. HU ISSN 0864 – 7410)
[4] Fogarasi L. – Douba M. – Sembery P.(1996): Relations between Surface Geometry of Hammer Mills and Energetic Parameters. Hungarian Agricultural Engineering 1996 No. 9 (54 – 57. p. HU ISSN 0864 – 7410)
[5] Korzenszky P. – Fogarasi L. (2006): Kinetic and Energetic Analysis of Grinders Faculty of Business Management at the University of Forestry, Journal of Management and Sustainable Development, 24-26. March 2006. (90-94. p ISSN 1311-4506)

AUTOMATIC STEERING OF POWER MACHINES WITH GPS NAVIGATION AID IN AGRICULTURE

József HAJDÚ[1] - István FÖLDESI[1] - András FEKETE[2] - József DEÁKVÁRI[1] - László KOVÁCS[1] - László MAGÓ[1]
[1] Hungarian Institute of Agricultural Engineering, Gödöllő
[2] Corvinus University of Budapest, Budapest

1. Introduction

There are different GPS-based navigation systems to reduce steering error especially with high speed and large working width operations. The navigation system is either a part of an automatic steering system, or it is a navigation aid having a special display indicating the direction of the proposed steering correction.

GPS-based navigation system should be used for minimizing overlapping and skips/gaps between consecutive runs with seeding, spraying, fertilizing, soil tillage, harvesting and especially when operating machines of large working width.

GPS-based navigation system is needed for different agricultural vehicles used for precision agriculture, especially for such purposes as soil sampling and data recording, field mapping, performing site specific operations, designating definite leading lines, following a definite leading line (by GPS navigation and manual steering) and following a definite leading line by GPS based automatic steering.

2. Objective

The objective of the work reported herein was to measure, analyze and compare the steering error with different steering modes, such as steering with GPS-based automatic vehicle steering, GPS-based navigation aid (manual steering according to the indications displayed by the navigation aid) and conventional manual steering (without any navigation aid).

3. Method

Experiments were performed along flat fields where a straight line was determined along the edge of the test field to be the leading line. The coordinates of this line were stored in the memory of the on-board computer to which the dGPS was connected and the tractor was driven along this line and the wheel tracks of the tractor provided with the actual leading line.

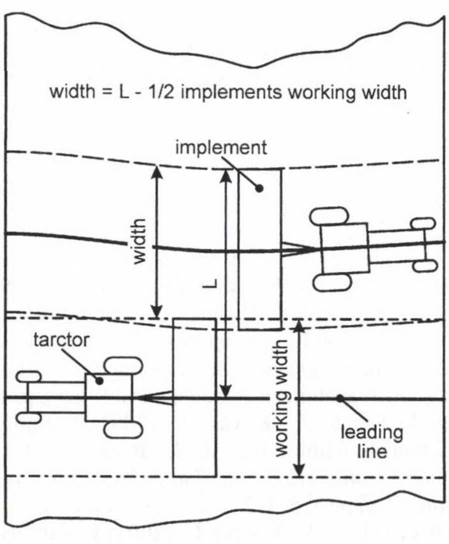

Fig. 1 Field experiment and the determination of "width"

Test runs were done with a four-wheel drive tractor and with four different implement combinations. The main characteristics of the implements used for the experiments were, as follows:

- disk harrow: working width: 6.9 m, average speed: 7.5 km/h
- field cultivator: working width: 8.7 m, average speed: 11.5 km/h
- seed drill: working width: 9.0 m, average speed: 10.0 km/h.
- fertilizer spreader: working width: 27 m, average speed: 14.0 km/h.

The purpose of the driver was to follow the straight leading line by

- automatic steering system,
- manual steering according to the indications displayed by the navigation aid and,
- manual steering without any navigation aid.

The automatic steering system used for the experiments was the John Deere „Auto Tracking" that controls the servo steering of the tractor via solenoid valves.

The GPS used for the experiments was a StarFire iTC with dual frequency receiver and the receiver had a built in gyroscope to compensate the roll (rotation on horizontal axis) to ensure approximately 100 mm path to path accuracy.

The navigation aid (parallel tracking) was supported by John Deere „Parallel Tracking" device having StarFire SF2 iTC antenna with dual frequency receiver and built in gyroscope and the steering was performed by manual steering according to the display of the „Parallel Tracking" device.

Four test runs were performed with each tractor and implement combination with the three different steering modes. The result of the experiments was determined by the distance between the leading line (base line) and the central lines of the wheel tracks for four test runs. The maximal and minimal value of the working width, the average value of the width, the average error of the width and the standard deviation of the width were determined. 40 to 50 measurements were performed along the 400 to 500 m long test runs.

The best characteristics to describe the quality of steering are the error and the range. The error characterizes the variations in the working width that is the difference between the set point of the working width and the average value of the actual working width. Another beneficial characteristic is when taking into account the maximum and minimum amplitude of the variation. This characteristic can be calculated from the difference of the maximum and the minimum value of the working width on a definite length.

Therefore the results of working width measurements were evaluated with different steering modes and the characteristics of the working width were determined, as follows: average value, maximum value, minimum value, the range that is the difference of maximum and minimum value and the error of the steering. (Földesi, *et al.*, 2006)

4. Results

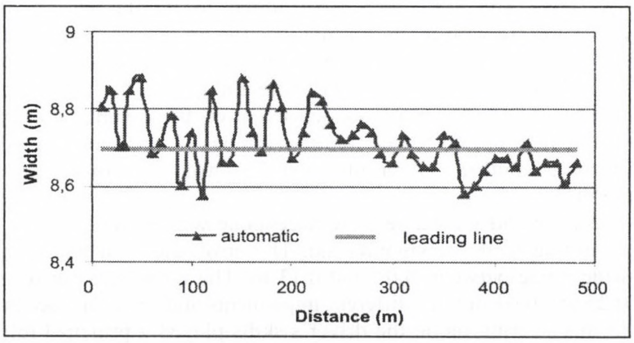

Fig. 2 Working width in the function of the run length by the tractor and field cultivator combination with automatic steering
(average speed: 11.5 km/h, working width of the equipment is 8.7 m)

The working width in the function of the run length by the tractor and implement combination is shown for automatic steering (Figure 2), for steering according to navigation aid (Figure 3) and for conventional manual steering in Figure 4.

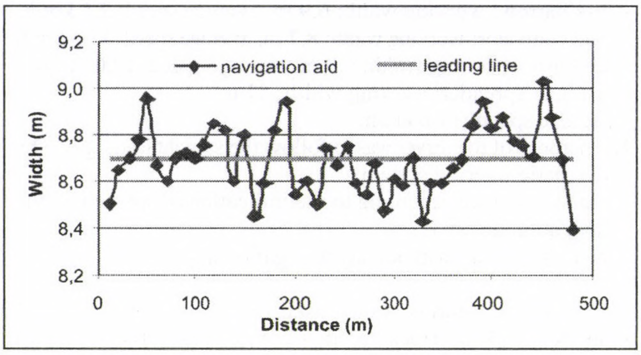

Fig. 3 Working width in the function of the run length by the tractor and field cultivator combination with steering according to navigation *(average speed: 11.5 km/h, working width of the equipment is 8.7 m)*

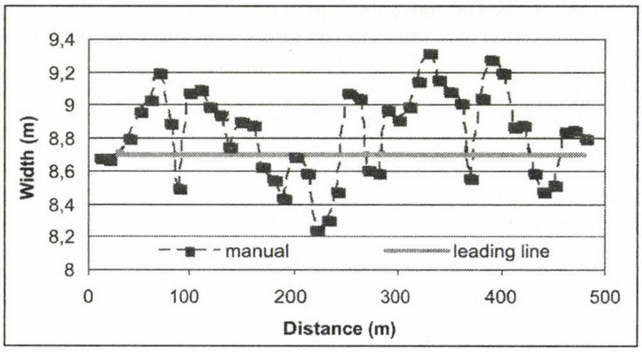

Fig. 4 Working width in the function of the run length by the tractor and field cultivator combination with manual steering *(average speed: 11.5 km/h, working width of the equipment is 8.7 m)*

The results obtained with the closed loop automatic steering system were independent on the skills of the driver. The driver with the navigation aid was aware of the relative position of the vehicle and he played the role of a part of the control system (sensor, controller and actuator), therefore the driver's skills had a definite influence on the quality of the results. With conventional manual steering without any navigation aid the driver had to find out the relative position of the vehicle without any objective information and had to do the steering according to his skills.

The results of working width measurements are shown in Tables 1 to 4 with different implements and steering modes. The characteristics of the working width (average value, error, maximum value, minimum value, difference of maximum and minimum value) were determined.

The error and the range were found to be the best with automatic steering mode. In this case the error was small, 0.01 to 0.08 m. The range was quite narrow between 0.21 and 0.58 m with different implements and different speeds. In automatic steering mode the error was dependent on the accuracy of the positioning by GPS and on the tuning of the closed loop steering control. Other disturbances had no considerable influence.

The error and the range were acceptable with manual steering according to the navigation aid. The error was in a relatively wide range between 0.01 and 0.13 m. The range was between 0.23 and 0.64 m with different implements and different speeds. In this steering mode the driver's skills played a principal role in the quality of following the leading line. The accuracy of the GPS was important, but other disturbances had no importance. Naturally, the reliability of the steering is not good in this mode since the error increases with the fatigue of the driver.

The error and the range were not acceptable at manual steering without any navigation aid because there were large variations. In this case, the driver's skills and the visibility played considerable role in the quality of the steering. The error and the range increased with higher forward speed and with wider working width. The error was between 0.02 and 2.24 m and the range was between 0.33 and 3.50 m.

Naturally, the steering error was found to be dependent on the steering mode. The forward speed of the tractor and implement combination had a considerable influence on the error, as well. However, the error was dependent on the working width and the visibility of the edge of the previously cultivated/covered area. The results of the tests with four different implements showed that the average error in the working width was 0.01 to 0.02 m with automatic steering, 0.01 to 0.08 m with the navigation aid and 0.02 to 2.24 m with manual steering. (Fekete, *et al.*, 2005)

Table 1 The average error in the working width at automatic steering

Steering mode	Average working width, m	Working width, m	Average error, m
Disk harrowing	6.91	6.9	**0.01**
Field cultivator	8.72	8.7	**0.02**
Seeding	8.92	8.9	0.02
Fertilizer spreader	27.01	27.0	0.01

Table 2 The average error in the working width at manual steering with the navigation aid

Steering mode	Average working width, m	Working width, m	Average error, m
Disk harrowing	6.96	6.9	0.06
Field cultivator	8.69	8.7	**0.01**
Seeding	8.87	8.9	0.03
Fertilizer spreader	26.92	27.0	**0.08**

Table 3 The average error in the working width at manual steering

Steering mode	Average working width, m	Working width, m	Average error, m
Disk harrowing	6.92	6.9	**0.02**
Field cultivator	8.83	8.7	0.13
Seeding	8.93	8.9	0.03
Fertilizer spreader	29.24	27.0	**2.24**

5. Conclusion

The error of the working width was found to be the best with automatic steering where it was independent on the driver's skills. The error was acceptable in several cases with the navigation aid. However, the error was dependent on the driver's skills and on paying attention to the display. With manual steering the error measured was too high in several cases and it was dependent on the driver's skills and attention.

References

[1] Fekete, A., Földesi, I., Kovacs L. (2005) Steering error with GPS-based vehicle navigation aid. *Book of Abstracts of 5th European Conference of Precision Agriculture*, p. 89-90.

[2] Formato A., Faugno S. Paolillo G. (2003) Contribution to the design of an autopilot for tractors: consideration on the set-up of the system. *Programme Book of the Joint Conference of ECPA-ECPLF*. Wageningen Academic Publishers. p. 403-405.

[3] Földesi I., Fekete A., Kovács L. (2002) Variations in the nutrient content within the field. *Book of Abstracts of International Conference of EurAgEng on Agricultural Engineering, Budapest*, p. 1-7.

[4] Földesi I., Fekete A., Kovács L. (2003) Feasibility of GPS-based vehicle navigation aid. *Proceedings of 4th European Conference of Precision Agriculture*, p. 397-398.

[5] Földesi I., Fekete, A., Kovacs. L. (2006) GPS-based Automatic and Manual Vehicle Steering. Bonn, XVI. CIGR World Congress, *VDI-Berichte* **Nr. 1958**

CREATION OF DEVELOPMENT SYSTEM FOCUSING ON PRODUCT-RANGE

Lászó FENYVESI – Szilvia KÉSMÁRKI-GALLY ERDEINÉ
Hungarian Institute of Agricultural Engineering, Gödöllő

Introduction

The macro-economic location, evaluation, operation of subsidy systems, CAP-reform and necessity of agricultural production are sources of debates all over the world. Besides certain balance explanations they are the traditions and mainly political reasons that are behind the agricultural "regulations" formed in separate regions. The European subsidy system is most probably due to change [1, 6] that results definitely in production support decrease.
The current system is not only deforming the real economic situations deteriorating the healthy development of entrepreneurs but also eliminates the need and importance of development and innovation.
The change in the agrarian-regulatory system is increasing the competition and makes innovation more important in the economic production.
Agricultural production can be successful via its products consequently creation of development system focusing on product-range is the main target. The method of „market-conscious technology development" [7] is suitable for this task.

Agricultural production systems in Hungary between 1986 and 1990

The socialist agricultural reorganization not free of stress had created the Soviet-type of agricultural large-scale farms: the cooperatives and the state-owned farms in Hungary via state-measures. Contrary to other countries of the "socialist camp" large-scale farms in Hungary often under the influence of ideological effects and regulated according to state planning have started to improve as of the end of the 1960's.
The engines of the development were the organizations so called "production systems" created to produce products or product-groups. The theoretical basis of the system was worked out and introduced by Imre Dimény [2] agrarian minister at that time. The "Dimény-model" was simple and it is shown in Figure 1.

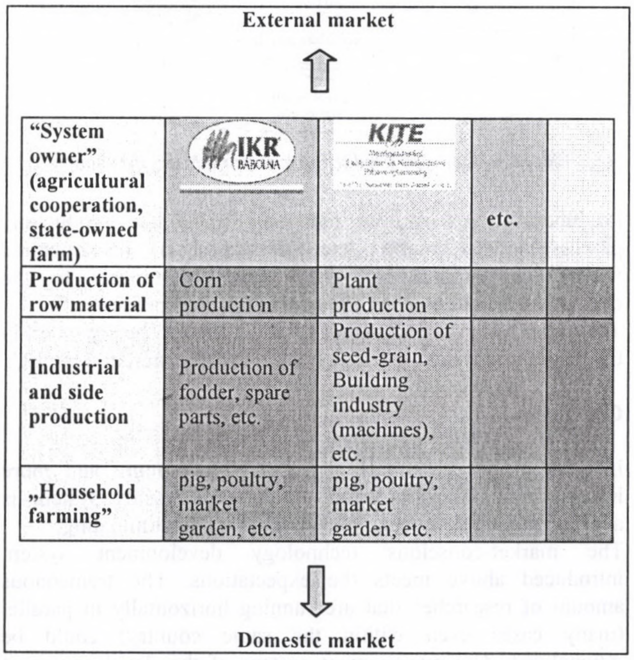

Figure 1 Model of production systems in Hungary (1968-1990)

There was one "system owner" (agricultural cooperation or state-owned farm) who was managing production, provided information, production inputs to the "members" (other farms in the organization) within the production systems that operated as innovation centers.
Development was ensured basically via self-training based continuous self-development that was accompanied by targeted research-innovation work. The marketing activity of each production system was good as well: most of the names and logo's are still well-known abroad. The system was market-oriented: the so called Council for Mutual Economic Assistance (CMEA) involving all the socialist countries was almost guaranteeing reception of agricultural products. The system supported the majority of internal consumption and there were even products of the highest quality shipped to the western markets: to markets of European Union and other markets of the world. Production happened at the level was defined by the market.
The timely fluctuation of agricultural production was smoothening by auxiliary activities: rural industrial and construction work. Employees of large-scale farms were allowed to manage their own farming in the construction typical of that era: in the so called "household farming". Overall the system provided important rural development tasks as well: supported village-communities, education, culture, and increased need for creating better standards both in private and in public.
The systems could integrate the work of branch research institutes well since they were relying on individual professional institutes based on the product-range. The main tasks were to have the individual professional tasks vertically harmonized properly and to have the applied technology optimized at the right time and in the right place ("present" column of Table 1).

Table 1 Connections of tasks of the market-oriented technology development [3]

Professional fields	*Production-market "Present"*	*Research-development "Future"*
Economy, Marketing	Concrete properties	Continuous market model
Place of product	Concrete geographical site and size	Possibilities of extensive Production
Biology	Available Hungarian sorts of wheat	Extending of productive characteristics
Agro-technology	Prescribed and controlled technology for quality production	New concepts of agricultural processes
Technical processes	Minimum programme By available machines Enlarged programme By newly developed machines developments, investments (storage facilities, driers etc.)	Reduction of soil load Conservation tillage Reduction of operations Distribution of fertilizer Decreasing of energy requirement Precision tillage Cost decreasing economical analysis

Horizontal researches had to be started to find solution to issues arising at different professional fields (horizontal lines of Table 1) that creates the technologic opportunities of the future.
Other integration belonging to the agrarian-business formed in the era (e.g. "Agrotröszt" supporting the transfer of inputs, ÁFÉSZ organizing retail, or "Mezőgép Tröszt" integrating machinery industry) were natural creations of agricultural production systems.

In Hungary following the political transition (at the beginning of the 1990's) the disintegration of the production systems introduced above, the quick-altering agrarian market, the fast-changes in land ownership and utilization structure and the new entrepreneurial forms resulted in a huge break. There has to be a new, innovation-executing production system worked out utilizing all the past experience, which

- helps the regional optimization of production,
- provides quick market flexibility,
- has effect on the whole country and
- efficiently helps the spreading of innovation [4].

Production system executing innovation and operating in market economy

Agricultural production is defined by several professions (Figure 2). The engine of economic increase is the continuous technical-economic renewal [8]: the innovation that is to be founded by high-level of basic- and applied researches [5].
According to our approach they are the research, development, production and market that form the agrarian production system together and basic researches are part of it. In case this connection cannot be formed within a specialty, the completed research result cannot be utilized. The bridge between the basic research and production is to be served by branch research institutes of each country (hatched area in the Figure 2).

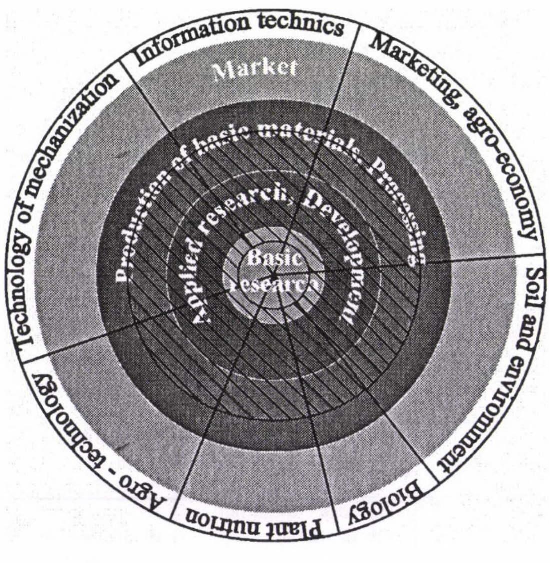

Agrarian research centers

Figure 2 Connection of market, production, R&D and professional fields [3]

As mentioned above vertical connections of professional duties arising during the production process are very important. An example of this is that the market expectations (possibilities) regarding a specific product given during economy-evaluation will be "limited" by biological basis, by local characteristics (soil, water, climate, etc.), by agronomic and technical knowledge due to what we receive the results if the product can or cannot be produced successfully at the specific area in the specific time-frame. In the main-stream of the production system suggested by us (Figure 3) there is not one „system-owner farm" located but basically the technology-forming, research managing institutes, the branch research centers.
The main stream having the role of the system owner periodically runs the analyzing cycle relative to vertical connections demonstrating if the product can be economically produced among the known circumstances. The system ensures self-development and self-regulation this way since analysis are made based on experience and knowledge typical in the specific area.
Decision is made via the consideration of economic advantages and scientific possibilities regarding on which field, with the involvement of which other research institutes and basic research bases horizontal researches to be completed.
It is essential that the technology development system is to be connected to the production system for the fulfillment of innovation and utilization of results of research-development. There must be farming units existing taking the risk for fulfilling the research results. Involvement of entrepreneurs (e.g. food processing industrial, agricultural chemicals, agricultural machinery) who can play an important role in success of the product besides agricultural producers is significant.
The technology development system for each product is managed by a board that consists of not only researchers but producers and they own significant managerial skills.
The substantive element of the system is an information system that transfers information to producers and provide proper feedback from R&D organization. This professional information system supports the market-conscious technology development of individual products in other words ensures the operation of the production system (Figure 3).

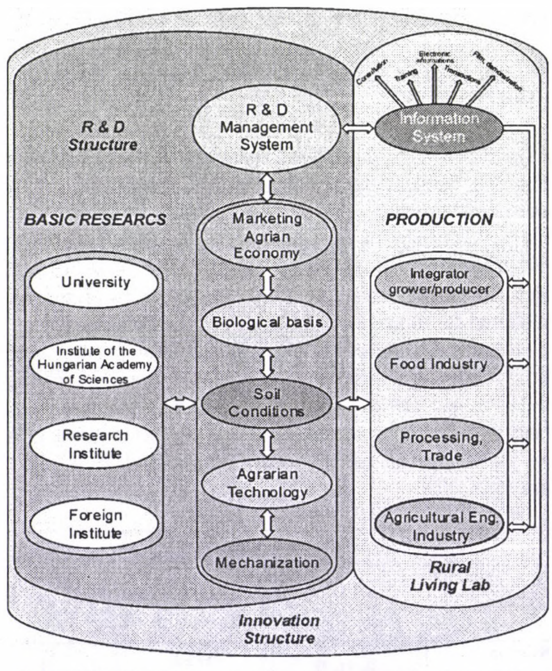

Figure 3 Model of production system realizing innovation

Producers/farmers receive the most up-to-date production, process industry, market, etc information in GIS-structured format via internet and they can communicate to the development system when the system operates properly.
The organization called „Rural Living Lab" can be separated in the model that is among the „Living Labs" registered in the EU.

Conclusion

Innovation in agricultural production gains more and more importance as the European agricultural subsidy system is altering and production supports are gradually eliminating.
The market-conscious technology development system introduced above meets the expectations. The tremendous amount of researches that are running horizontally in parallel (many cases even within the same country) could be rationalized. The management system of the development of individual products, services (e.g. tourism, hospitality, and

special rural development tasks) could be localized at the best cultivation areas.

Significant part of the agrarian subsidies focusing on food-market development could be utilized in more effective operation of the introduced system increasing income and competitiveness of producers in a great extent.

Technology development and production system efficiency could be improved significantly via operating the effective information system based on GIS, this way increasing competitiveness of agrarian production of Hungary and the European region.

The system would ensure the preferred agricultural-sector labor-management in the long run (synchronizing capabilities and production), optimal utilization of R&D institute system, increasing competitiveness of production while maintaining sustainability and developing landscape management.

The opportunities beyond Europe must be mentioned hereby as well since the „system" is providing continuously improving information to its members enabling the defined possibilities of technology transfer and the development of connecting trades (e.g. machines, propagation means, and chemicals).

References

[1] Buckwell-Report (1999): Towards a Common Agricultural and Rural Policy for Europe. Report of an Expert group.

[2] Dimény, I. (1971): A gépesítés ökonómiája a mezőgazdaságban. Akadémiai Kiadó. Budapest, 235.

[3] Fenyvesi L. et al. (2003): A mezőgazdaság műszaki fejlesztésének lehetséges megoldása. Gazdálkodás. Budapest: Mátra-tan, 47 (5) 1-15.

[4] Fenyvesi, L., Késmárki-Gally Erdeiné, Sz. (2005): Marketing Oriented Technology Development of Vegetables Production on Arable-Land. 33rd International Symposium on Agricultural Engineering. Faculty of Agriculture University of Zagreb. Agricultural Engineering Department. Opatija, 21-25 February 2005. 425-433.

[5] Husti, I. (1998): Problems and possibilities of the Hungarian agricultural innovation. Hungarian Agricultural Engineering. Budapest, 11, 39-41.

[6] Huylenbroeck, G., Gurand, G. (2003): Multifunctional Agriculture: A New Paradigm for European Agriculture and Rural Development-Perspectives in rural policy and planning. Great Britain, 239.

[7] Késmárki-Gally, Sz., Fenyvesi, L. (2004): A Market-conscious Technology Development Model. Studies in Agricultural Economics. Research Institute for Agricultural Economics. Budapest, 101, 143-154.

[8] Késmárki-Gally Sz. (2006): A műszaki fejlesztés szerepe a magyar mezőgazdaság fejlődésében. Szent István Egyetem. Doktori értekezés. Gödöllő, 145.

QUALITY MANAGEMENT SYSTEMS FOR SUSTAINABLE DEVELOPMENT

Klára BÉRES - István HUSTI
Szent István University, Gödöllő

Introduction

To lead and operate an organization successfully, its necessary to direct and control it in a systematic and transparent manner. Success can result from implementing and maintaining a management system that is designated to continually improve performance while addressing the needs of all interested parties. Managing an organization encompasses quality management amongst other management disciplines. A quality management system is a sustainable system to direct and control an organization with regard to quality.
The quality and its continual improvement is one of the most important area for the organizations of competitive economy. These organizations depend on their customers and therefore should understand current and future customer needs and strive to exceed customer expectations. That is why the sustainability of the customer focused organizations depends on the level of satisfaction of their customers. The producing and servicing companies – apart from their activities – therefore turn higher attention to implementing and sustainable developing of their quality management systems.

Material and methods

This paper focuses on establishing, developing, auditing and registration of quality management systems. We show two road maps, as models, based on our experiences and references. These models can help to implementing and checking the main elements of the quality management systems, apart from their activities.

Results and discussion

1st Road Map: Implementing A Quality Management Program

Quality management programs can take many shapes and forms and will be most effective if they are individualized to meet the needs of a specific organization. While each program will look different, successful quality management programs have key characteristics that are critical to the efficient functioning of the program. The next nine steps that can be used to develop and implement a solid and sustainable quality program.

***Step 1:** Confirm Commitment of Leadership & Establish Supportive Organizational Structure*
- Establish support of program leadership for Quality Management (QM) and confirm commitment.
- Commit resources to support QM activities.
- Provide education about CQI tools and techniques to all levels of staff, including senior leadership.
- Establish a method to inform all levels of staff, including senior leadership and Board of Directors about QM initiatives.
- Delineate expectations of staff related to QM.
- Delineate specific QM responsibilities of staff.

***Step 2:** Establish Quality Management Plan*
- Establish Quality Guidance Team, Steering Committee or utilize existing leadership meetings to oversee the QM program.
- Develop an organizational QM plan which delineates goals and objectives for the QM program.
- Establish QM priorities.
- Develop a time line or calendar of activities for the year.
- Select a QM approach, such as PDSA.
- Clarify QM responsibilities of staff.

***Step 3:** Determine Performance Measures & Collect Baseline Data*
- Based on QM priorities, determine performance measures.
- Develop indicators to measure performance.
- Define measurement population and delineate eligibility criteria.
- Create a data collection plan to include: – Sampling strategy – Determine method of data collection, i.e. chart abstraction, interviews
- Create data collection tools – Create instructions for data collection tools – Train personnel who will collect data – Conduct pilot test of tool
- Establish process of communicating with staff about measurement process
- Collect data

***Step 4:** Analyse Data*
- Analyse data and review the results.
- Identify areas where additional data is required.
- If historical data are available, compare for trends.
- Display and distribute data to communicate findings and results.
- Identify areas for improvement and select a quality improvement project.

***Step 5:** Develop Project-Specific CQI Plan*
- Establish project-specific QM team that represents all staff integral to the service or issue.
- Identify a team-leader.
- Delineate specific and sustainable goals for the team.
- Allocate time and resources for the team.
- Delineate team responsibilities.
- Develop timeline for reporting findings and improvement strategies.

***Step 6:** Study and Understand the Process*
- Analyze the root causes.
- Utilize CQI tools and techniques to understand the process, such as flow charts, facilitated brainstorming, cause & effect diagrams, fishbone, etc.
- Document and track progress by using activity logs, issue identification logs, meeting minutes, etc.
- Report progress to senior leadership and staff on a regular, defined basis.

***Step 7:** Develop and Implement an Improvement Plan*
- Identify potential solutions to make improvement to the systems of care.
- Recognize quick fixes and longer term solutions.
- Try a small test of change and analyse results.
- Refine improvement plan.
- Develop timeline for implementation of plan.
- Delineate team responsibilities.
- Implement changes.
- Track changes and improvement actions.

***Step 8:** Remeasurement*
- Determine interval for remeasurement.
- Remeasure indicator after change has been implemented.
- Look for incremental improvement.
- Communicate results to team, staff and leadership.
- Determine need for and/or level of remeasurement on an ongoing basis.
- Develop a plan for sustained improvement.

***Step 9:** Celebrate Success*
- Communicate results of the project to all levels of the organization, including consumers when appropriate.

- Congratulate team in public forum, i.e. staff meetings, Board of Director meetings.
- Select a new project and begin at Step 1.

2nd Road Map: ISO 9000 Registration

A quality system that meets ISO 9000 requirements can be confusing, costly, time consuming and sustainable.
There are many right ways to satisfy the requirements of the ISO 9000 standards, and their experiences can be valuable learning tool for organizations just beginning the "journey".
The road map shown in **Figure 1** has three main components:
- ***milestones*** to ISO 9000 registration,
- ***internal activities*** for each milestone, and
- ***consulting and training services***.

The **time line** indicates the intervals between milestones as well as the 18-month average it takes most companies to achieve registration. This time frame is only an approximation, the actual time depends on the initial status of quality system, the presence of management commitment, and the degree of involvement of every member in the organization.

Step 1: *Securing management decision and commitment*
The first step to ISO 9000 registration begins with management making and informed decision to implement an effective quality system.
Before the leaders can make a commitment to ISO 9000 registration, they must understand what it is and why it is necessary. Once the organization's leaders have decided to pursue registration, they must develop a strategic plan for implementing ISO 9000. The plan should include the scope of registration, an initial assessment of the organization, the resource requirements, and a tentative time line.

Step 2: *Establishing and training internal resources*
The next step is to establish an infrastructure that includes a management representative, steering group, and area coordinators.
The management representative has the authority and responsibility for ensuring that the ISO 9000 standards requirements are implemented and maintained.
Since the implementation of a quality system is not a one-person job, the steering group is essential to help guide the effort and make strategic decisions. Led by the management representative, the relatively small team should include leaders from a cross section of functions within the organization.
Every area involved in the ISO 9000 pursuit needs a coordinator who provides input to and acts on the strategic directions of the steering group.
The people assigned to *all three of these jobs* need to know about the standards requirements and how they apply to their own functions. A two-day interactive seminar should be sufficient to provide the necessary knowledge and skills for implementation.

Step 3: *Conducting internal audits*
As the registration effort gets under way, the organization needs to determine its starting point to continuously measure progress. Internal quality audits are an effective measurement tool, and they mark the beginning of the third milestone.
The initial round of internal audits compares the current quality system – including documentation, policies, and practices – to the requirements of the appropriate ISO 9000 standard. The result is a thorough report on the areas that need to be upgraded or improved to implement an effective quality system that meets the ISO 9000 standards requirements.
From these audit results, the management representative and steering group can set priorities based on business needs and develop a more detailed implementation plan.

Step 4: *Documenting efforts*
Internal quality audits will identify the areas in which standard practices are missing or areas in which the practices exist but are not documented.
The quality manual is an important aspect of documentation because it describes the policies and principles by which the organization manages quality. At this stage, only a rough draft of the quality manual is needed.
There are many approaches to writing a quality manual, and a one-day training session can be valuable for the team assigned this task.

Step 5: *Choosing a registrar*
At this point – before the actual audit takes place – it is important to establish a relationship with a third-party registrar. This organization should be accredited to ensure that the registration provided will be recognized by customers.

Step 6: *Documenting and implementing practices*
At some point, documentation efforts will begin to taper off as the documented quality system is put into place. As work is finished on documenting and implementing improved practices, auditing continues and the quality manual is finalized.

Step 7: *Learning from the pre-assessment*
During the pre-assessment, the third-party auditors audit the organization and its quality manual to ensure compliance with the documented system. The length of the pre-assessment varies with the organizations size and complexity and with the auditors practices.

Step 8: *Undergoing registration assessment*
The registration assessment is performed by the registrar several months after a quality system in completely documented and implemented. This allows the registrar to find objective evidence that the organizations actions comply with its quality system and with ISO 9000 standards.

Step 9: *Achieving registration*
If the outcome of the assessment is a recommendation for registration, the organization will receive a certificate. If the registrar found minor discrepancies, the organization will have about four to eight weeks to correct them. Major discrepancies will preclude registration and will require a partial or complete re-audit of the system.
Registration is really just the beginning of the ISO 9000 process: it serves as the foundation for ongoing quality and business improvements. An organization must continue its internal audits, management reviews, and corrective actions.
The registrar will return periodically to conduct surveillance audits to ensure that the quality system is still in compliance.

Conclusions

The twice nine milestone-models provide a well-marked path to implementing and sustainable developing the quality management system. By following this models, organizations are better able to prioritize needs and resources to implement a cost-effective and sustainable quality management system that meets the ISO 9000 standards.

References

[1] Quality Management Systems. Fundamentals and vocabulary (ISO 9000:2000). Hungarian Standard.
[2] HOCKMAN, K. K.- GRENVILLE, R. - JACKSON, S.: Road Map to ISO 9000 Registration. Quality Progress. May 1994. p.: 39 - 42.

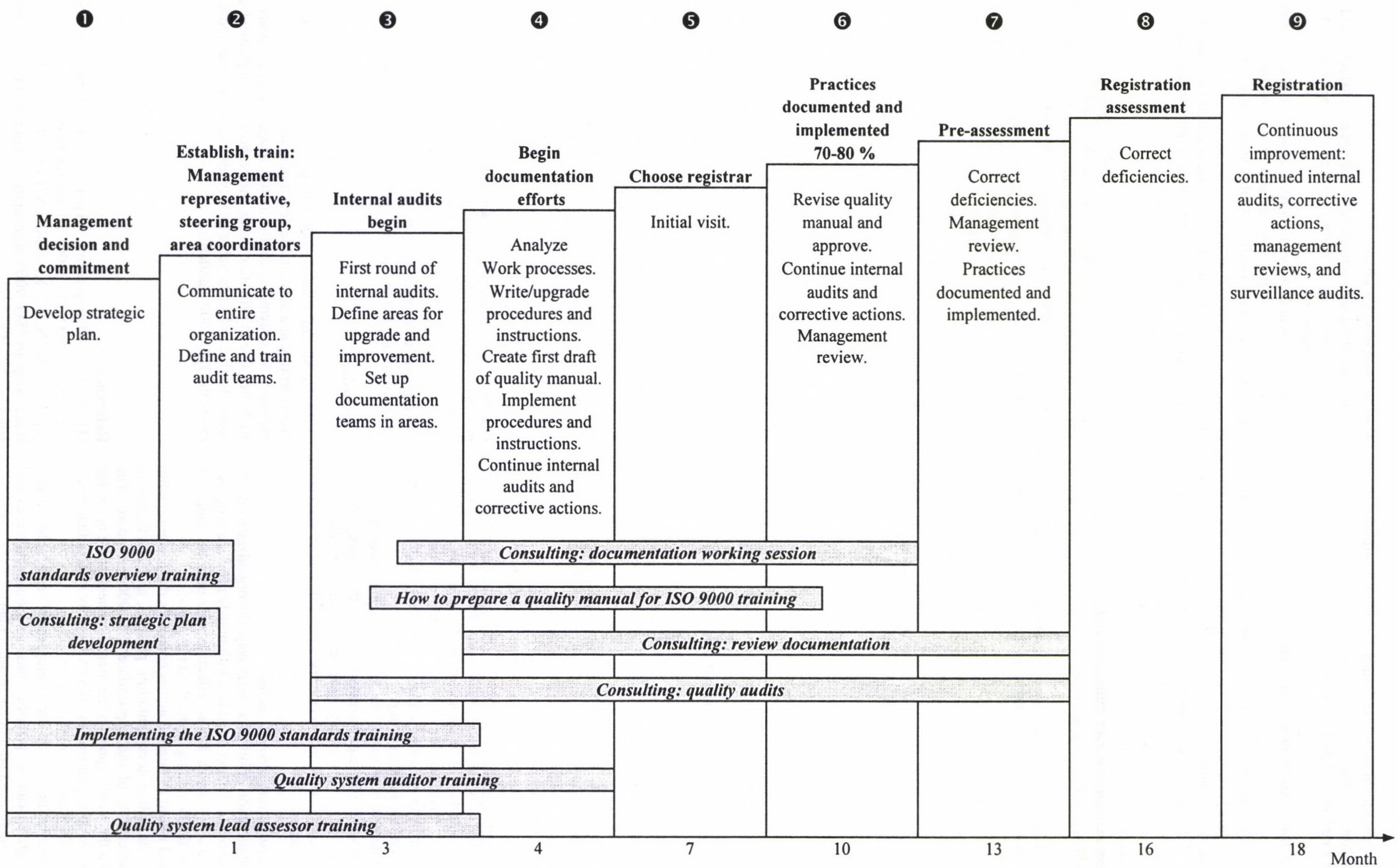

Figure 1 Road Map to ISO 9000 Registration (Own drawing, based on 2.)

LOW COST MECHANISATION SOLUTIONS FOR EFFECTIVE FARMING ON SMALL AND MIDDLE-SIZED ARABLE FARMS

László MAGÓ
Hungarian Institute of Agricultural Engineering, Gödöllő

1. Introduction

It is essential to develop a cost effective fleet of machinery for the present day various standard sizes of plants. In the case of the small units it is essential to develop equipment and cost saving mechanical solutions, but there is also demand for the building up of systems of machinery with modern, cutting edge technology and profit improving attributes for the middle-sized farms, which more favourable specific cost level.

The changing and modernising of the Hungarian fleets of machinery, the majority of which is obsolete is unavoidable. Farmers working from different amounts of capital on farms, which provide different levels of mechanical development potential, have to develop mechanisation solutions using the wide range of types and price range of the power and work machinery.

Taking into consideration the current partitioned structure of the farms the goal was established to determine that in the case of the different branches of plant production on small and middle-sized farms which combination of fleet of machinery can be used effectively.

2. The method

Testing of the mechanised processes of agricultural harvesting was carried out using models. In the model a crop rotation plan was adopted which mirrors the Hungarian production characteristics using wheat and oil plants. Depending on the size of the farm the proportion of the sewed area of each plant was established keeping in mind the agronomical and production technological conditions.

At the basic level the experiments were focused on the lowest investment cost power machinery range of products in Hungary. With this machinery because of the low investment cost the amortisation cost is less and thus the cost of utilisation is low. The determination of the basic data of the costs of machine utilisation has been carried out, based on the database of the FVM Hungarian Institute of Agricultural Engineering [2].

The *model calculations* involved the key plant size data of the formation of machinery systems in the range of plant size ranging from 5 to 1000 hectares. On the basis of these data, statements can be made regarding a larger segment of the estate structure, and conclusions may be drawn regarding machinery utilisation and mechanisation.

3. Results

3.1. Conclusions drawn regarding the composition of the power machinery system and the performance of hours run, based on the results of the model calculations.

3.1.1.The composition of machine systems of minimal utilisation cost broken down in categories of power machinery depending on the sizes of plants.

In the course of carrying out our survey the universal power machinery was categorised according to *engine performance*, as well as taking into consideration the *function* of being a cereal harvesting machine. The composition of the power machinery systems rendered to a particular area was determined on the criteria of *power machinery categories*. Taking into consideration the crop structure, growing technology, conditions of mechanised work typical of the Hungarian particularities and the composition of categories of *cost effective power machinery systems* which are formed on the criterion of plant size, *regular interrelations* can be established.

The surveyed power machinery system that can be rendered to the smallest plant size, in the case of ***tractors***, consists of machines of 40 kW, a performance that is the minimum requirement for the quality performance of soil work. If the size of the area is higher, then first the performance of the machinery making up the fleet (from the size of 30 hectares tractors with 60 kW performance are required), next the number of tractors increases. Thus, tractors of 40 and 80 kW performance are mentioned *together* in a machinery system for plant size of 100 hectares or upwards. From the plant size of 300 hectares the function of power machinery mentioned above is filled by tractors of 60 and 120 kW performance, which have sufficient capacity for the increased workload. For the plant size of 500 hectares or upwards the number of tractors increases in proportion to the growth of requirement for capacity.

It is necessary to note that, in the case of large plant size, the cost level of machinery utilisation may be further decreased by increasing the number of performance-based categories and optimising the distribution of work among machinery connections of various performance levels (**Magó 2004**). [5]

In order to increase utilisation, *transportation* tasks should also be realised by the means of tractor-trailer connections.

The utilisation of an own, low capacity ***cereal harvester*** may be justified above the plant size of **100 hectares**. In the case of a plant size exceeding 500 hectares, the large extent of the specialised mechanised work requires the utilisation of harvesters with larger delivery value. According to the calculations, a 1000-hectare farm requires the utilisation of at least two combine harvesters.

3.1.2. Optimal mechanisation levels concerning tractors, depending on plant size

The **number of tractors** required by plants of various sizes is as follows:

1) In the case of a plant size **not exceeding one hundred hectares**, we calculated with *one tractor*.

2) In the case of a plant size ranging from **one to five hundred hectares**, two tractors of different performance levels are required.

3) In the case of a plant size **exceeding five hundred hectares**, two tractors are required from both performance categories in order to carry out the work operations in time and in good quality.

When analysing the number of own power machines per *area unit* it can be stated that, in the case of a power machinery system of minimal utilisation costs, the *coverage* on farms of ***over 50 hectares*** is favourable. The economically most favourable value can be calculated ***over 200 hectares***, in this case a maximum of *one power machine* is sufficient for the cultivation of 100 hectares of land.

The specific performance of engines per hectare decreases substantially in the function of plant size. While on small plant sizes 2-8 kW/Ha engine performance is required for every hectare, in the case of medium sized plants this value falls within the range of 1-2 kW/Ha. In plants of large size the work operation may be carried out with a requirement of ***0.7 kW/Ha***.

3.1.3. The ranges of plant sizes of the "activation" of the power machinery categories

The individual power machinery categories are "*activated*" when they first appear in the power machinery system developing in the function of the growing plant size. For the "activation" of each power machinery category this is a specific range of plant size. (For example: *80 kW performance category:* directly from 100 hectares and upwards, *120 kW performance* *category:* from 300 hectares and upwards. The attachment of a new category also influences the costs of utilisation and investment on the level of machinery systems. **(see Figure 3)**.

In connection to the above, **up to the plant size of 100 hectares**, the system of machinery is formed on the basis of power machines belonging to each of the performance categories. In the range of plant size **not exceeding 30 hectares**, if we aim to utilise our own machines, in order to decrease the fixed costs, it is reasonable to utilise machines of the *lowest performance level and purchase cost*, which are still capable of performing the required workload. If the plant size and number of work tasks grow, the solution is the *increase of the level of performance* rather than the number of machines. Thus, the category of 60-kW tractors becomes a part of the optimal machinery system **from 30 hectares upward**. 80-kW tractors are part of the system **from 100**, whereas 120-kW tractors are part of the system **from 300 hectares** upward. It is necessary to point out that size in itself does not guarantee the fulfilment of the appropriate number of work hours and favourable utilisation.

The use of own *harvester* – depending on performance and delivery value – is economically justified **over the plant size of 100 hectares**. It can be stated that the following issues must be consequently taken into consideration prior to the "*activation*" of a new machine:

– is it not possible to perform the tasks by the means of *internal redeployment* rather than by making a new purchase;
– can the missing capacity be covered by *machine rental* or other *external service*;
– is it possible to utilise the *surplus capacity* resulting from the new purchase (eg. lease work);

3.1.4. The number of performed hours run in the function of plant size

With differing plant sizes the number of performable hours run has influence on the composition of categories of the power machinery system;

- In the case of the examined *smallest plant size* (**up to 50 hectares**) *low exploitage* may be achieved with tractors: maximum 400-500 hours run per year.
- In the case of *medium size plant* (**50 to 300 hectares**) this quantity is *larger,* 800-1400 hours run per year.
- With *large size plants* (**above 300 hectares**) the various categories of tractors achieve significant performance (1000-1800 hours run per year).

A cereal harvester with well-chosen capacity can achieve *good* exploitage at 300 hours run per year in the case of plant size *above 300 hectares*, by which the cost of operation becomes *reasonable*.

The number of hours run projected on a *unit of area decreases* with the increase of plant size. *In small plant sizes* 10-15 hours run per year is realised. *In the range of 30 to 300 hectares* this value is 8-10 hours run per year, and, *above this range*, a value of *6 hours run per hectare* can be observed when realising the *efficient work plan.*

It can be observed that both in the number of machines and with regards to the performed hours run, the most *exploited tractor* ***belongs to the category of 120 kW***. The performance of this significant labour time is achieved by the power machine of the given category, when both soil work and transportation tasks are carried out. (See **Figure 1**)

3.2. The costs of purchase and use of machines

3.2.1. The specifications of the function of investment and operation costs of machines projected on the size of plant

The result calculated for the specific *machine operation costs per hectare decreases* ***hyperbolically*** in the function of plant size (see **Figure 2**) and it borders the upper values of a real broken hyperbolic function (**Takács 2000**). (see **Figure 3**) [7]

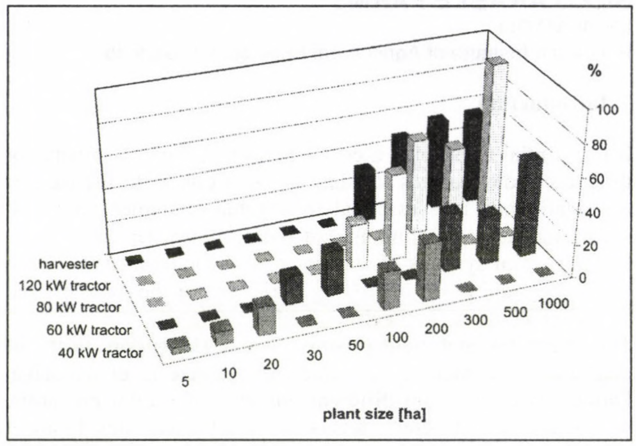

***Figure 1** The extent of exploitation with the various categories of power machines in the case of the examined plant sizes*

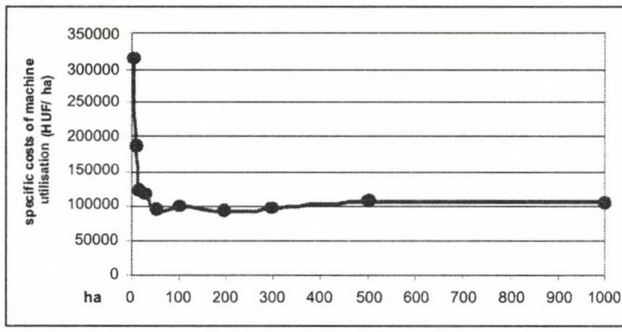

***Figure 2** Specific costs of machine utilisation in the function of plant size*

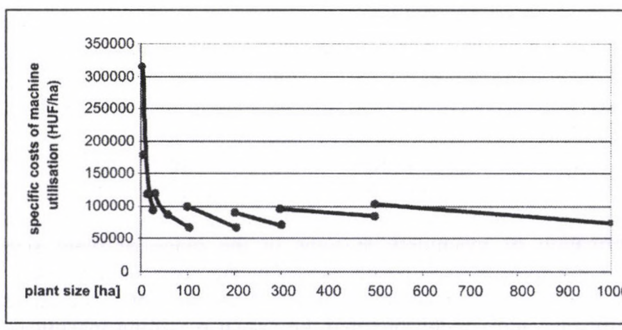

***Figure 3** The broken function of the costs of specific machine utilisation per hectares, indicating the extra costs of switching to power machines of greater performance in order to increase capacity (1 EUR = 250 HUF)*

From the plant size of 100 hectares it gradually approaches an imaginary line that parallels the horizontal axis, thus indicating the operation cost level of a constant machinery system formed in the case of a large plant size.

3.2.2. The composition of the utilisation costs of the machine system

3.2.2.1. Broken down in the cost of power and work machines

Based on the survey it can established that the utilisation costs of the machine system is divided between power and work machines, depending on the plant size, at the ratio of 65-82 % and 35-18 %. In the case of smaller plant sizes, the utilisation cost of the power machines is proportionally too high, for in this case, the cost of power machines, due to the low level of their utilisation, is highly unfavourable, that is to say, very high. As for the work machines, we could calculate with low utilisation cost machinery of simple design and low technical standard, that could be adapted to low-performance power machines.

3.2.2.2. Broken down into categories of power machines

Figure 4 illustrates that in the case of very small plant sizes (5 to 10 hectares) the specific costs of power machine utilisation are rather high even if machines of the lowest possible performance but still appropriate work quality are utilised. From the plant size of 20 hectares and upwards the specific utilisation cost of a 40 kW tractor is reduced to the level of cost specific to the cost level of other power machines.

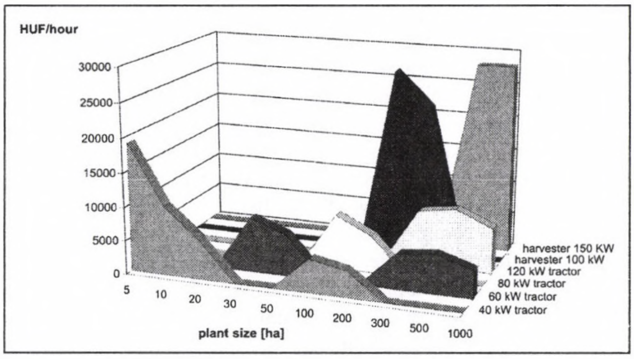

Figure 4 The specific utilisation cost per hours run for the various power machines in the plant sizes examined (1 EUR = 250 HUF)

The utilisation costs of tractors used on over 20 hectares are at an acceptable level already at the time of the activation of the given power machine. With the increase of the plant size and the level of utilisation, this value decreases further.

The cost per hours run for the **cereal harvesters** is substantial. While the cost of utilisation decreases with the increase of the level of utilisation of low-performance combine harvesters, in the case of high-performance machines the number of machines increases together with the growth of the plant size, while the hour run per machine is unchanged, thus the specific costs of utilisation remain unchanged too.

It must be admitted that the utilisation of the own harvester solely for the own crops is not economical up to the plant size of 100 hectares, thus it is more favourable to perform the work tasks through the use of lease work.

3.3. Comparison of the utilisation costs of the elaborated model of machinery system of a small plant using high-performance power machines and the costs incurring when aging machines are used

The examinations also extended to cases when, in the case of small and medium sizes plants, not the most cost effective power machines are used for certain technological tasks, that is to say, our fleet consists of power machines of higher performance than justified.

We can confirm that in this case the value we calculated for the costs of machinery model introduced above is 4-5 times higher. **(see Figure 5)**

When the reason for using power machinery of higher performance than justified is that these are aging machines and no amortisation cost should be counted with, and there are no costs of regular maintenance under guarantee, and we only have to calculate with the replacement of low price level, post-manufactured spare parts as repair cost, then still, the cost of machine utilisation in the cases of the given sizes of plant are twice as high as in the cases of plants where the category of the power machines was optimally selected.

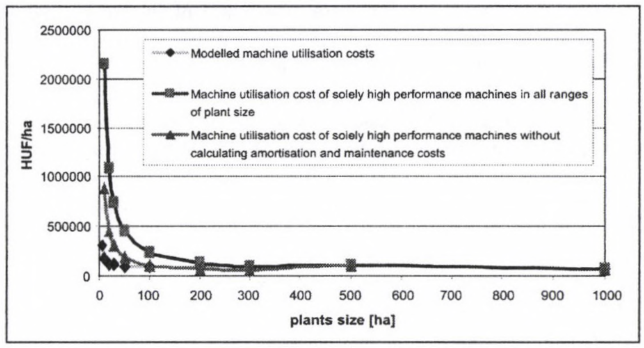

***Figure 5 Comparison of costs of a model of machinery system elaborated for small and medium sized plants with the costs of high-performance power machines in a small plant and the costs of aging machines** (without calculating amortisation and maintenance costs)*

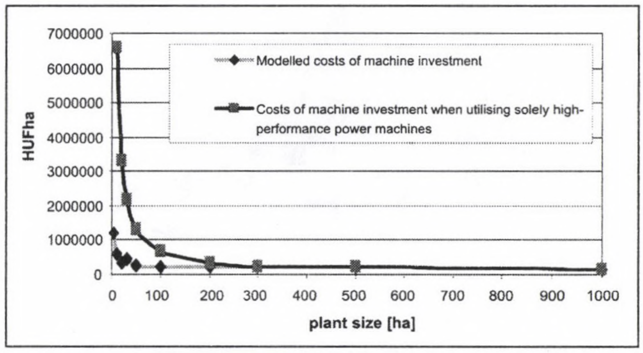

Figure 6 Comparison of investment costs of a model of machinery system elaborated for small and medium sized plants with the investment costs incurring when high-performance power machines are used in a small plant

If we regard the investment costs, we can find similar proportions. Al so in this cases we have to calculate with investment costs 4 and 5 times as high even if on the small and medium sized plants where that task are carried out not by the power machines of sufficient performance and the connecting work machines but by power machines of unreasonably high performance. **(see Figure 6)**

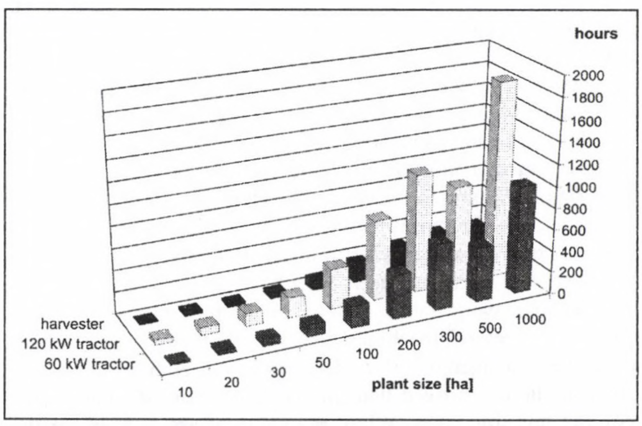

Figure 7 Performance of hours run by medium and heavy-duty universal power machine categories used in all plant sizes including small plants

Figure 7 illustrates well how the multiple costs of machine utilisation mentioned above develop. It demonstrates that 60 and 120 kW tractors achieve substantially less hours run per annum on plants under 200-300 hectares than expectable. This is also true of cereal harvesters. The low level of exploitage means drastic operation costs, as **Figure 8** demonstrates. According to our calculations, for a 60kW power machine the cost of machine utilisation on a 10-hectare plant exceeds HUF 80.000/hour run, in the case of a 120kW power machine this value is over HUF 120.000/hour run.

We did not even consider the situation if a farm smaller than 50 hectares decides to purchase a new combine harvester, therefore the specific cost of utilisation for harvesters was determined only up to this plant size, which is still over HUF 100.000/hour run.

Of course, the operation of low-repair-cost aging machines run without regular service background has more "favourable" costs than the above substantial costs of machine operation. In this case cost per hour run for a power machine is about HUF 17-20.000, for a harvester, serving a plant of 50 hectares it is only HUF 13.000/ hour run.

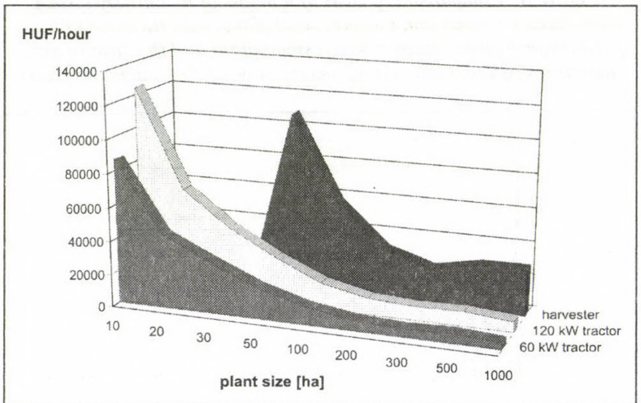

Figure 8 The specific utilisation costs per hours run for medium and heavy-duty universal power machine categories in the examined plant sizes including small plants

This is the reason for the fact that many farmers, who work on small and medium sized plants, carry out their work tasks with aging medium or heavy-duty universal tractors and do not experience a substantial excess of costs related to machine utilisation, for the amortisation burdens of the machines do not appear, and the maintenance of the machines is carried out by themselves at low costs.

4. Conclusions

The results of the calculations prove that every individual work operation should be performed by the machine connection that can be utilised to the maximum extent, which has sufficient capacity to carry out the given work task of the given plant size at the appropriate time and in adequate quality. By achieving this, the work can be performed at the *lowest operational cost.*

This system of conditions may be easily realised in plants of large size, however, in the case of small and medium size farms one has to be far more cautious and has to carefully analyse both the costs of investment and machine utilisation.

In the case of farms between 5-10 hectares it must be decided whether the work tasks should be performed by the own unutilised fleet of machines or low-cost lease work, which makes the management of the farm more vulnerable.

Our calculations proved that the mechanisation of small plants requires multiple costs. While the value of assets used for the mechanisation of a plant ***over the size of 50 hectares*** is **HUF 210-220.000/hectare**, the same value for a farm of a ***few hectares*** is over ***HUF 1.200.000/hectare***, even if the tasks of sowing and harvesting are usually performed by the use of lease work on these small areas.

With regards to machine utilisation, these values are the following: whereas on ***plants over 20 hectares***, on the basis of the model calculations, a machine utilisation cost of **HUF 100-120.000/hectare** may be realised, ***on the small plants*** this cost may triplicate and exceed **HUF 300.000/hectare** due to the low level of exploitage, even if part of the tasks are performed by lease work.

These figures were calculated presuming the best possible level of machine utilisation among the given conditions, and low technical level of machines.

In the case of *small plants* the power machines perform ***less than 500 hours run per annum***. With efficient work organisation, professional, and sometimes tight arrangement of work order, on a *medium sized plant* one power machine may perform a substantial number of hours run. In this case, in our calculations, ***1000 hours run per annum*** per power machine may be realised.

In the case of *large size plants*, the utilisation of a heavy-duty universal power machine performing mostly tillage tasks is favourable in the range of ***1000-1800 hours run per annum***, whereas the utilisation of a secondary tractor performing the tasks of sowing, nutrient supply and plant protection becomes acceptable in the range of ***500-1000 hours run per annum***.

On the basis of earlier national plant surveys it can be stated that in the small and medium sized plants the power and work machines that could be regarded as new investments are in line with the system of machines modelled in the function of plant size introduced above (**Magó 2007**). [6]

The farmers working on small plants mostly rely on one 40-60 kW power machine in their work, whereas power machines of the medium sized plants are in line with the machine system modelled in the course of the calculations, however, in order to meet the requirements of the production technology and the requirement of performance of the employed work machines, we can often see a primary tractor of higher performance or the number of secondary tractors is higher.

5. Acknowledgement

The author would like to express his gratitude to the OTKA Fund for the financial support (F 60210).

References

[1] **Fenyvesi L., Gockler L., Hajdú J., Husti I.**: (2003) A mezőgazdaság műszaki fejlesztésének lehetséges megoldásai. Gazdálkodás, XLVII. évf. No. 5. 1-15 p.

[2] **Gockler L**: (2007) The Purchase Price and Running Costs of Agricultural Machines in 2007, Mezőgazdasági Gépüzemeltetés 2007. No.1., FVM Mezőgazdasági Gépesítési Intézet. Gödöllő,.

[3] **Hajdú J., Gockler L.**: (2005) Relationship between Farm Size and Mechanisation, Hungarian Agricultural Engineering, Periodical of the Committee of Agricultural Engineering of the Hungarian Academy of Sciences, Vol. 18/2005. p. 50-54.

[4] **Husti I.**: (2004) Why is the Mechanisation of Hungarian Small and Medium Size Farms so Difficult, Hungarian Agricultural Engineering. No. 17. p.: 74-75.

[5] **Magó L.**: (2004) Farm Machinery Fleet Planning Concerning Machinery Utilization, Proceedings of the 62nd International Conference Agricultural Engineering "Innovation and Integration", Technical University Dresden, Germany, 07-08. October 2004. VDI Berichte 1855. Düsseldorf: VDI-Verlag, p. 265-273.

[6] **Magó L.**: (2007) Reasonable Usage of Different Tractor Categories in Small and Medium Size Plant Production Farms, Proceedings of the 32nd CIOSTA - CIGR Section V Conference, Nitra, Slovakia, 17-19. September 2007. Proc. Part 2., p. 475-482.

[7] **Takács I.**: Elemzés, Egyetemi jegyzet. SZIE, GTK. Gödöllő, 2000.

BASIC TASKS OF THE AGRICULTURAL INVESTMENT PROCESS

Miklós DARÓCZI
Szent István University, Gödöllő

1. Introduction

The competitiveness of the Hungarian agriculture can only be maintained and improved by continuous technical development. The efficient utilization of the amounts invested, the own capital, the loans and state subsidies is of crucial importance. The **Department of Engineering Economics and Management** has been doing researches for several decades on agricultural investments. The **primary objective** of this paper is to develop the decision-preparation process, particularly focusing on the investment efficiency aspects. Decisions on investments determine the activity and future success of an enterprise basically and for long term. Properly preparing the investment decisions and selecting the most favorable version are essential for both the enterprises and the national economy.

Economic calculations of the investment have been utilized in Hungary for decades. Despite the uncertainty and hazard, belonging naturally to the investments, a dozen of well applicable techniques have been elaborated by **Engineering Economics** and **Management science**. Thanks to the development of informatics, the economic calculations and the sensibility analyses can be carried out much more thoroughly and rapidly than a couple of years ago.

The proper training of entrepreneurs and managers on the theoretical background and the methodology as well as the applicability of the subject can be extremely helpful in preparing and making decisions related to agricultural investments.

2. Methods of the research

The **main objective** of my work is to evolve a theoretical model or a method, which can be successfully applied in preparing decisions of investment. This dynamic and symbolic model can be capable of supporting investment decisions of a certain enterprise or a certain branch of business. During the elaboration of my model, I have focused on the **main steps** of the complicated process of decision-preparation. The **functioning model** runs under MS EXCEL, which is widely known and can be accessed easily.

3. Results

The most important objective of this study is the elaboration of the model and methodology for supporting the decision-preparation of an investment. Great advantage of the elaborated version, that it seeks the answer **in a complex way** for every essential questions of a decision-preparation of an agricultural investment. Taking the different aspects into consideration, the model was formed to be:

- a **well applicable** tool for the management of the enterprise,
- even with an **average** technical knowledge, and hardware-software background,
- and even on the **most different** production structure and plant size.
- The model was elaborated to **support** processes of complex decision-preparation,
- and to **serve** the effective utilization of development sources.

The model is based on the main steps of the technical development tasks (**Figure 1.**).

3.1. Specifying the degree of supply of fixed assets of the enterprise

I have used the "**balance equation**" or rather inequality method, well known in the related papers, to determine the degree of supply of physical means. The calculation was based on the production structure and the applied production technologies. The proper elaboration of the latter indicates the quality and quantity of work which can be done through the planned means at a given time.

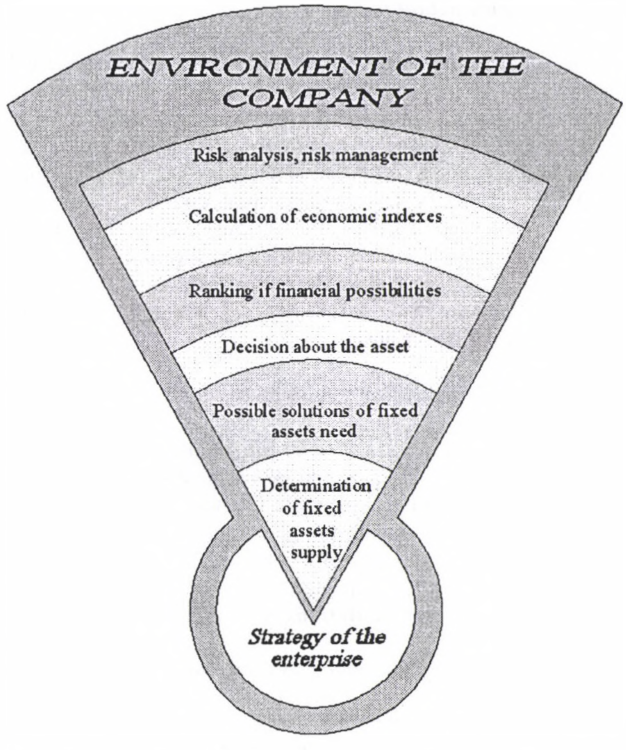

Figure 1 Basic tasks of the agricultural investment process Source: self-constructed

$$m \leq x * h * p$$

where:
m: quantity of the work to be done [shift-hours, nha]
x: number of the machines [pcs]
h: term available for the accomplishment of the work [shift-day]
p: specific capacity of a given tool [ha/shift-hours].

The determined **resource utilization** must be compared for both quality and quantity with those **available**, already analyzed, applicable buildings and operable machines. The received "**rate of supply of physical means**" points out if new means are required (buildings, machines, equipments) or the available ones (perhaps after renovation, expansion or conversion) are capable of carrying out the task within optimal **biological** and **agro-technical** time limits.

3.2. How to provide the required fixed assets

If the **results of the physical means supply** indicate that further means are required for the enterprise, it should be examined which way they can be obtained. For a **long-term resource employment,** in case of machines, there are two solutions for the acquisition: the so-called "**machine ring**" and the **machine-cooperative society**. For **temporary resource employment,** on the other hand, either **machine renting** or **hiring contractors** can be the best solution.

The simplified **break-even analysis structure** offers a solution for deciding between purchasing machines or hiring contractors. It indicates evidently the quantity range of work, above which the former, and under which the latter is more advantageous. Beside the arising fixed and variable costs, the model shows the realized savings, too.

3.3. Selecting the actual means

This part of the model is for selecting the **actual physical means** and development version. On the **buyers market** several dozens of means, equipments and technical solutions are available for the investor. Therefore, technical, technological, economical, ergonomic, environmental and other considerations have to be made before selecting an actual model.

For the complex comparison, the various features have to be converted in order to be comparable, i.e. the units should be eliminated and they must have the same direction.

The **order** among the possibilities can be defined by **the weighted sum of the values**

3.4. Tendering of financing possibilities

This part of the model deals with the **financing possibilities** and their tendering which should be **acquisitioned** to provide the required means. There are more financing models that can be taken into account during the preparation of the investment decision. The following scheme of model calculation helps better understanding of the tendering process. **The basic equations used in the calculations** are summarized **in Table 1.**

Table 1 List and denotations of the essential financing versions, basic equations

Deno-tation	Name of the version		Deno-tation
A	Investment from own resources	"A" + subsidizations	E
B	Investment from loan	"B" + subsidizations	F
C	Acquisition through financial leasing	"C" + subsidizations	G
D	Acquisition through financial leasing + investing own sources		
H	Acquisition through financial leasing + investing own sources + subsidizations		

Version	Equation
A	$B_0 = Se$
B	$B_0 = Se + Ht + Hk$
C	$B_0 = Se + Lht + Lhk$
D	$B_0 = Se + Lht + Lhk - Tn$
E	$B_0 = Se + T$
F	$B_0 = Se + T + Ht + Hk - Hkt$
G	$B_0 = Se + T + Lht + Lhk - Lhkt$
H	$B_0 = Se + T + Lht + Lhk - Lhkt + Tn$

Bé:	Market value
Se:	Own resource
B_0:	Total expenses
B_0*:	Present value of the total expenses
D_t:	Discount rate (%)
Ht:	Capital redemption of credit
Hk:	Redemption of interest of credit
Hkl:	Interest rate of credit (%)
Lht:	Repayment of leasing credit
Lhk:	Interest rate of leasing (%)
Tn:	Increase of capital
Tnk:	Interest of the investments (%)
T:	Subsidization (%)
Hkt:	Interest rate subsidization of credit (%)
Lhkt:	Interest rate subsidization of leasing (%)

Source: *self-constructed*

The most favorable financing solution for the entrepreneur is the one having the lowest expenses in the given situation and bringing the highest increase of income and having the most beneficial features for the enterprise.

3.5. Economic calculation of the investment

This element of the model helps to calculate the profitability indexes, determine the viability related to the **development possibilities** and the formed versions, and classifying them according to the calculated indexes. There are several kinds of static or dynamic indexes to be calculated (**Table 2**), for the sake of different features of the various profitability indexes of an investment, the differences among the indexes, and the **complex profitability evaluation**.

Table 2 List of static and dynamic indexes

Static indexes:
Expenditure for each unit of capacity (K)
Rate of profitability (J)
Static payback period (T_{stat})
Profitability of foreign exchange (D_g)
Dynamic indexes:
Net present value (NPV)
Internal financial rate of return (IRR)
Dynamic payback period (Tdin)
Benefit-cost rate (BCR)

Classification of the investment versions is not possible based on the net present value, the internal rate of return, and the benefit-cost ratio. The most suitable index for tendering is the **net profit – investment cost rate** (N/K), which is the net present value of the positive years divided by the net present value of the negative years of the post-investment period. The most beneficial version for the enterprise is the one having the highest **N/K** value.

The calculations and the presented tendering method can be widely applied in practice for tendering various investment versions.

3.6. Risk analysis, risk management

The last part of the elaborated **model** deals with the final fit of selected development version into the economic management of the enterprise. Knowing the final numbers, it should be examined how the single and continuous expenditures affect the **cash-flow** and the **credit rating** of the enterprise as a whole. Another important question, which will be later examined, is that how the already realized development influences the strategy of the enterprise.

The most important aspect when drawing up the **cash-flow,** that each change of the revenues, expenditures, tax-payments of the enterprise, due to the investment, should be taken into account even the indirect effects, too. The costs, on the other hand, incurred before independent of the investment must not be taken into account. It is practical to break down the **cash-flow plan** to each month.

There are several methods for analyzing the **risk**. The relating part of the model is based on the method of the **sensibility analysis** which breaks down the result-variable (e.g. internal rate of return) into components. It examines the effect of each components exerted on the result altering the variables particularly keeping the others unchanged.

References

[1] The economy and management of the agricultural mechanization. (Edited by Husti István) Műszaki Könyvkiadó. Budapest, 1999. p.: 100-137.; 184-206. ISBN 963 356265 1

[2] Modeling investment-profitability calculations. VII.th International Agro-Economic Conference Gyöngyös, 28-29. March 2000, Volume I. p.: 221-226

[3] From the strategy to the actual development projects. IX.th International Agro-Economic Conference Gyöngyös, 25-26. March 2004 p.: 6 CD

ABRASIVE WEAR TESTING OF ENGINEERING POLYMERS

Gábor Kalácska - László Zsidai - Zoétán Bors
Szent István University, Gödöllő

1. Used Materials

Beside some typical engineering polymers we focused on the different polyamide versions (table 1.) regarding the large number of real applications of theses materials in abrasive engineering solutions.

Table 1

PA 6G-H Mg catalitc cast polyamide 6	*PA 66E* Extruded PA 66	*PA 6GMo* Cast PA 6 + MoS_2	*PA 6GOL* Cast PA 6 + oil
PA 66GF30 Pa 66 + 30% glass fibre	*POM C*	*PETP*	*PETP TX* PETP + PTFE

2. Prearation of the test specimens

The test specimens were machined out from semifinished material forms. The final dimension was:
Ø8x15 mm

2. Developed testrig

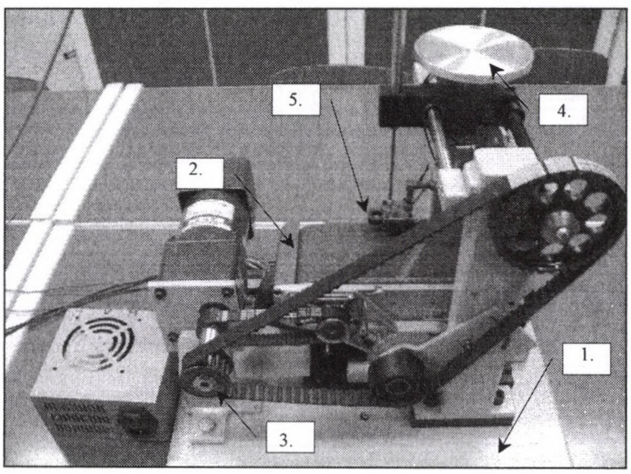

Fig. 1 New testrig

The main units of the equipment (Figure 1.) are as follows: the table (1.), the abrasive cloth (2), the elements of the drive mechanism (3), the loading structure (4), and the measurement and data collection unit (5).
The abrasive cloth is an abrasive paper of the type P60 KK504X NEO fastened to the drum of the grinding machine. The subsequent, planned measurements will be performed by the application of an abrasive cloth of a different surface roughness. The machine is fastened with its processing surface facing upward, the abrasive plane is parallel with the base surface of the equipment.
The steady, straight-line motion of the cloth is coupled with a lateral feed motion of the sample piece, thus it does not pass over the same abrasive surface twice but it always contacts a new abrasive element. Due to the exact adjustment and regulation of the speed of the abrasive cloth (peripheral speed of the driven cylinder), a separate electric motor is responsible for the drive mechanism. Apart from driving the abrasive cloth, the motor also directs the transverse movement of the sample piece (in relation to the cloth). The coordinated relationship of movements is possible due to the pre-calculated transfer ratios. The drive mechanism consists of ribbed belts.

The load structure forms a single unit with the sample unit grip head traveling on a threaded spindle performing the feed motion. The grip head is located at the bottom of the load structure. The test piece has a cylindrical shape one front surface of which is pressed to the cloth. The diameter of the cylinder is 8 mm and its length is 15 mm. It is important to fasten the tested sample piece in the grip head without the possibility of any movement and also to prevent any substantial deformation because it can influence measurement results. The grip head has strain gauges which make possible the measurement of forces exerted on the test piece during the test. The gauges are connected in a Wheatstone bridge.
The input parameters of the electronic measurement system are as follows:
t –time (s)
F_x – abrasion friction resistance calculated from the movement of the cloth (N)
F_y –abrasion friction resistance calculated from the lateral feed motion of the test piece (N)
F_z –load value in the normal direction (N)
S_{zv} –displacement from the abrasion of the sample piece. (mm)

3. Measurement process

we have performed three measurements on one polymer type each, corresponding to the load level values, using loads of 5, 10 and 20 N, respectively. The resting surface pressure can be calculated using the following formula:

$$\sigma = \frac{F}{A} = \frac{F_t}{\frac{d^2 \cdot \pi}{4}}$$

4. Evaluation of wear

The k value representing wear can be calculated as a quotient of the mass difference of the test piece and the friction path traveled.

$$k = \frac{\Delta m}{s} \quad \left[\frac{mg}{m}\right]$$

After dividing the result [mg/m] by the load force [N], the value of the specific abrasion wear is obtained. It has a reference to the system because it takes into consideration the normal load of the abrasive system.

$$k_f = \frac{\Delta m}{s \cdot F} \quad \left[\frac{mg}{m \cdot N}\right]$$

This figure shows how many mg of abrasive loss is suffered by the test piece used in the system as a result of 1 m of abrasive path and 1 N of load force.
The general specific abrasive wear can be calculated by the following formula:

$$k_{fá} = \frac{\Delta m}{\frac{s \cdot F_t}{A}} = \frac{\Delta m}{s \cdot p} \quad \left[\frac{mg}{m \cdot \frac{N}{m^2}} = \frac{mg \cdot m}{N}\right]$$

The results of the measurements are shown in table 2.

5. Results

The fig.2. shows the wear losses.
It is instructive to evaluate the results of force and abrasion measurements as a function of time (proportional to the abrasive path) (Figure 3. and 4). We have approximated the values of the

Table 2 Calculated wear based on weight measurements

Polymer	F_0 [N]	F_t [N]	F_x [N]	F_y [N]	F_e[N]	Weight [g] Before test	After test	Δm [g]	s [mm]	k [mg/m]	k_f [mg/mN]	$k_{fä}$ [mg*m/N]
PA 6G-H	5	11,65	14,92	2,60	15,15	0,950	0,928	0,022	5067,21	4,34	0,373	0,0069
	10	15,72	20,55	3,34	20,82	0,972	0,953	0,019	5118,85	3,71	0,178	0,0032
	20	25,07	32,30	5,49	32,77	0,917	0,885	0,032	5122,07	6,25	0,191	0,0036
PA 66E	5	11,99	14,90	2,22	15,06	0,967	0,951	0,016	5151,12	3,11	0,206	0,0038
	10	16,52	20,52	3,22	20,77	0,982	0,955	0,027	4967,15	5,44	0,262	0,0050
	20	25,36	32,06	5,10	32,46	1,006	0,960	0,046	4963,93	9,27	0,285	0,0053
PA 6GMo	5	11,88	14,57	2,23	14,74	0,962	0,932	0,030	5225,35	5,74	0,389	0,0073
	10	16,18	20,53	3,29	20,79	0,988	0,960	0,028	5293,13	5,29	0,254	0,0046
	20	25,30	32,05	5,30	32,48	0,978	0,921	0,057	5225,35	10,91	0,336	0,0061
PA 6GOL	5	11,65	14,72	2,36	14,91	0,821	0,788	0,033	5199,53	6,35	0,426	0,0088
	10	16,06	20,41	3,35	20,69	0,789	0,754	0,035	5157,58	6,79	0,328	0,0070
	20	25,47	31,22	5,26	31,66	0,779	0,724	0,055	5205,99	10,56	0,334	0,0073
PA 66GF30	5	11,59	14,51	2,48	14,72	1,113	1,056	0,057	5170,49	11,02	0,749	0,0139
	10	16,41	20,04	3,22	20,29	1,114	1,038	0,076	5034,93	15,09	0,744	0,0138
	20	25,01	31,22	5,49	31,70	1,028	0,911	0,117	5102,71	22,93	0,723	0,0137
POM C	5	11,47	14,53	2,50	14,74	1,121	1,044	0,077	5096,25	15,11	1,025	0,0191
	10	16,12	20,56	3,64	20,88	1,127	1,015	0,112	5235,04	21,39	1,025	0,0194
	20	25,53	31,75	5,70	32,26	1,122	0,938	0,184	4999,43	36,80	1,141	0,0216
PETP	5	11,65	14,52	2,18	14,68	1,063	1,030	0,033	5157,58	6,40	0,436	0,0082
	10	15,72	20,23	3,07	20,46	1,116	1,056	0,060	5306,04	11,31	0,553	0,0103
	20	25,24	32,26	5,25	32,68	1,110	1,016	0,094	5118,85	18,36	0,562	0,0107
PETP TX	5	11,93	14,87	2,21	15,03	1,128	1,074	0,054	5176,94	10,43	0,694	0,0134
	10	16,35	20,64	3,19	20,89	1,119	1,046	0,073	4850,96	15,05	0,721	0,0139
	20	25,53	31,29	5,10	31,70	1,190	1,079	0,111	4938,11	22,48	0,709	0,0133

F_0	-load, [N]
F_t	-load with self-weight of the unit, [N]
F_x	-x direction (main sliding direction) friction force, [N]
F_y	-y direction (feed motion) friction force, [N]
F_e	-resulted abrasive friction force, [N]
Δm	-change in weight of the test specimen, [g]
s	-sliding distance, [mm]
k	- quotient of the mass difference of the test specimen and the sliding path, [mg/m]
k_f	- specific abrasive wear, [mg/mN]
$k_{fä}$	- general specific abrasive wear, [mg*m/N]

abrasive curve by a linear polynomial. By analyzing the equation of the straight line, we obtain

$$y = A \cdot x + b$$

where A: – the slope of the straight line of wear (change of vertical displacement (mm)), a characteristic figure concerning the degree of abrasion speed.

By comparing the a values, the abrasion relationships of individual polymers can be compared.

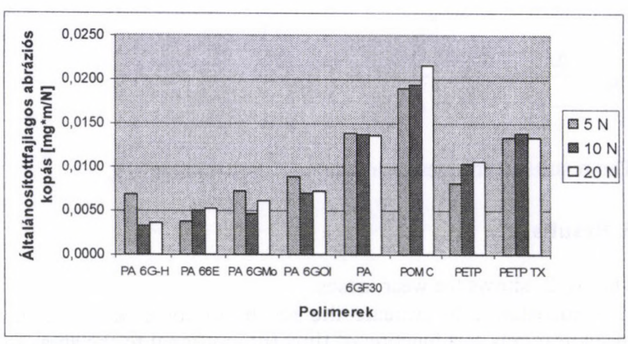

Fig. 2 General specific abrasive wear

Table 3 Linear equations of abrasive friction forces in the function of sliding distance under 20 N

	Approximated equations of friction forces
PA 6G-H	0,000251x + 19,109178
PA 66E	0,000113x + 20,589989
PA 6GMo	0,000113x + 20,589989
PA 6GOL	-0,000048x + 18,730922
PA 6GF30	0,000129x + 18,506395
POM C	0,000155x + 20,241552
PETP	-0,020815x + 19,415361
PETP TX	0,000135x + 19,933754

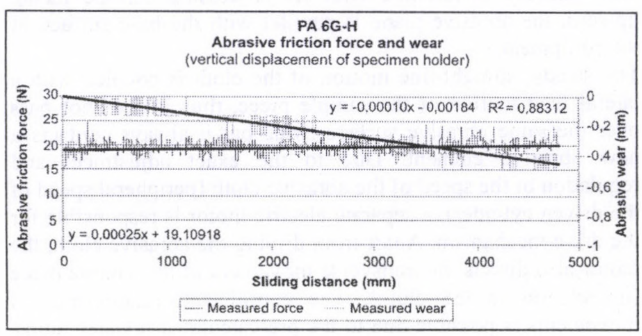

Fig. 3 PA 6G-H abrasive friction force (N) and wear (mm)

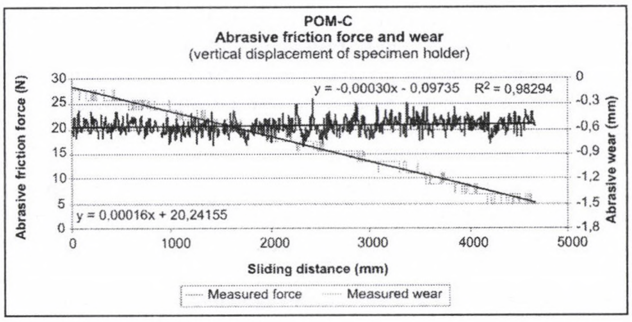

Fig. 4 POM-C abrasive friction force (N) and wear (mm)

6. Summary

• Using the new testing equipment – modified "pin-on-cylinder" measurement principle – the abrasive process can be studied along a longer friction path and by studying a more diverse set of information as opposed to the traditional "pin-on-cylinder" measurements.

• The previous statements published earlier in literature by Ratner proved to be conditionally true (i. e.: linear abrasion dynamics, - the decisive role of tenaciousness and breaking expansion). They have proven to be true for natural polymers but the mathematical relationships can be influenced by the abrasion circumstances and they are not true for all composites.

• In the linear abrasive dynamic region, the measurement results can be used to define the "specific micro cutting resistance" of individual polymers. (Table 4.)

$$c = \frac{F_{átl}}{A_0}$$

Table 4 Specific micro cutting resistance (MPa)

PA 6G-H	0,279	**PA 66 GF30**	0,273
	0,379		0,376
	0,614		0,599
PA 66E	0,278	**POM C**	0,274
	0,394		0,395
	0,603		0,611
PA 6GMo	0,277	**PETP**	0,275
	0,379		0,383
	0,592		0,620
PA 6GOL	0,309	**PETP TX**	0,290
	0,441		0,402
	0,690		0,596

• Based on the evaluation of the diagrams so far, it can be established that the tenacious but highly solid natural, cast polyamide 6 exhibited the smallest degree of wear and the POM copolymer wore of most rapidly..

• The PTFE (Teflon) additive increasing tenacity did not result in a decrease of wear in PETP (material marked with "PETP TX"), but it wore much more than rigid, natural PETP. Thus, the Ratner theory cannot be applied for this composite version – when comparing materials of identical basic matrices.

• Based on further measurements and results, the speed of abrasion wear and specific abrasion wear can be analyzed as a function of material properties which may deliver further new scientific results in the future.

References

[1] Kalácska Gábor: Mezőgépek - Mezőgépészeti tribológia. Szerkesztette Kalácska G. GATE és VE jegyzet. Ph.D. és Tribológia szakmérnök képzés. 1999. Második kiadás: 3C Grafika Kiadó Kft Gödöllő, 2003. p. 1-92.

[2] Kalácska G. – Kozma M. – Zsidai L. – P. De Baets:

[3] Engineering plastics in the technical development of mining equipment and machines. Gépészet 2000 konferencia. Budapest. 2000 május. p. 573-578.

[4] Zsidai L. – Kalácska G. – Pálinkás I. – Ost W.: Modular development of dynamic tribological test rig. . = HAE. N.19/ 2006. Hungarian Academy of Sciences. p. 15-18.

[5] Kalácska- Kozma: Tribológiai vizsgáló berendezés fejlesztése műanyag kompozitokhoz. MTA Agrárműszaki Bizottság, Kutatási és Fejlesztési Tanácskozás. Kiadvány. Gödöllő, 1999 január. 2. kötet p. 216 – 220.

[6] Kalácska G. – Zsidai L. – De Baets P. – Vercammen K: Dinamikus tribométer fejlesztése. . MTA Agrárműszaki Bizottság, Kutatási és Fejlesztési Tanácskozás. Gödöllő, 2001 január, 3. kötet p. 223-226.

[7] Eberst O. – Pop S. – Kalácska G: Application of polymers in abrasive tribosystems. MTA Agrárműszaki Bizottság, Kutatási és Fejlesztési Tanácskozás. Gödöllő, 2002 január. 1. kötet p. 268-272.

[8] Antal – Fledrich – Kalácska – Kozma: Műszaki műanyagok gépészeti alapjai. MINERVA-SOP BT. Sopron, 1997 p 1-56.

[9] Eberst O. – Pop S. – Kalácska G. – Keresztes R. – Zsidai L. – DeBaets P.: Abrasive wear of engineering polymer gears. International multidisciplinary Conference. North University of Baia Mare. May 2005. Scientific bulletin. 2nd Volume. p. 171-177.

[10] Yamaguchi - Yukisaboro: Tribology of plastic materials. Amszterdam, Tribology series 6, Elseviere 1990.

THE IMPACT PATHWAY METHOD FOR ESTIMATING EXTERNAL COSTS OF ELECTRICITY GENERATION

Sándor MOLNÁR[1] - Nenad DEBRECIN[2] - Tea KOVAČEVIĆ[2] - Márk MOLNÁR[1]
[1]Szent István University, Gödöllő
[2] Zagreb Unviersity, Faculty of Electrical Engineering and Computing

Introduction

External costs of electricity refer to the costs of damage imposed on society and the environment by an electricity generation chain, but not accounted for in the market price of electricity. Electricity generation impacts include effects of air pollution on health, buildings, crops, forests and global warming; occupational disease and accidents; and reduced amenity from visual intrusion or emissions of noise. Effects of air pollution on human health are the most significant among them. The equivalent monetary value of health damage, i.e. external cost, is calculated here for two types of fossil fired power plants, located in Croatia, with the analysis covering Croatian- and European-wide scope of effects.

Method Description

Because of their diverse character, electricity generation impacts are expressed in a common measure, so called external costs. External costs can be calculated using the so called impact pathway methodology, which relates to the sequence of events linking a "burden" to an "impact", and subsequent valuation. The impact pathway methodology consists of the following steps: (i) quantification of emissions, (ii) calculation of the associated ambient concentration increase by means of atmospheric dispersion and transport models, (iii) estimation of physical impacts using various exposure-response functions, and (iv) finally monetary evaluation of damages. The tool used to assess external costs caused by power plant operation is the EcoSense software [1].

Focus of this analysis is put on the effects of ambient air pollution on human health, as one of the priority impacts of electricity generation. Since air pollutants are transported over large distances, crossing national borders, their impacts are quantified both for population in Croatia and for the whole of Europe. Europe is mapped onto a grid comprised of 100x100 km sized cells, i.e. receptors. Long-range transport and dispersion of pollutants is assessed by a Lagrangian trajectory model, which examines incoming trajectories of air parcels arriving from different directions to the receptor point. The outputs from the model are atmospheric concentrations and deposition of emitted species and secondary pollutants in each grid cell.

Incremental air pollution attributable to power generation is a mixture of pollutants emitted from stack (particulate matter, sulfur dioxide, nitrogen oxides) and those formed subsequently in chemical reactions in the atmosphere (sulfate and nitrate particles, and tropospheric ozone). Both primary and secondary pollutants cause certain health effects, mostly connected to respiratory and circulation problems. Quantitative relationships have been established linking air pollution with health endpoints (Table 1). Acute effects occur on the same day as increases in air pollution or very soon thereafter, while chronic effects are delayed and develop as a result of long-term exposure. More susceptible to symptoms are older people and those who suffer from respiratory diseases, e.g. asthmatics.

Increased air pollution can not really cause 'additional' deaths, it can only reduce life expectancy. Length of life lost in cases of acute mortality is likely to be short - a few weeks or months. If mortality is caused by chronic illness, life reduction is considered to be several years. Here is the example of how additional mortality and restricted activity days can be calculated based on the given exposure-response functions:

Mortality (number of cases) = exposure-response factor/100 × baseline mortality × population of the observed area × pollutant concentration increase (μg/m^3).

Restricted activity days (number of days) = exposure-response factor/100 × population of the observed area × percentage of adults × pollutant concentration increase (μg/m^3).

Table 1 Summary of exposure-response functions and monetary values [2]

Impact Category	Monetary value (ECU) (1)	Pollutant	Exposure-response factor (2)
Acute mortality (3)	155.000	PM_{10} and nitrates	0,040%
(expected life reduction: 9 months)		$PM_{2.5}$ and sulfates	0,068%
		SO_2	0,072%
Chronic mortality (3, 4)	83.000	PM_{10} and nitrates	0,390%
(expected life reduction: 12 years)		$PM_{2.5}$ and sulfates	0,640%
Hospital admissions,	7.870	PM_{10} and nitrates	$2,07\times10^{-6}$
respiratory problems		$PM_{2.5}$ and sulfates	$3,46\times10^{-6}$
		SO_2	$2,04\times10^{-6}$
Hospital admissions,	7.870	PM_{10} and nitrates	$5,04\times10^{-6}$
cerebrovascular problems		$PM_{2.5}$ and sulfates	$8,04\times10^{-6}$
Restricted activity days (4)	75	PM_{10} and nitrates	0,025
		$PM_{2.5}$ and sulfates	0,042

(1) mortality values given at a discount rate of 3%, based on years of life lost; 1 ECU = 1,25 US$ (1999).
(2) slope of the exposure-response function is expressed in percentage change in annual mortality rate per unit of pollutant concentration increase (% change per μg/m^3) for mortality, while in number of events per person per μg/m^3 for morbidity.
(3) baseline mortality in Croatia is 11 per 1000.
(4) age group 14-65, in Croatia 68% of total population.

Mortality impacts can be valued based on the willingness to pay (WTP) for reduction of the risk of death, or on the willingness to accept compensation (WTA) for an increase in risk. One year of life lost is estimated at 98.000 ECU, if no discounting is applied. If the discount rate is set to 3%, which is recommended for environmental damage valuation, money loss in case of acute death is 155.000 ECU, while 83.000 ECU if a fatal outcome is caused by a chronic illness. Morbidity impacts are valued based on medical treatment cost and lost wages.

Application of the Impact Pathway Method on Croatia

The aim of the analysis made here was to estimate costs of health damages through air pollution caused by two possible power generation technologies in Croatia in the near future: coal and natural gas fired facilities. Hypothetical power plants, one coal and one gas combined cycle (CC) unit, are assumed to comply with current domestic emission standards [3], so the emission rates equal the upper emission limits. Both power plants are same in size, 350 MW net capacity. Their emission data are given in Table 2.

It was observed how each of those two power plants, if placed at a certain location in Croatia, would affect (a) population in

Croatia, and (b) the whole of Europe. Power plants were moved across the country to check how the external costs vary with location. To determine the health impacts on population in Croatia only, grid cells belonging to Croatia were isolated in the matrix of results. The total affected population in Croatia is 4,8 million, while in the whole of Europe around 540 million. Spatial distribution of primary and secondary pollutant concentrations, combined with population distribution and the appropriate exposure-response functions is used to calculate health impacts on the population in Croatia and Europe and the associated external costs due to operation of the observed two power plants.

Table 2 Emission rates of the analyzed power plants

Emissions	Coal fired		Natural gas fired	
	mg/m^3	g/kWh	mg/m^3	g/kWh
Particulates	50	0,15	0	0
SO_2	400	1,21	0	0
NO_x	650	1,97	100	0,52
CO_2	2,84E+5	862	0,66E+5	344

After examining several locations, possible for future power plants, a range of external costs was obtained. Results are shown in Table 3. More detailed description of the method and the results can be found in [4].

Table 3 External costs: summary of results

	Coal fired facility	Gas fired facility
Scope:		
Croatia only (4,8 million)	mUS$/kWh	mUS$/kWh
Particulates	0,29 – 0,33	0
SO_2 (including sulfates)	0,59 – 0,93	0
NO_x (including nitrates)	0,63 – 1,96	0,18 – 0,54
Total*	***1,51 – 3,22***	***0,18 – 0,54***
Scope:		
Europe (540 million)	mUS$/kWh	mUS$/kWh
Particulates	1,99 – 2,95	0
SO_2 (including sulfates)	13,93 – 15,72	0
NO_x (including nitrates)	23,59 – 28,10	6,91 – 8,16
Total*	***39,51 – 46,77***	***6,91 – 8,16***

* health damages due to tropospheric ozone (precursor: NO_x) not included.

The obtained external costs comprise only health impacts due to airborne emissions (particulates, SO_2, NO_x). Impacts of ground-level ozone, which is caused by NO_x, and of global warming, caused by greenhouse gases, are not included. Due to lack of reliable ozone models, external costs of NO_x via ozone are set to the uniform value of 1.500 ECU per ton of NO_x for the whole of Europe. External costs of global warming are subject to large uncertainties, so they vary from 3,8 to 139 ECU per ton of CO_2. The geometrical mean value was taken as the best estimate for global warming damages: 29 ECU/t.

External costs of power generation in fossil fuelled power plants are obtained as the sum of (i) airborne emissions damages, which are site specific, (ii) ground-level ozone damages that are for now considered uniform for the whole of Europe, and (iii) global warming damages that are considered uniform in the whole moderate climate zone. Those numbers are given in Table 4.

External costs can be included in power system expansion planning, i.e. selection of the optimal future capacity mix. They can be added to production costs of candidate generation units and in that way incorporated into the optimization goal function. Such exercise was conducted in the following analysis. The aim was to find the capacity mix with the lowest annual production costs, which still complies with the given requirements.

Table 4 Cases depending on the level of external costs included in optimization

External cost (mUSD/kWh)		Case name
coal	3,22	External cost Croatia
gas	0,54	
nuclear	0,1	
coal: 46,77 + 3,69*	50,46	External cost Europe (including ozone damage)
gas: 8,16 + 0,98*	9,14	
nuclear	0,1	
coal: 46,77 + 3,69* + 30,05**	80,51	External cost Europe-total (including ozone and global warming damage)
gas: 8,161 + 0,98* + 12,47**	21,61	
nuclear***	0,1	

* due to tropospheric ozone, ** due to global warming, *** based on [6]

The effect of external costs on the optimal expansion plan

On the basis of electricity consumption forecast and scheduled retirements of the existing power plants, projections of the needed new generating capacities have been made [5]. It turned out that additional capacity of 4500 MW will have to be installed in the period 2001-2030. Fossil-fired (coal and natural gas) and nuclear power plants, together with several hydroelectric facilities, are chosen as candidates for system expansion. All candidate power plants are designed to comply with current environmental standards in Croatia. Coal units will be equipped with electrostatic precipitators for particulates removal and with wet scrubbers for desulphurisation. Low-NO_x combustion measures will be applied to reduce NO_x emissions to the allowable levels. The existing power plants will not be equipped with any additional emission abatement devices before they are retired.

Annual production costs are obtained as a sum of levelized fixed costs (comprised of annual capital cost recovery and yearly fixed maintenance cost) and annual variable costs (comprised of fuel cost and variable maintenance cost).

In the selection process of the optimal capacity mix in the following 30-year period four cases were observed, each with different external cost value added to direct costs of expansion candidates. In the first case no external costs were added, so the optimization was conducted based on direct costs only. In the second case, called *Ext. costs Croatia*, the calculation was made with the external cost for Croatia, as given in Table 3, which means that only damages within Croatia are taken into account. The upper value in the range was chosen following the conservative approach. The third case incorporated the external costs for the whole of Europe, plus the average ozone damage for Europe (*Ext. costs Europe*). In the fourth case, *Ext. costs Europe–tot*, the external costs from case 3 were increased by the value of global warming damages. The list of cases and the attached external costs is given in Table 4.

It has to be stressed that external costs are added only to candidate and not the existing units, because the purpose of this analysis was to examine the influence of external costs on resource selection and not on power system operation. Therefore, once the optimal capacity mix is determined, it is assumed that facilities are dispatched according to their direct costs, i.e. the economic loading order. In other words, external costs here are not meant to be imposed on any party, neither the producer nor the customer, and therefore should not affect the price of electricity.

The optimal capacity mixes in those four cases are shown in Figure 1, as cumulative values for the entire planning period. In all cases it is supposed that natural gas availability is unlimited.

If no external costs are added, the optimal capacity mix consists only of gas CC power plants, since they have the lowest direct costs. Adding the external costs for Croatia would not affect the optimal solution much, because gas fired power plants would still have the lowest total costs. However, if the value of external costs is high enough, optimal expansion plan does get strongly affected. That happens in the third and fourth case, where European-level external costs are added. In the third case, where no global damages were included, three nuclear units enter the optimal capacity mix, whereas in the fourth case, where the global warming damages are also included in the cost function, optimal solution involves even four nuclear units.

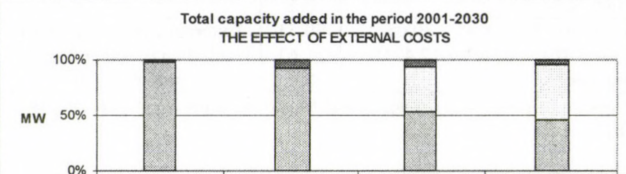

	No external costs added	Ext. costs Croatia	Ext. costs Europe (incl. ozone)	Ext. costs Europe-tot (incl. ozone + GW)
HYDRO	83	326	286	180
NUCLEAR	0	0	1800	2400
GAS	4440	4140	2340	2140
COAL	0	0	0	0

***Figure 1** Total added capacity by fuel, depending on the external cost level*

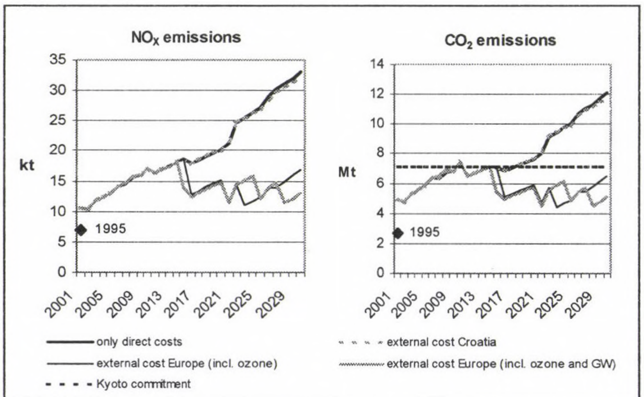

***Figure 2** Emissions of NO_x and CO_2 in the observed period*

The structure of new capacities is reflected on emission levels, as shown in Figure 2. If there is no nuclear facilities installed, emission follow an upward trend. Emissions of NO_x in the year 2001 are expected to be 10 kilotonnes. During the observed period they would triple if only gas facilities are built. Only if more nuclear units are deployed, NO_x emissions could be kept at low levels, around 20-30% percent higher than today. Emissions of SO_2 and particulates in all of the observed cases are expected to drop to negligible amounts till the year 2030, because no coal or oil units are added.
An additional very important consequence is that CO_2 emissions are decreasing as well, although no direct measures to reduce CO_2 are applied. Croatian commitment in Kyoto is to start reducing total country's CO_2 emissions so that the average value in the period 2008-2012 is 5% lower than in 1990, and that the emissions are kept at that level afterwards. The corresponding requirement for the power sector is to reduce CO_2 emissions to 7,1 million tonnes per year. The average CO_2 emission in the period 2008-2012 would be around 6,8 Mt/year. This value is similar in all cases since bigger differences occur only in the second half of the planning period, due to the retirement of the existing units. Although the value is below the Kyoto limit, the rising emission trend suggests the goal of long-term reduction would not be met. Only the case with large share of nuclear power could keep CO_2 emissions below the Kyoto limit in the long run.

Conclusions

This paper is one of the first attempts to evaluate electricity externalities in Croatian power system, therefore the focus was put on priority impacts. Those are health effects of air pollution caused by coal and gas fired facilities, candidates for construction in the following 30 years. It has to be stressed that external costs of coal power plants can be lowered by further reducing their emissions, i.e. by applying more efficient abatement technologies already available on the market. Of course, that would induce some additional direct costs.
The results show that damages linked to coal power plants are much larger than those linked to gas fired facilities, since the latter are responsible only for NO_x emission and nitrates. The largest share in the damage costs accounts for mortality effects. The highest damages are attributable to particulate matter, on the local level directly while on the regional level in the form of sulfates and nitrates. Health damages highly depend on the number of people affected – that is why damages within Croatian borders are much lower than on the European scale.
When incorporated into electricity system expansion planning, the external costs that include only the population within Croatia do not significantly influence the optimal capacity mix, but the European-wide external costs do so in a great deal. In the latter case, the competitiveness of gas units is reduced in favour of nuclear units. It is very important to define geographical scope within which the impacts should be internalized, since that can seriously influence decision making in the country of emissions origin.

Research was partially supported by TéT HR 4/2004

References

[1] EcoSense 2.0 User's Manual, Institut für Energiewirtschaft und Rationelle Energieanwendung (IER), Universität Stuttgart, 1997.
[2] ExternE National Implementation Germany, Final Report, IER, Stuttgart, 1997.
[3] Regulation on permissible emission levels for stationary sources pollutants (in Croatian), Narodne novine, Službeni list 140/1999, Zagreb.
[4] Feretić et al: CRP "Case study for Croatian electrical energy system on comparing sustainable energy mixes for electricity generation", FER Zagreb, 1999, prepared for IAEA, Research Contract No 9526/RB.
[5] Energy Strategy of Republic of Croatia (in Croatian), Ministry of Economy, Zagreb, 1998.
[6] Rabl, Curtiss, Spadaro et al: Environmental Impacts and Costs: The Nuclear and the Fossil Fuel Cycles, Report to European Commission DGXII, Armines (Ecole de Mines), Paris, 1996.

Contents of N° 20/2007

Contents of the "Mezőgazdasági Technika" periodical of the year 2007.

MEZŐGAZDASÁGI TECHNIKA
2100 GÖDÖLLŐ, TESSEDIK S.U.4.

Do you want to know more from

Hungarian Agriculture Machinery!

SENDTMIS ORDER FROM TO:

The Hungarian Agricultural Machinery Journal
H-2001 Gödöllő, Tessedik Sámuel u. 4.

ORDER FORM

I want order the Hungarian Agriculture Machinery Journal

from .... day .... month 200......

The subscription fee: 3240 HUF

Name: ....

Adress: ....

Code, City: ....

Country: ....

Date: .... day .... month 200.......

....

signature